# MICROFACIES ANALYSIS OF THE BAJOCIAN—BATHONIAN DHRUMA CARBONATES, CENTRAL SAUDI ARABIA

BY

**AVIANDY WIDYA ISMANTO**

A Thesis Presented to the
DEANSHIP OF GRADUATE STUDIES

**KING FAHD UNIVERSITY OF PETROLEUM & MINERALS**

DHAHRAN, SAUDI ARABIA

In Partial Fulfillment of the
Requirements for the Degree of

# MASTER OF SCIENCE

**In**

**GEOLOGY**

**MAY 2018**

KING FAHD UNIVERSITY OF PETROLEUM & MINERALS

DHAHRAN- 31261, SAUDI ARABIA

**DEANSHIP OF GRADUATE STUDIES**

This thesis, written by **AVIANDY WIDYA ISMANTO** under the direction of his thesis advisor and approved by his thesis committee, has been presented and accepted by the Dean of Graduate Studies, in partial fulfillment of the requirements for the degree of **MASTER OF SCIENCE IN GEOLOGY.**

Dr. Khalid A. Al-Ramadan
(Advisor)

Dr. Abdulaziz Al-Shaibani
Department Chairman

Dr. Lamidi O. Babalola
(Member)

Prof. Salam A. Zummo
Dean of Graduate Studies

Prof. Michael A. Kaminski
(Member)

24/5/12
Date

© AVIANDY WIDYA ISMANTO

2018

## *Dedication*

*This work is dedicated to my beloved parents and sister for their enormous support, inspiration, and motivation.*

# ACKNOWLEDGMENTS

In the name of Allah, the most gracious, most merciful. All the praises and thanks are due to Allah who has given me the opportunity and capability to finish my study at KFUPM.

My deep appreciation goes to my advisor, Dr. Khalid Al-Ramadan, for the knowledge, patience, encouragement, and guidance that he has shown me over the past few years that I have been in the Geosciences department. His motivation always encourages and stimulates innovation inside my brain, thus I feel more mature as a geoscientist.

I would like to thank my thesis committee members, Dr. Lamidi O. Babalola and Prof. Michael A. Kaminski for their sincere support and constructive comments over the years:

I acknowledge the funding support provided by King Abdulaziz City for Science and Technology (KACST) through project No. NSTIP-13-OIL1694-04.

The support enjoyed from the Geosciences Department's faculty members, staff, and colleagues during my study are duly acknowledged especially. The departmental Chairman Dr. Abdulaziz Al-Shaibani and Graduate Coordinator of Geosciences Department, Dr. SanLinn I. Kaka are thanked for their kind support and assistance. Special appreciation goes to Mr. Hameed, Mr. Aziz Khan, Mr. Abbas, Mr. Fyl Louie, Mr. Abdulrasyid, Mr. Abdulkhaleq, Mr. Fuad and Mr. Abdullah for helping in sample preparation and analyses. The assistance and support received from my colleagues including Omar, Moaz, Mazin, Ibrahim, Naveed and Mahmoud are really appreciated.

Many thanks go to CPG-KFUPM Indonesian community (Septriandi, Arum, Leon, Pram, Argo, Hanif, Dipta, Bayu, Ghozian, Nanda, Ryan, Bagus) and all the other Indonesian students at KFUPM (Rama, Try, Adha, Ihsan, Adi, Lutfi A, Lutfi M, Zamzam, Yusuf, Ghazi, Pak Teguh, Kang Latif, Kang Yusri, Kang Rangga, Tausiff bhai and many more). Basketball and football communities in Eastern Province are also appreciated for the joy they have brought during my stay at KFUPM.

# TABLE OF CONTENTS

# LIST OF TABLES

# LIST OF FIGURES

# LIST OF ABBREVIATIONS

| | |
|---|---|
| XRD | : X-Ray Diffraction |
| SEM | : Scanning Electron Microscopy |
| EDX-SEM | : Energy-dispersive X-ray- Scanning Electron Microscopy |
| FWWB | : Fair-weather Wave Base |
| SWB | : Storm Wave Base |
| PPL | : Plane-Polarized Light |
| XPL | : Cross-Polarized Light |

# ABSTRACT

Full Name : [Aviandy Widya Ismanto]

Thesis Title : [Microfacies Analysis of the Bajocian-Bathonian Dhruma Carbonates, Central Saudi Arabia]

Major Field : [Geology]

Date of Degree : [May 2018]

The Middle Jurassic Dhruma Formation as a part of the Jurassic succession in Saudi Arabia is one good example of an ancient carbonate ramp to be studied. Dhruma outcrops are well-exposed about 60 kilometers west of Riyadh, in Central Saudi Arabia. The Dhruma Formation is comprised of three distinctive members (Lower, Middle, and Upper Dhruma) and seven distinct informal units (D1—D7 Units). Based on ammonite, gastropod, and brachiopod faunas, the Dhruma Formation was assigned an Early Bajocian to Middle Callovian age. The Dhruma Formation is mainly composed of a thick carbonate sequence with a thin bedded clastic sequence in the basal part. These units are developed on a homocline carbonate ramp system.

Integrated field and laboratory investigations (e.g., sedimentological and petrographic analyses, X-ray diffraction, scanning electron microscopy and porosity-permeability analyses) were carried out on outcrop section (D2 to D4 Units) to identify the microfacies and interpret the depositional environments of the succession.

This study identified eight distinctive microfacies including peloidal skeletal wackestone, skeletal peloidal packstone, skeletal oolitic packstone, peloidal grainstone, oolitic grainstone, skeletal floatstone, burrowed wackestone and mudstone. These microfacies were interpreted to have been deposited in lagoon, shoal complex, and open marine environments. The lagoonal setting is represented by peloidal skeletal wackestone and skeletal peloidal packstone. Skeletal oolitic packstone, peloidal grainstone, and oolitic grainstone were deposited in the shoal complex. Lastly, the open marine setting is characterized by skeletal floatstone, burrowed wackestone, and mudstone.

Porosity and permeability results showed that the highest values and the most likely high-quality reservoir is the burrowed wackestone in which the dolomite calcitization (dedolomitization) process generally occurs. Micritization, dolomitization, and cementation processes in mudstone and peloidal skeletal wackestone reduce porosity and permeability values.

# ملخص الرسالة

**الاسم الكامل** : أفياندي ويديا ايسمانتو

**عنوان الرسالة** : دراسة السحنات الدقيقة للصخور الجيرية لمتكون ضرما بوسط المملكة العربية السعودية

**التخصص** : جيولوجيا

**تاريخ الدرجة العلمية** : مايو 2018

يعد متكون ضرما ذو العمر الجوراسي الأوسط نموذجا جيدا لرصيف جيري قديم في الجزيرة العربية. وتظهر مكاشف هذا المتكون بشكل جيد على بعد 60 كم غرب الرياض في وسط المملكة العربية السعودية. ويشمل المتكون ضرما ثلاثة أعضاء (سفلي، أوسط، وعلوي) أو سبعة وحدات (D1—D7). ويتكون غالب متكون ضرما من صخور جيرية سميكة مع وجود طبقات رقيقة من صخور فتاتية في الجزء السفلي. تهدف هذه الدراسة لتفسير البيئات الترسيبية لمتكون ضرما وبخاصة الوحدتين (D3—D4) عن طريق دراسة الميدانية والمعملية للسحنات الدقيقة.

بناء على الدراسة المجهرية تم تمييز ثمان سحنات دقيقة في تلكا الوحدتين وهم: الحجر الجيري الواكي المحتوي على الحبيبات الحيوية والكريات الجيرية، الحجر الجيري المعبأ المحتوي على الحبيبات الحيوية والكريات الجيرية، الحجر الجيري المعبأ المحتوي على جسيمات سرئية وكريات جيرية، الحجر الجيري الحبيبي المحتوي على كريات عقدية، الحجر الجيري الحبيبي السرئي، الحجر الجيري الطوف المحتوي على حبيبات حيوية، الحجر الجيري الواكي المنقب، والحجر الجيري الوحل. توحي تلك السحنات الدقيقة ببيئة بحيرة ساحلية إلى بيئة بحرية مفتوحة. ويمكن تقسيم السحنات الدقيقة إلى ثلاثة أقسام. قسم يمثل بيئة البحيرة الساحلية ويحتوي على السحنات: الحجر الجيري الواكي المحتوي على الحبيبات الحيوية والكريات الجيرية، الحجر الجيري المعبأ المحتوي على الحبيبات الحيوية والكريات الجيرية. قسم يمثل بيئة ضحضاح (قليلة العمق) ويحتوي على السحنات: الحجر الجيري المعبأ المحتوي على جسيمات سرئية وكريات جيرية، الحجر الجيري الحبيبي المحتوي على كريات عقدية، الحجر الجيري الحبيبي السرئي. وقسم يمثل بيئة بحرية مفتوحة ويحتوي على السحنات: الحجر الجيري الطوف المحتوي على حبيبات حيوية، الحجر الجيري الواكي المنقب، والحجر الجيري الوحل.

وبناء على دراسة المسامية والنفاذية للوحدتين يتضح أن السحنة الأكثر مسامية هي الحجر الجيري الواكي المنقبة والتي ينتشر بها عمليات إزالة الدلمته. ويتضح أيضا أن عمليات التجُّير، التَّسْمُنت، الدلمتة قد أدت إلى تقليل قيم المسامية والنفاذية لسحنات الحجر الجيري الوحل والحجر الجيري الواكي المحتوي على الحبيبات الحيوية والكريات الجيرية.

# CHAPTER I

# INTRODUCTION

## 1.1 Background

In the past few decades, carbonate rocks have been studied in both surface and subsurface to recognize their heterogeneity and complexity. Hydrocarbon resources in carbonate reservoirs hold more than 30% of the world's proven reserves (Figure 1.1; Ehrenberg and Nadeau, 2005; Schlumberger, 2009). Thus, around 60% of the world's oil reserves, 70% of which are hosted in carbonate reservoirs, are in the Middle East region. The Middle East also holds 40% of the world's gas reserves and 90% of these lie in carbonate rocks (Schlumberger, 2009).

Due to its economic importance, the Jurassic carbonate succession of Saudi Arabia named the Shaqra Group, is well-known as one of the most significant carbonate reservoirs around the world (Schlumberger, 2009; Cantrell et al., 2014). Jurassic reservoirs of Saudi Arabia and neighboring countries (i.e., Qatar, Bahrain, and offshore UEA) have prolific hydrocarbon resources (Alsharhan and Magara, 1994). The Jurassic succession in Saudi Arabia is named the Shaqra Group, and is comprised of seven carbonates and evaporite formations namely, the Marat, Dhruma, Tuwaiq Mountain, Hanifa, Jubaila, Arab and Hith Evaporite Formations (Figure 1.2; Powers et al., 1966; Al-Husseini, 1997; Sharland et al., 2001). The rocks of this succession represent an excellent model of an ancient carbonate ramp to be studied (Beydoun, 1986; Sharland et al., 2001). In particular, Arab C and D reservoirs in the Arab Formation host the highest oil reserves in the world in the Ghawar field (Cantrell et al., 2014) and the Middle Jurassic Tuwaiq

Mountain and Hanifa Formations act as the main carbonate source rocks for the Jurassic Petroleum System (Murris, 1980; Cantrell et al., 2014).

The examination of carbonate rock using microfacies analysis is widely used as a basic approach to characterize carbonate rocks. The carbonate Dhruma Formation, spanning the Bajocian to Bathonian ages (170—166.1 m.y.), represents the lower part of the Shaqra Group (Arkell et al., 1952; Powers et al., 1966; Hughes, 2004). Steineke (1939) introduced the name ”Dhruma” in its type locality at Khashm adh Dhibi in which a-375 meters thick carbonate sequence crops out forming a cliff. The thickness of the Dhruma Formation in its stratotype situated southwards in Wadi Birk is about 264 meters thick and it almost pinches out near Khashm ar Zifr (Powers et al., 1966). The formation is predominantly carbonate in its stratotype, becoming siliciclastic near Khashm Al-Khalta and Al-Haddar (Powers et al., 1966). However, somewhere near the central part of Rub’ Al-Khali Basin, clean carbonate is recorded in subsurface wells while in the northeastern part of Saudi Arabia the formation is composed mainly of dark-colored mudstone and argillaceous shelf limestone with varying amounts of sand-sized limestone and shale interbeds (Powers et al., 1966). The thickness of Dhruma Formation reduces towards the southeastern part of the Rub’ Al Khali Basin where it attains a thickness of 40—80 meters, thins to 20 meters at the Qatar Arch. The formation thickens towards the northeast reaching about 300-m of thickness as a basinal mudstones facies in Kuwait and Iraq (Alsharhan and Magara, 1994; Stewart, 2017).

Geological studies of carbonate rocks have been intensively developed since the early 1950’s when carbonate rocks in many countries around the world were discovered as oil

and gas reservoirs (Flugel, 2010). The examination of carbonate rock using microfacies analysis is widely used as a basic approach to characterize carbonate rocks. Carbonate microfacies analyses provide a micro-scale detailed analysis and interpretation of rocks using the microscope and various geochemical analyses. The term microfacies was first coined by Brown (1943) and Cuvillier (1952) as a study of petrographic and paleontological characteristics of a rock in thin sections. Flugel (2010) stated that microfacies is all sedimentological and paleontological studies by using thin sections, slabs or rock samples to classify and describe carbonate facies. In addition to that, Flugel (2010) explained that microfacies analysis could establish an interpretation and classification of carbonate rocks, therefore a model of the depositional environment can be constructed.

## 1.2 Problem Statement and Objectives

The Jurassic Shaqra Group of Saudi Arabia has been investigated by many researchers (Arkell et al., 1952; Powers et al., 1966; Murris, 1980; Al-Husseini, 1997; Ziegler, 2001; Hughes, 2004; Enay et al., 2009; Cantrell et al., 2014). A number of investigations have been conducted on the microfacies of the Jurassic formations of Saudi Arabia in both surface and subsurface wells (Okla, 1986, 1987; Hughes, 2004; Al-Dhubaib, 2010; Al-Mojel, 2010; Malik, 2016; Al Ibrahim et al., 2017). However, there is still a gap in the microfacies analysis concerning all members of the Dhruma Formation in the study area (Darma' Quadrangle) that will lead to a critical thinking of how microfacies analysis can help achieve a better understand the paleoenvironments and develop a depositional model of the Dhruma Formation.

Even though all the Jurassic formations form a significant petroleum system in Saudi Arabia, the lower and middle parts of the Dhruma Formation in which the Faridah and Sharar reservoirs are equivalent to those of the D4 Unit on the surface, still has the potential to be investigated (Alsharhan and Kendall, 1986; Hughes, 2004). This research focused solely on the Middle Dhruma Formation consisting of the D2 (Dhibi Limestone Member), D3 (Jufayr Member) and the D4 (Uwaynid Member) Units. The detailed sedimentological study and petrographic analysis of carbonate rocks is used to decipher and understand the paleoenvironment of the studied members in the study area.

The main objectives of this research are as follows :

1. Construct a detailed analysis of the sedimentology in the study area through sedimentary observations including sedimentary structure and texture, and other key features during the fieldwork.

2. Identify the microfacies of the D2–D4 Units of the Dhruma Formation and decipher their depositional environment.

3. Integrate microfacies analysis and depositional environment with the petrophysical properties (porosity and permeability) to determine the reservoir potentials of the identified microfacies.

## 1.3 Study Area

The study area, situated between 24°12'02.4"N, 46°13'54.1"E and 24°12'04.2"N, 46°14'35.5"E is about 60 kilometers westward of Riyadh, Central Saudi Arabia (Figure 1.3). The examined outcrops are easily accessed from the Riyadh-Makkah highway to the

south. The study area is located in a small village, Harafat Nisah. The exposures of the studied members (the D2—D4 Units of the Dhruma Formation) are adjacent to the Saudi White Cement Factory extending almost north-south direction. Figure 1.4 shows the geological map of the study area in the Darma Quadrangle and its stratigraphic relationship with the other sedimentary formations in the quadrangle. The sections include section 1 and 2 which are in the west of the study area representing the uppermost part of D2 Unit (Dhibi Limestone Member), D3 Unit (Jufayr Member), lower part of D4 Unit (Uwaynid Member) of the Dhruma Formation, respectively (Figure 1.5b), furthermore, section 3 consists of the D4 Unit in the eastward side (Figure 1.5a). The first section has approximately a thickness of 50 meters. The latter forms a cliff of 25 meters. These sections are roughly separated by 7 kilometers distance.

## 1.4 Thesis Structure

The research presents the result of a study of microfacies analysis of the Bajocian-Bathonian Dhruma Formation's outcrops in Central Saudi Arabia using an integration of field and lab techniques. The thesis consists of six chapters. The first chapter introduces the research, discusses the problem statement the listing of the research objectives and concluded with a brief description of the study locality. Chapter 2 discusses the geological overview of the study area with respect to the paleotectonics and paleoenvironments of the Jurassic of the Arabian Plate with emphasis on Saudi Arabia. In addition, previous work related to bio- and litho-stratigraphy and microfacies of the Dhruma Formation is explained. The interpreted depositional model from this study is then compared with the carbonate depositional model developed by Wilson and Flugel. The third chapter presents the research methodologies including field description,

microfacies and biofacies analyses and interpreted depositional environment of all microfacies that are presented in Chapter 4. Chapter 5 discusses the integration of microfacies and biofacies analyses to achieve the main research objectives including modeling the depositional environments of the identified microfacies. Additionally, petrophysical properties of Dhruma Formation in the study area are discussed. Finally, the last chapter concludes the main findings of the work and is followed by recommendations for future work.

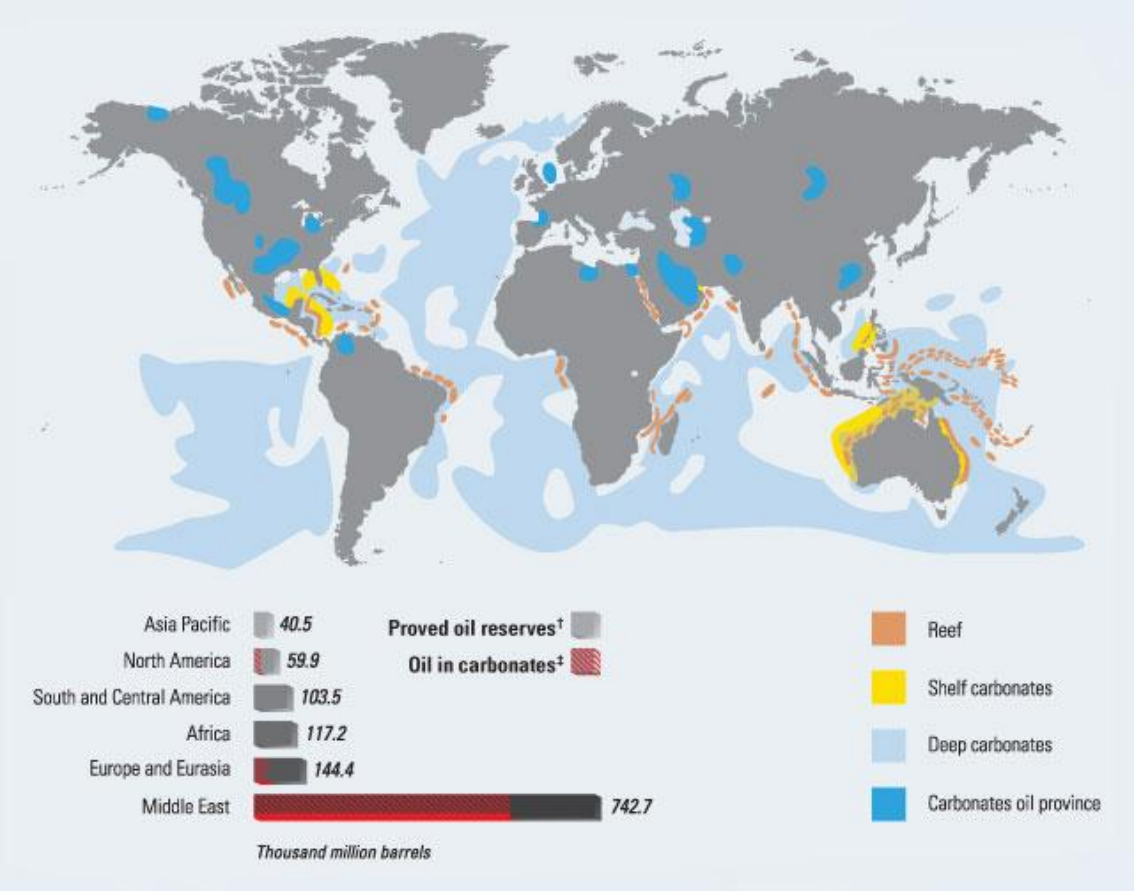


Figure 1.1. World distribution of carbonate reservoirs offer the most significant challenges and opportunities to develop new strategies and technologies (Schlumberger, 2007).

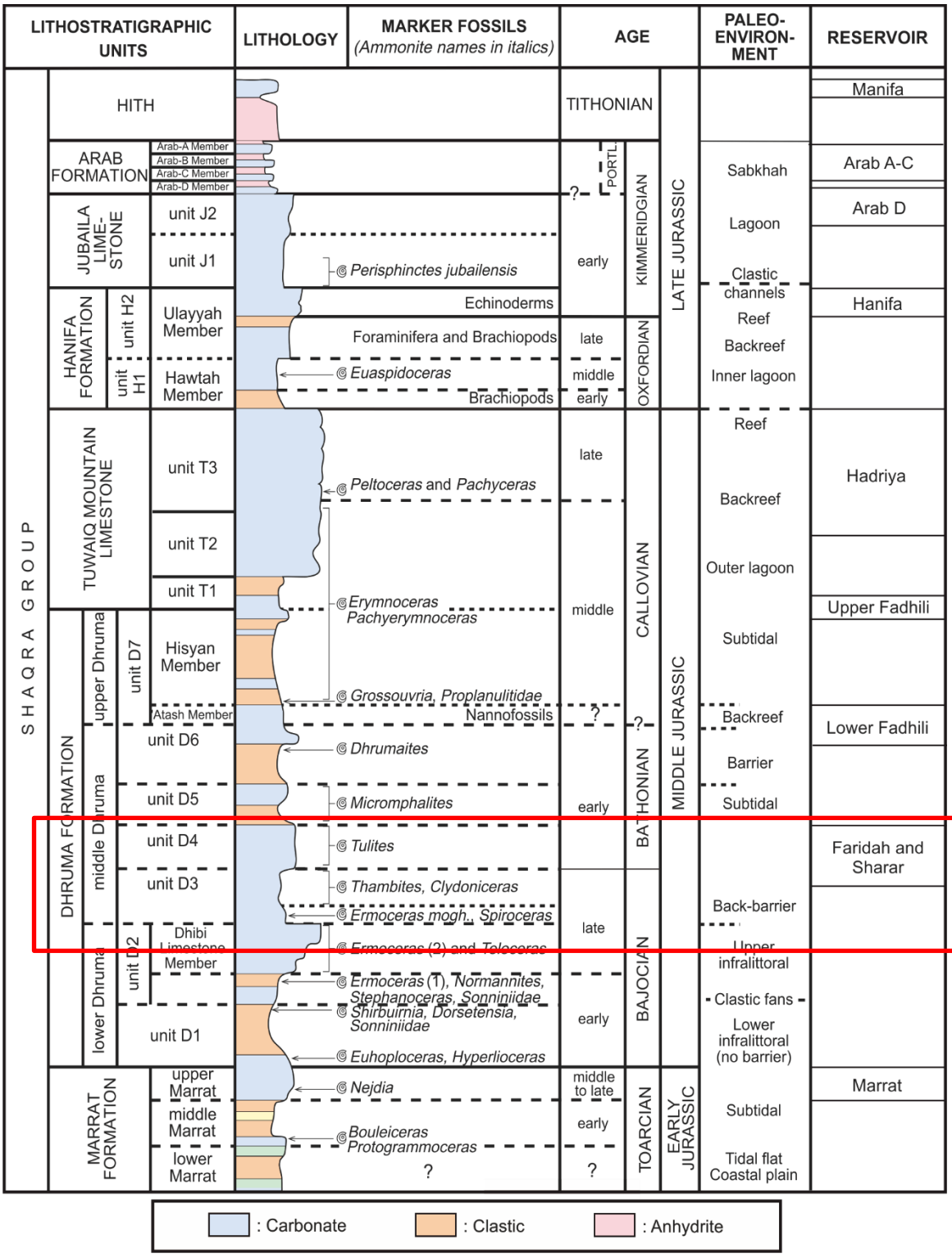


Figure 1.2. Litho- and bio-stratigraphy of the Jurassic Shaqra Group of Saudi Arabia established by the presence of ammonite faunas (modified after Enay et al., 2009). The red rectangle highlights the studied members.

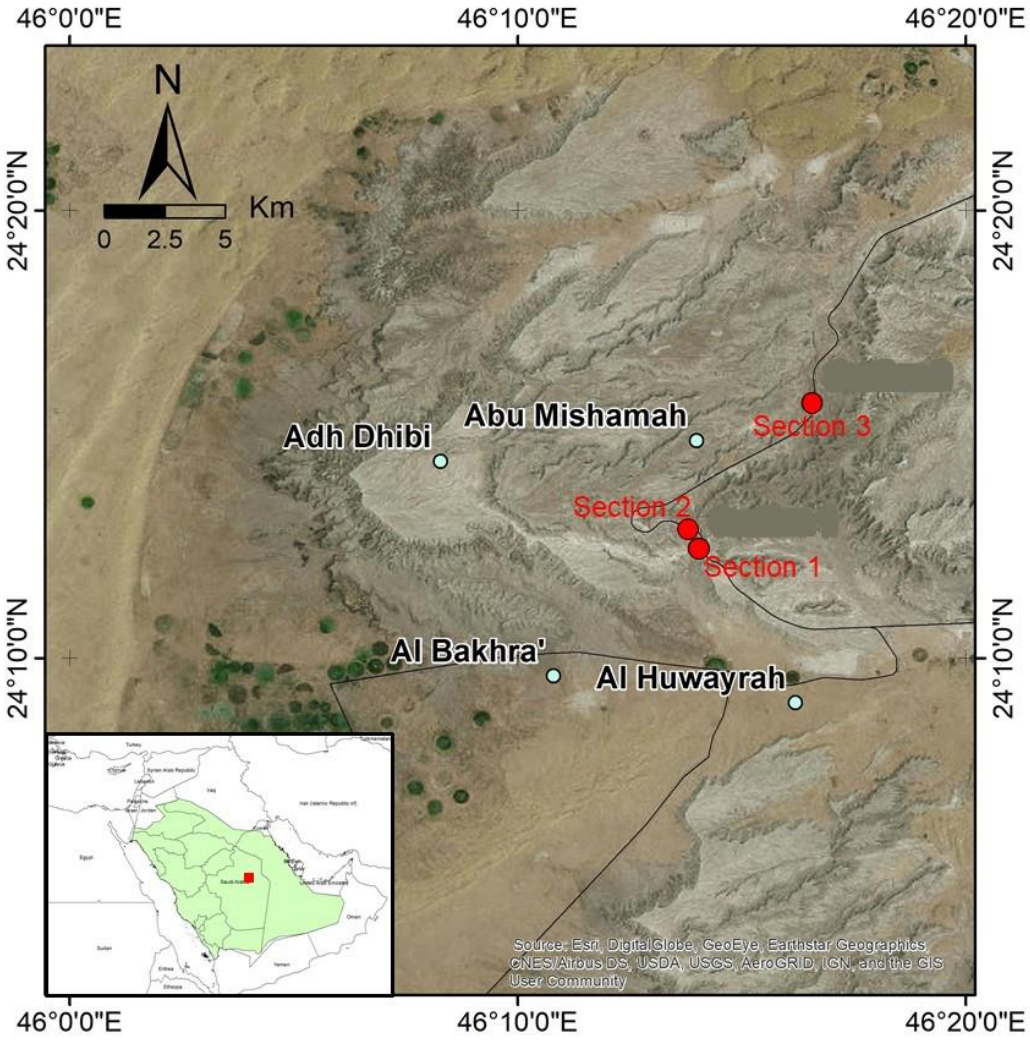


Figure 1.3. The studied outcrops are located in the southwest of Riyadh. The studied sections are easily accessible from Mekkah-Riyadh highway and are close to the Saudi White Cement Factory and Hafirat Nisah village. See Figure 1.5. for the outcrop photomosaic of the studied sections.

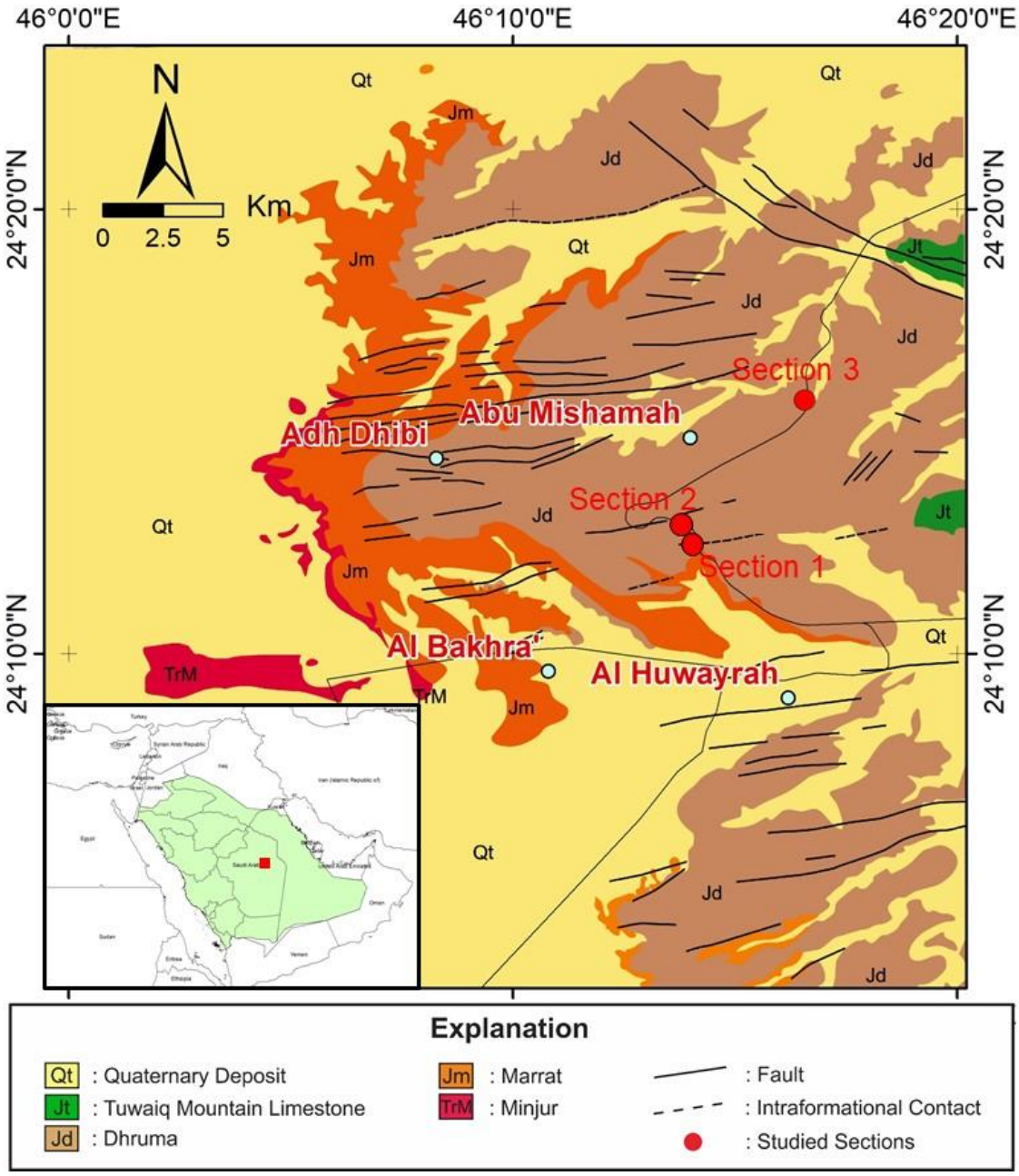


Figure 1.4. Geological map of the location area (modified after Manivit et al., 1985). The Dhruma Formation is represented by light brown color and is bounded unconformably by the Upper Jurassic siliciclastic Marrat Formation (orange color) to the west, conformably overlain by the Middle Jurassic Tuwaiq Mountain Formation (green color) to the east and surrounded by Quaternary deposits.

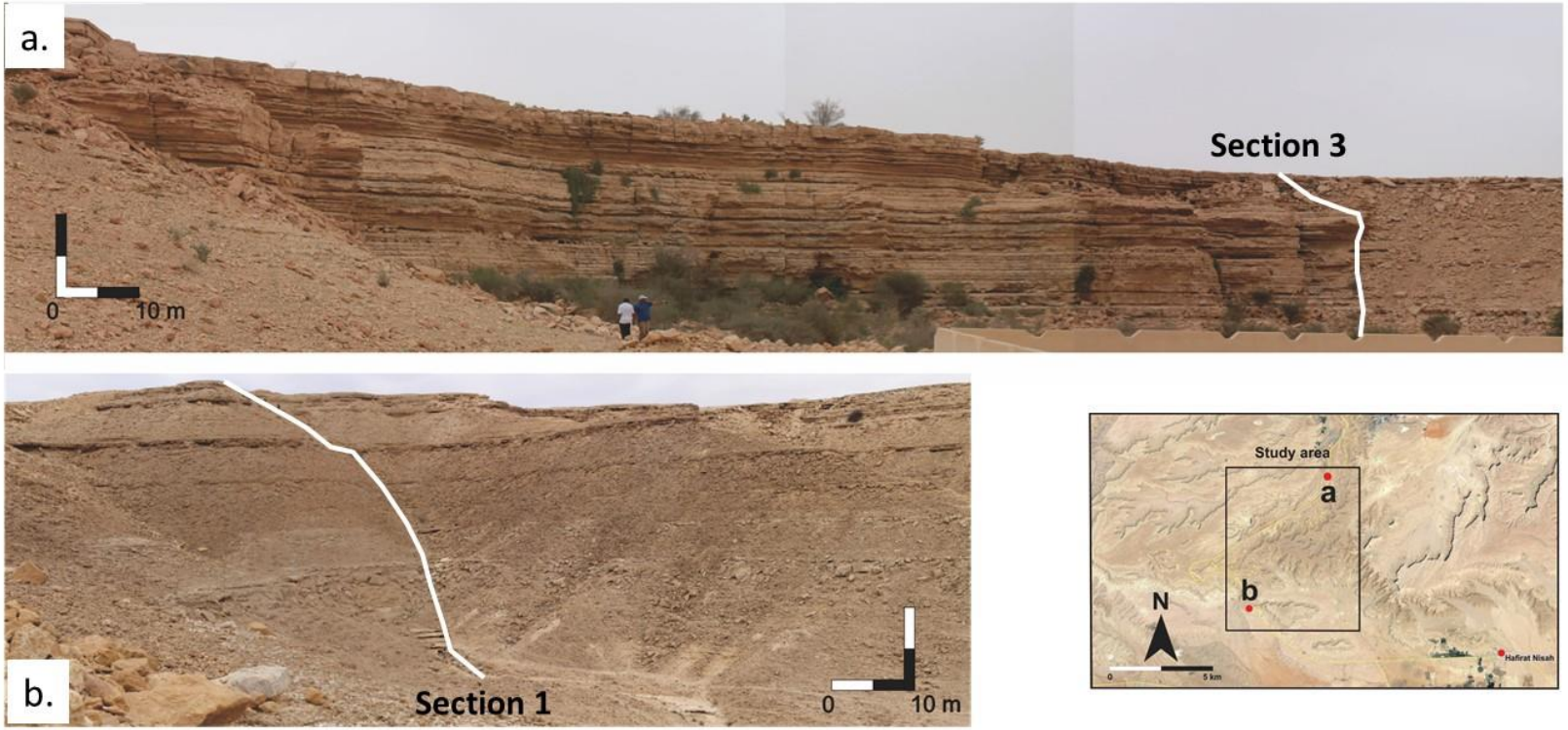


Figure 1.5. a. Section 3 consists predominantly of thick carbonate sequence in which a total of 25 meters represents the D4 Unit of the Dhruma. b. Section 1 of the D2—D3 Units of Dhruma Formation with a thickness of 33 meters. The white lines show the track in which all samples have been collected.

# CHAPTER II

# LITERATURE REVIEW

## 2.1 Introduction

Basement-controlled structures have been affecting the upper sedimentary successions since the Paleozoic (Konert et al., 2001). Therefore, the tectonic regime of the Arabian Plate can be represented as three major directions including the dominant N-S to NNE-SSW structural trend (Arabian Trend), the NE-NNE trend left-lateral strike-slip fault, the NW-SE trend as a response to the Indian Plate movement and the NE-SW trend due to the collision of Arabian-Eurasia Plates and opening of Red Sea (Edgell, 1992; Ziegler, 2001; Stewart, 2017). These directions represent in the present-day motion of the Arabian Plate (Konert et al., 2001; Ziegler, 2001). Thus, most of the Mesozoic carbonate and siliciclastic megasequences throughout the Gulf region were deposited on the basement complex and they host major reservoirs (Alsharhan and Nairn, 1997; Ziegler, 2001; Cantrell et al., 2014; Stewart, 2017).

The Jurassic sequence of Saudi Arabia is well-defined in both surface and subsurface, however, relatively few studies have been conducted on the Lower to Middle Dhruma, hence, it is the focus of this research.

## 2.2 Jurassic Tectonic Evolution of the Arabian Plate

Arabian Plate was located at 5° N to 25° S during the Triassic and drifted northward to the equator due to the Mediterranean rifting during the Early Jurassic (Ziegler, 2001). Moreover, the Arabian Plate maintained its location around the equator until the present-

day. During the Early Permian to Early Jurassic, an epeiric carbonate platform covered a wide area of the Arabian Plate with the major source of terrigenous clastics from the present day Arabian Shield (Murris, 1980). According to Sharland et al. (2001), the tectonostratigraphic framework of the Arabian Plate is subdivided into eleven tectonic megasequences (AP1—AP11) based on a similar structural setting and accommodation spaces which represent major unconformities as defined by Hubbard (1988). The Jurassic period of the Arabian Plate is categorized as the seventh tectonic megasequence (AP7). The AP7 lasted for 33 m.y. and occurred when the Arabian Plate was under extension regime and passive margin during the formation of the Neo-Tethys Ocean. During the Middle Jurassic, the carbonate platform of Arabian Plate was relatively different than the Early Jurassic development of intra-shelf basins which were separated by paleo-highs, namely the Rimthan Arch and Qatar Arch as depicted in Figure 2.1 (Murris, 1980; Ziegler, 2001). The carbonate shelf covered a wide and broad area from the Arabian Shield in the west to the Zagros Fold Belt in the east at a low angle dip (approximately 1°) (Murris, 1980).

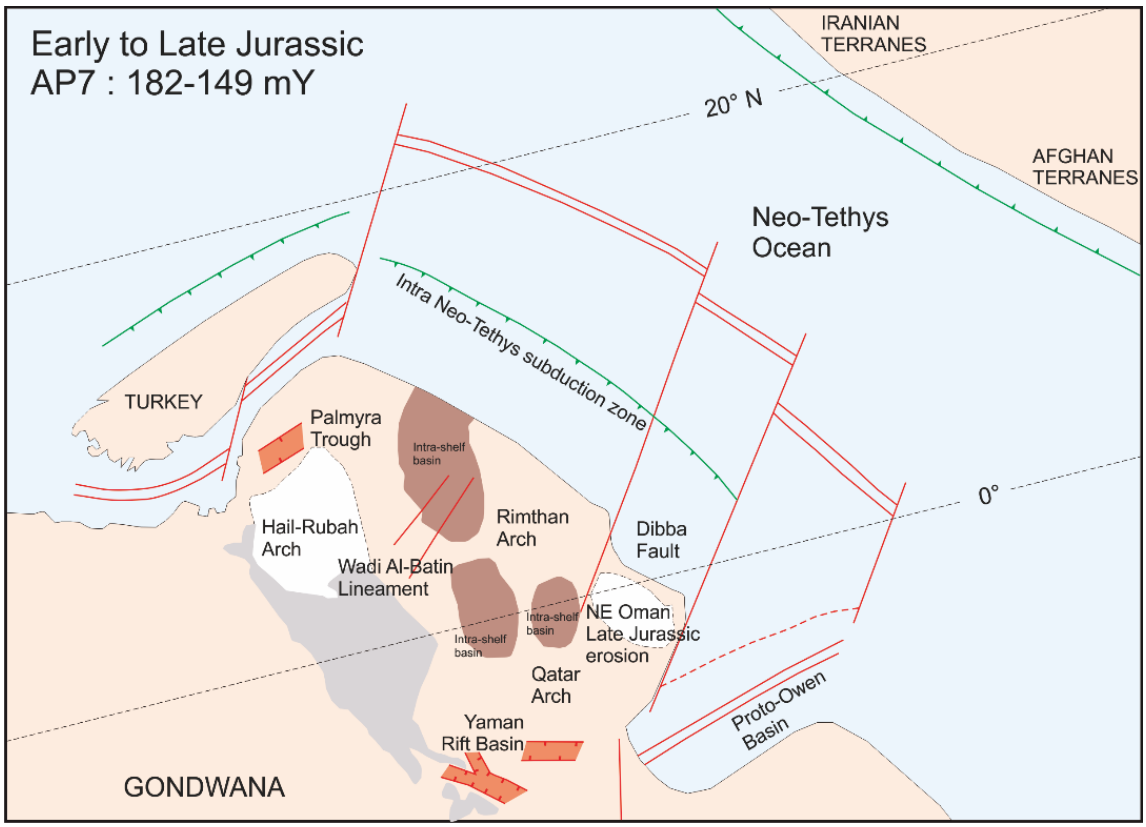


Figure 2.1. The Seventh Arabian Plate (AP7) megasequence lasted during Early to Late Jurassic (182—149 m.y.) (modified after Sharland et al., 2001). Intra-shelf basins were greatly impacted by numerous faults and lineaments such as Dibba fault, Wadi al-Batin lineament trending generally NE-SW because of the early stage of the subduction and the closing of the Neo-Tethys Ocean

The tropical setting (~30°N—15°S) during the Jurassic was ideal for sedimentation and the growth of carbonate throughout the margin of the Arabian Plate. Although the variations in relative sea-level and terrigenous influx from the present-day Arabian Shield were low in the Jurassic, most areas in the north and south of the plate had been developed and covered by clastic deposits (Figure 2.2; Sharland et al., 2001; Ziegler, 2001).

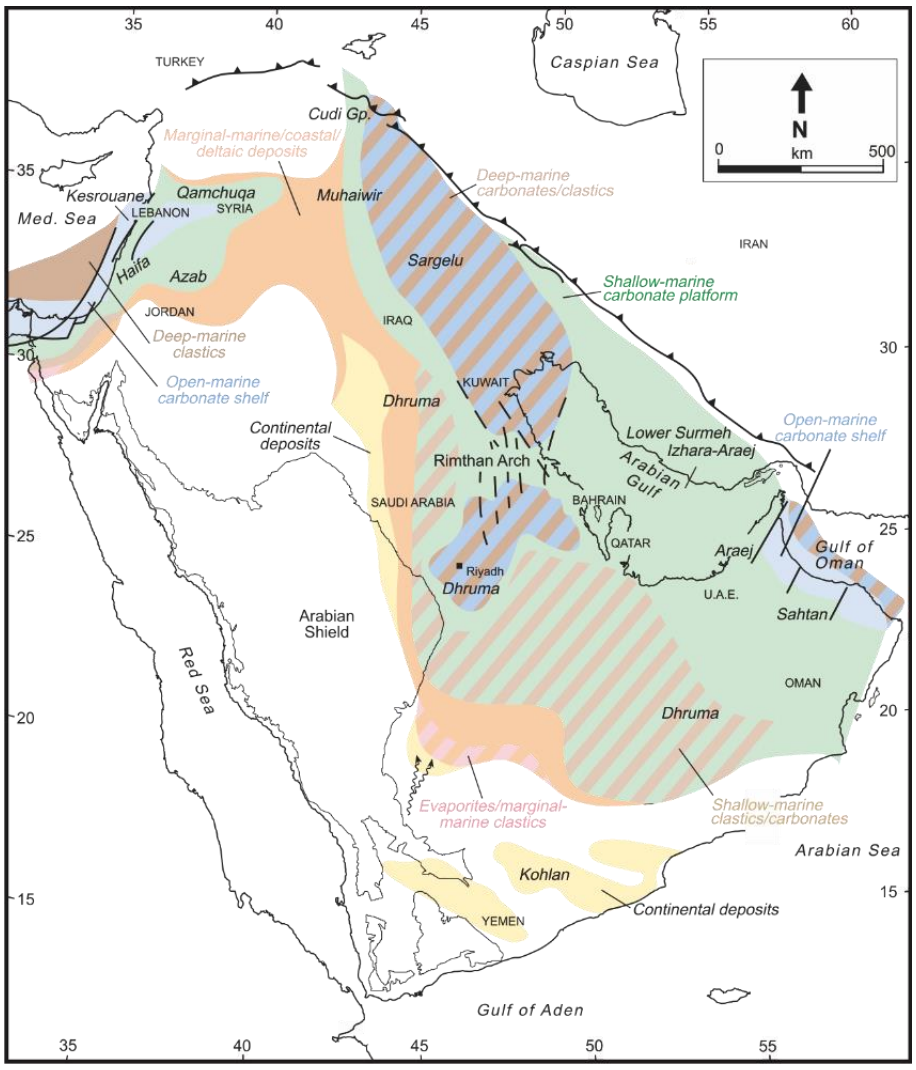


Figure 2.2. Paleoenvironment of the Arabian Plate showing a changing of lithology from marine deposits (carbonate origin) in central Saudi Arabia to deltaic system in southwest Saudi Arabia based on the examination of the biostratigraphic data including brachiopods and ammonites (Enay et al., 2009).

## 2.3 Jurassic Shaqra Group of Saudi Arabia

The Jurassic stratigraphic succession of Saudi Arabia is categorized as a second order cycle while each formation within the Jurassic successions constitutes a third order cycle (Al-Husseini, 1997; Sharland et al., 2001). The lower part of the Shaqra Group started with the deposition of the Marrat Formation which unconformably overlies the Triassic Minjur Formation. The Toarcian Marrat Formation is composed predominantly of

interbedded marine sandstone, claystone and carbonate deposits (Manivit et al., 1985). The Middle Jurassic Dhruma Formation sits unconformably on the Marrat due to short periods of non-deposition (Manivit et al., 1985). It is predominantly comprised of limestone with minor claystone in the central part of the outcrop belt in Saudi Arabia, while the south and north of the outcrop belt are composed of detrital rocks (Figure 2.3; Powers et al., 1966; Manivit et al., 1985; Enay et al., 2009).

Above the Dhruma Formation lie the unconformable beds of the middle to late Callovian age Tuwaiq Mountain Formation. The Tuwaiq Mountain Formation was deposited on a shallow marine lagoon with an abundance of stromatoporoids-bearing carbonates (Powers et al., 1966). The carbonate sequence of the Upper Jurassic commenced with the deposition of the Hanifa Formation which is composed mainly of fine-grained limestone in the basal part and stromatoporoid carbonate facies in the upper part (Powers et al., 1966). This formation is disconformably overlain by the Upper Jurassic Jubaila limestone. The lower part of the Jubaila Formation consists of very fine-grained to sand-sized limestone whereas the upper part composes of silt-sized limestone of subtidal environment (Powers et al., 1966). The Arab Formation is in sedimentary continuity and overlies the lower Kimmeridgian Jubaila Formation. This formation is composed generally of packstone and a very fine-grained limestone intercalated with anhydrite layers (Powers et al., 1966). The upper part of the Shaqra Group is the anhydrite of the Hith Formation covering most of the Arabian Platform (Ziegler, 2001).

## 2.4 Dhruma Formation of Saudi Arabia: Litho-and Bio-stratigraphy

Steineke (1939), who is the pioneer of detailed sedimentological study of the Jurassic sequence, placed the Dhruma as a member of the Tuwaiq Mountain Formation. Bramkamp (1945, in Powers et al, 1966) raised the Dhruma to formation status, and the Tuwaiq Mountain Group to be elevated. In 1952, Steineke and Bramkamp measured the Dhruma in detail and dropped the Tuwaiq as a formation. Steineke (1958) revisited the outcrop and measured both type localities of the Dhruma Formation at Khashm adh Dhibi and Khashm al Mazru'i. Further study of the sedimentology of the Dhruma Formation was carried out by Powers et al. (1966). The authors subdivided the Dhruma into three formations; the Lower, Middle and Upper Dhruma Formations at its type locality. Later, Manivit et al. (1985) measured several sections in Darma' quadrangle and developed the geological map of this quadrangle with the explanatory notes on the sedimentological interpretations and lithology (Figure 2.3).

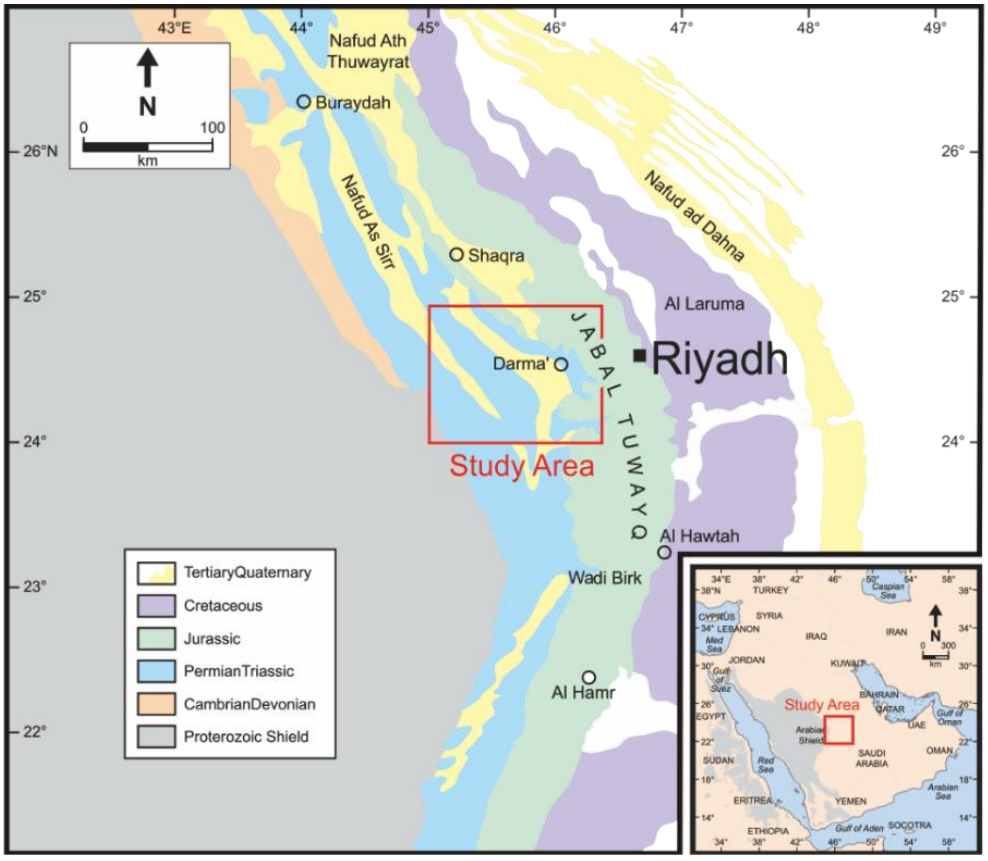


Figure 2.3. Generalized geological map of central Saudi Arabia. The Middle Jurassic Dhruma is unconformably bounded by Permian-Triassic formations and other younger formations. Note that the red square is the location of the study area where the Dhruma Formation crops out at Darma' Quadrangle (modified after Enay et al., 2009).

Dhruma outcrop at Khashm adh Dhibi is about 383 meters (later revised to 447 meters) (Figure 2.4; Powers et al., 1966; Manivit et al., 1985). The base of the formation is placed at the contact between the interbedded shale-limestone of the Lower Dhruma and carbonate of the Upper Marrat Formation. Meanwhile, the upper limit of the formation with the overlying formation is marked by the contact between the Upper Dhruma interbedded clay-shale beds and the basal limestone of the Tuwaiq Mountain Formation (Steineke et al., 1958).

The Lower Dhruma Formation is composed of two members, Balum (D1) and Dhibi Limestone (D2) (Powers et al., 1966; Manivit et al., 1985; Al-Husseini, 1997). At

Khashm adh Dhibi, the Lower Dhruma has a thickness of 127 meters that gradually thins to the north of the quadrangle. It is composed mainly of several thin layers of sand-sized limestone and fine-grained sandstone in the basal part and gradually changes into packstone of the Dhibi limestone (Arkell et al., 1952; Steineke et al., 1958). At Khashm adh Dhibi, the thickness of the D2 Unit is around 86 meters but the unit is almost invisible to be traced northward (Manivit et al., 1985). The lower part of D2 Unit is characterized by green marl and is overlain by a 35-meter of massive and burrowed limestone passing to fine-grained bioclastic. *Nautiloculina oolithica* at the base of the limestone, *Haurania deserta* and *Trocholina* sp.1 at the top of the D2 Unit have been reported in north and central of the Darma' quadrangle (Manivit et al., 1985).

The Middle Dhruma Formation is a 170-meters thick unit of carbonate rocks and is comprised of three formal units, the Jufayr (D3), Uwaynid (D4), Barrah (D5), and Mishraq (D6) Members (Powers et al., 1966; Manivit et al., 1985; Al-Husseini, 1997). They are comprised mainly of packstone with several thin layers of marl, shale, and oolite (Steineke et al., 1958). The D3 Unit is dominantly made of limestone with abundant bivalves and peloids, rare ooids and intraclasts. Abundant benthic foraminifera including *Pfenderina* sp. commonly associated with *Nautiloculina* sp., *Redmondoides* sp., and *Globivalvulina* sp. were found in the bottommost part. The D4 Unit is limestone rich in peloids, ooids, mollusks fragments interbedded with peloidal mud to wackestone. The Middle Dhruma has low preservation of microfauna as reported by Manivit et al. (1985). However, *Trocholina* sp.1 was reported as an abundant benthic foraminifera in the central and south of the Darma' quadrangle (Manivit et al., 1985).

Atash and Hisyan Members of the Upper Dhruma Formation reaches 86 meters thick at Khashm adh Dhibi and are composed mainly of limestone interbedded with shale (Steineke et al., 1958). Although only a few ammonites have been found within the Atash Member, some foraminifera (i.e., *Nautiloculina oolithica*, *Trocholina gr. elongata, Steinekenella crusei, Praekurnubia crusei, Pfenderina gracilis, Trocholina* sp.) are present in the north and south of the Darma' quadrangle (Manivit et al., 1985). In contrast, Hisyan Member has various ammonites at different levels and abundances of *Nautiloculina oolithica* and *Trocholina gr. elongata* (Manivit et al., 1985). Lately, Atash and Hisyan Members (D7 Unit) of the Upper Dhruma are considered as members of the Tuwaiq Mountain Formation due to genetic relationship between mud-dominated characteristics of the D7 Unit and the base of the Tuwaiq Mountain Formation (Hughes et al., 2009).

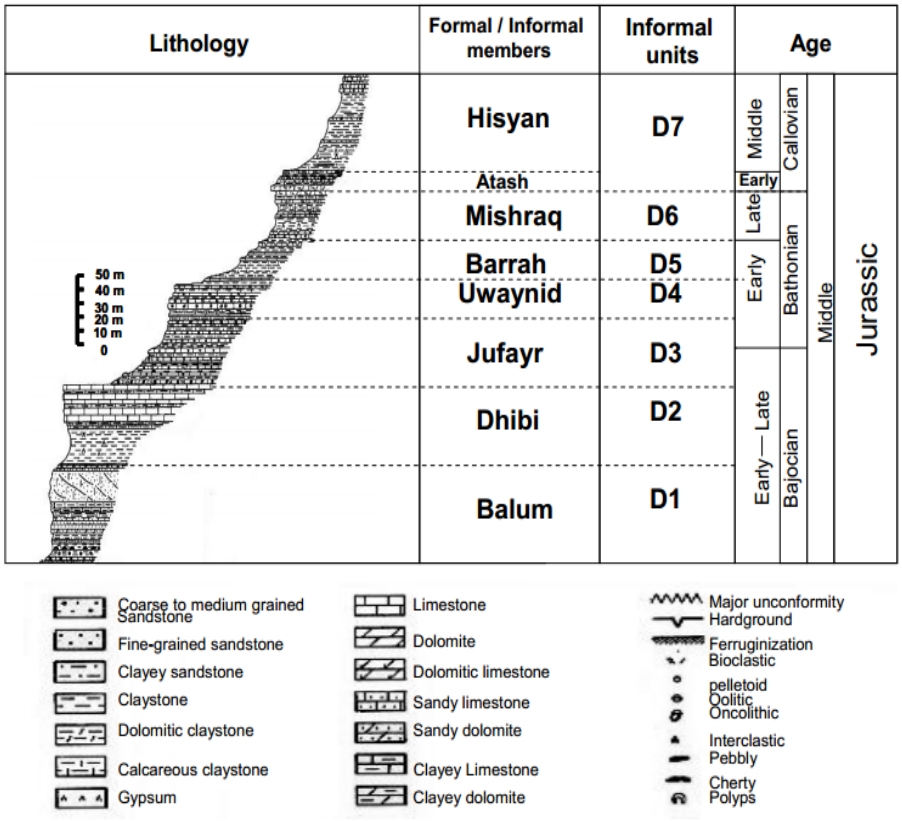


Figure 2.4. Lithostratigraphy of the Dhruma Formation in the outcrop belt of central Saudi Arabia. The 448-m gradually passed from sandy limestone of Balum Member to clayey limestone of Hisyan Member (adapted from Vaslet et al., 1983).

Steineke et al. (1958) established a stratigraphic sequence along the Arabian Plate during Paleozoic and Mesozoic. Based on a sequence stratigraphic study of global eustatic sea-level, Le Nindre (1990) and Manivit (1985) also developed sequence stratigraphy framework of the Jurassic sequence in Saudi Arabia. A recent study by Al-Husseini (1997) revised the sequence stratigraphic framework and correlated the sequences along Arabian Platform. The foundation of the sequence stratigraphic framework of the Arabian Plate was developed by Sharland et al. (2001) in both outcrop and subsurface studies. The author redefined its type section with respect to sequence stratigraphic surfaces (i.e., sequence boundaries and maximum flooding surfaces).

Enay (2009) found a discontinuity (hiatus) between D5 and D6 Units of Dhruma Formation due to relative sea-level fall and later proposed the Wadi Ad Dawasir “delta” as a new member of the Dhruma Formation. Al-Husseini (2009) defined Dhruma Formation as three distinct third-order chrono-sequences, from older to younger: The Lower Dhruma Sequence A consists of the Balum (D1 Unit and lower part of D2 Unit) and Dhibi Limestone (upper part of D2 Unit) sequences with MFS J20 marked on the top of Balum Member, Dhruma Sequence-B is comprised of the Uwaynid (D3 Unit), the Barrah (D4 Unit), the Mishraq (D5 Unit), and the Wadi Ad Dawasir ”delta” Members. The MFS J30 is present at the lowermost portion of the Mishraq Member and is represented by planktonic foraminifera of *Globuligerina* sp., and *Conoglobigerina* sp. (Kaminski et al., 2018). Dhruma Sequence-A consists of the informal D6 Unit, Atash. The Mishan Member of the D7 Unit contains the MFS J40 on the top of the Mishan.

The earliest biostratigraphic research on the Jurassic sequence in the Middle East was based on micropaleontological data using ammonites (Arkell et al., 1952), gastropods (Fischer et al., 2001), calcareous algae (Hughes et al., 2009). On the basis of fossil assemblages, the Dhruma Formation was dated to Early Bajocian-Middle Callovian age (Arkell et al., 1952; Hughes, 2004). The microfauna is not only useful for predicting its age, but also leads to the depositional environment in which they had lived. For instance, gastropods, *Kurnubia* sp., *Trocholina* spp., and *Nautiloculina oolithica* were deposited on a lagoon environment whereas *Lenticulina* sp. and sponge spicules were mostly found in the basinal areas as shown in Figure 2.5. Al-Dhubaib (2010) established the depositional environments of the Jurassic formations using both surface (outcrop) and subsurface data. The distribution of biofacies of outcrop (along Mekkah-Riyadh highway) can be traced to

the subsurface well (i.e., Khurais Complex, including Fadhili and Berri fields) and regional correlation across the Gulf countries can be developed. The author interpreted seven biofacies that have been deposited in an environment varying from lagoon to open marine setting. The deep to shallow lagoon is associated with *Redmondoides lugeoni, Siphovalvulina* sp.1, *Kurnubia palastinienses* and *Thaumatoporella parvovesiculifera* calcareous algae. Adjacent to this, shoal complex is composed mainly of milliloid foraminifera, calcareous algae of *Salpingoporella annulate* and the branched stromatoporoid *Cladocoropsis mirabilis*. The open marine is characterized by abundant *Lenticulina* sp., *Nodosaria* sp., the pelagic bivalve *Bositra buchi* and sponge spicules. The interpretation of these biofacies is consistent with the proposed model by Hughes (2004). Recently, Malik (2016) studied the muddy interval of the D4-D5 Units of the Dhruma Formation to establish and refine sequence stratigraphy based on micro-paleontological data.

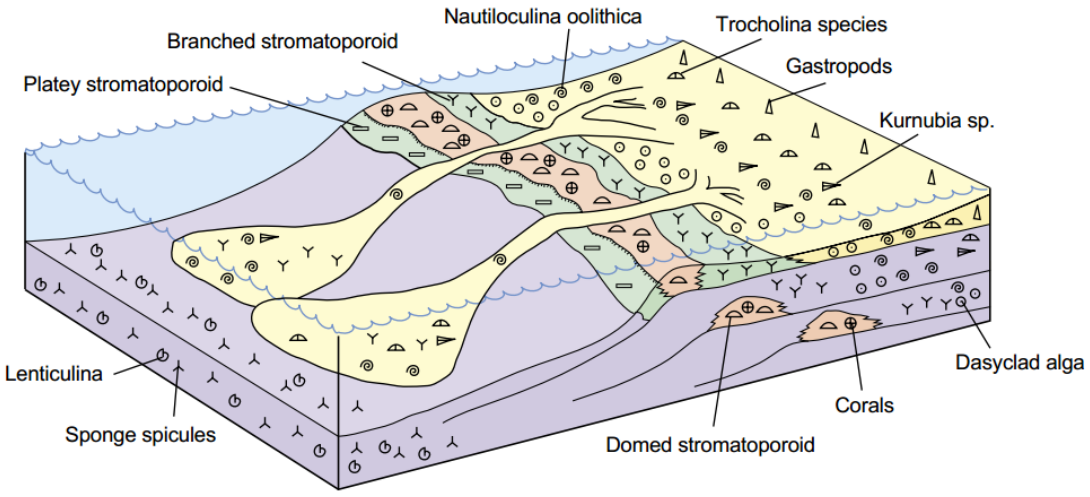


Figure 2.5. A diagrammatic cartoon showing a distribution of some bioclasts during the Middle to Late Jurassic. These biocomponents are a good indicator of depositional environment as they deposited and lived in-situ (Hughes, 2004).

## 2.5 Carbonate Ramp Microfacies

Carbonate ramp is an alternative model of carbonate platform. The term ramp is briefly defined as a sloping surface connecting continent and ocean without any pronounced break in slope that firstly introduced by Ahr (1967) (Figure 2.6a; Ahr, 1967). The author presented a new model of carbonate platform because shelf-slope break of carbonate platform is as far as 100 fathoms (~182.88 meters) as defined by Mill (1988). However, the shelf-slope break of a carbonate ramp can reach ten up to hundred kilometers (Wilson, 1974, 1975; James and Jones, 2015). Another factor in which the ramp may somewhat demonstrate diverse characteristic than that of rimmed shelves is the continuity of reef trends acting as a barrier, whereas in the case of carbonate ramp the reef is typically discrete and separate (Ahr, 1967; Read, 1982).

As mentioned by Read (1982), a carbonate ramp can be further subdivided based on slope break in the outer ramp as distally steepened and homoclinal ramps. The first refers to a shelf break (few to tens kilometers seaward) with slumps and turbidites deposits along the steepened slope (Figure 2.6c). On the other hand, the latter demonstrates relatively stable slopes without a shelf break, lack of gravity flows and slumps deposits (Figure 2.6b).

Burchette and Wright (1992) established a deep review on carbonate ramp and further subdivided it into several zones into inner-, mid-, and outer-ramp and concluded that it mostly occurs in passive margin, foreland basin, and cratonic-interior basin where the tectonic activity and the slope gradient are less.

Microfacies study that has been established by Wilson (1975) and Flugel (1979), and later revised by Flugel (2010), found the importance of micro-scale analysis integrating paleontological, sedimentological and geochemical approaches to examine carbonate rocks.

Wilson (1975) developed a standard for assessing a carbonate platform on the basis of the pattern recognition in the shelf-margin over textural and microfacies analysis (for further explanation of the classification, see Figure 2.7). The subject of the classification is the shelf-margin in both ramp and shelf settings including lime-mud accumulations on the slope of shelf-margin, reef setting on carbonate ramps, reef on carbonate buildup. To reach the maximum production and accumulation, reef of carbonate ramp must be restricted from terrigenous clastic influx and remain in the photic zone represented in the middle-ramp, thus the nearshore and the basin are the zone of minimum carbonate production. The author also presented several factors for assessing the water depth using various zone limits of algae. Stromatolites and calcareous algae are frequent in intertidal with a depth range of 10-15 ft and high salinity can be attributed to the most suitable living environment of dasycladaceae green algae. The occurrences of red algae vary from shallow subtidal to a depth of 800 ft. in warm water setting (tropic, normal marine water), while abundant lime mud in reef setting suggests below wave base environment.

El-Sorogy et al. (2017) examined the microfacies, depositional environment, and diagenetic processes of Dhruma Formation at Khashm adh Dhibi, Riyadh, central Saudi Arabia. They described and identified nine microfacies which range from deep shelf to organic buildup on platform margins.

Schlaich and Aigner (2017) conducted a study on Dhruma Formation in Oman integrating both outcrops at Jabal Madar, northern slope of Oman Mountain and also subsurface wells to establish its microfacies. The study described 12 lithofacies within 3 zones including low-energy in both distal and proximal also high-energy in between. These microfacies were further grouped into four lithofacies association and were ascribed to peritidal and lagoonal of low-energy zone, moderate-energy zone, and high-energy zone. The first lithofacies association is composed mainly of carbonate with micritic texture ranging from mudrocks, stromatolite and microbial laminites of relatively low-moderate energy, to high energy cross-bedded wacke-packstones with some scour fills present. The low-energy lagoon is predominantly of dolomitic limestone (mudstone) with abundant bioturbation of *Thalassinoides* indicating a marine environment. The bioturbation is often filled by echinoderms, bivalves, gastropods, peloids, and coated grains. Lagoon to shoal-margin of the moderate-energy zone is characterized by wacke-packstone containing bivalves, broken shells, some gastropods and brachiopods, peloids and few oncoids. The latter, high-energy zone, is composed of low-angle cross-bedding peloidal and oolitic pack-to grainstones with highly cemented that lack of porosity.

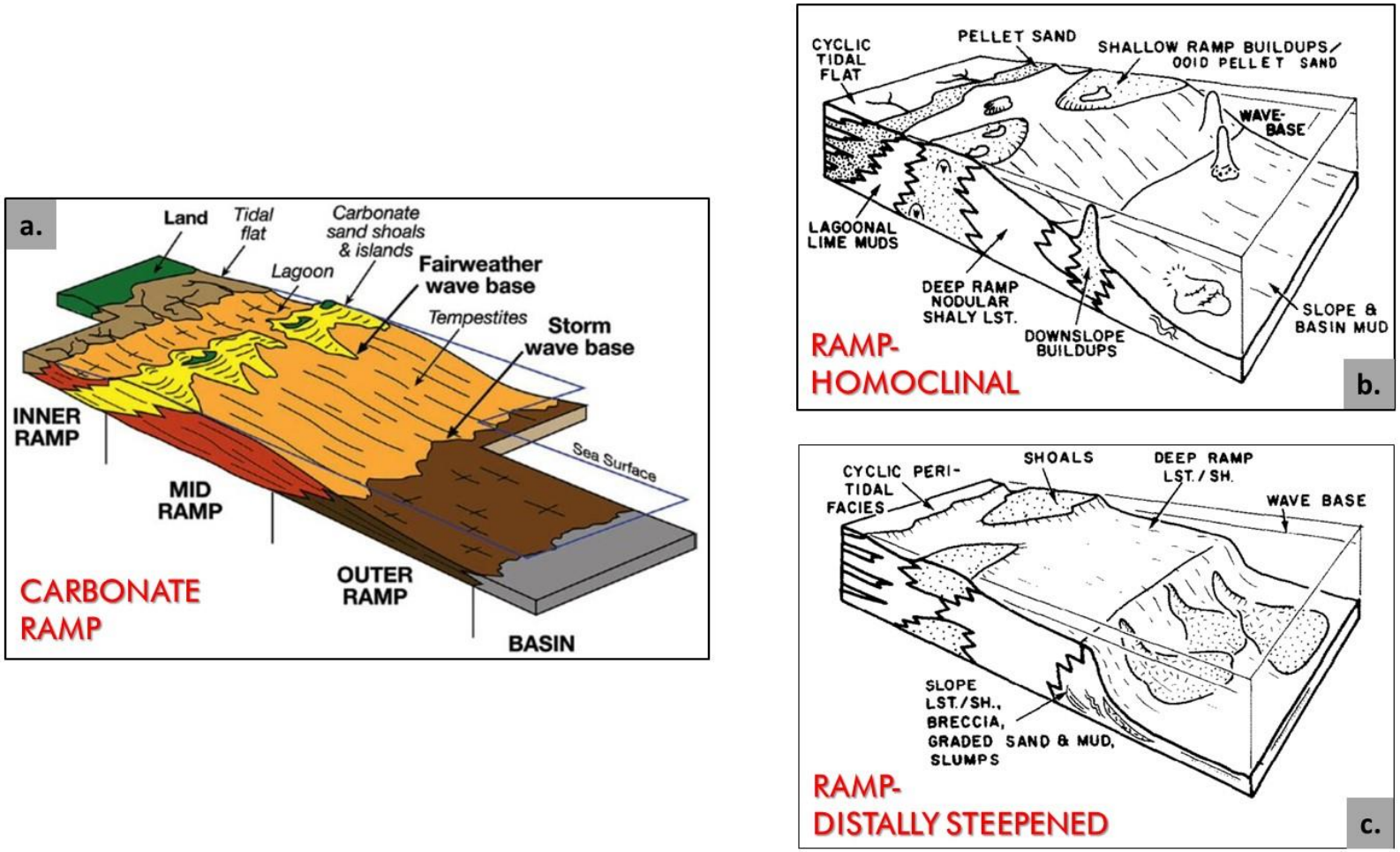


Figure 2.6. a. A diagram of a typical carbonate ramp including inner, middle, and outer ramp, also basinal areas (Burchette and Wright, 1992), A cartoon of b. homoclinal ramp and c. distally steepened ramp models (Read, 1982).

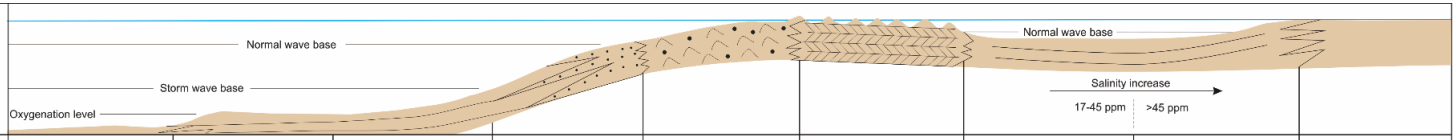


| Facies Number | 1 | 2 | 3 | 4 | 5 | 6 | 7 | 8 | 9 |
|---|---|---|---|---|---|---|---|---|---|
| **Facies** | *Basin*<br>a. Fine clastics<br>b. Carbonates<br>c. Evaporites | *Open shelf*<br>(open marine neritic)<br>a. Carbonates<br>b. Shale | *Toe to slope carbonates* | *Foreslope*<br>a. Bedded fine grain sediments with slumps<br>b. Foreset debris and lime sands<br>c. Lime mud masses | *Organic reef*<br>a. Boundstone mass<br>b. Crust on accumulation of organic debris and lime mud; bindstone<br>c. Bafflestone | *Sand on edge of platform*<br>a. Shoal lime sand<br>b. Sand with dune sands | *Open platform* (normal marine, limited faunas)<br>a. Lime sand bodies<br>b. Wackstone-mudstone areas, bioherms<br>c. Areas of clastics | *Restricted platform*<br>a. Bioclasts wackestone, lagoons and bays<br>b. Litho-bioclastic sands in tidal channel<br>c. Lime mud-tide flats<br>d. Fine clastic unit | *Platform evaporites*<br>a. Nodular anhydrite and dolomite on salt flats<br>b. Laminated evaporite in ponds |
| **Lithology** | Dark shale or silt, thin limestones (starved basin); evaporite fill with salt | Very fossiliferous limestone interbedded woth marls; well segregated beds | Fine-grain limestone; cherty in some cases | Variable, depending on water energy upslope; sedimentary breccias and lime sands | Massive limestone-dolomite | Oolitic lime sand or dolomite | Variable carbonates and clastics | Generally dolomite and dolomitic limestone | Irregularly laminated dolomite and anhydrite may grade to red beds |
| **Color** | Dark brown, black, red | Gray, green, red, brown | Dark to light | Dark to light | Light | Light | Dark to light | Light | Red, yellow, brown |
| **Grain type and depositional texture** | Lime mudstone; fine calcisiltles | Bioclastic and whole fossil wackestones; some calcisiltles | Mostly lime mudstone with some calcisiltles | Lime silt and bioclastic wackestone-packstone; lithoclasts of varying sizes | Boundstones and pockets of grainstone; packstone | Grainstone well sorted; rounded | Great varity of textures; grainstone to mudstone | Clotted, pelleted mudstone and grainstone; laminated mudstone; coarse litho-clastic wackestone in channels | |
| **Bedding and sedimentary structures** | Very even mm lamination; rhytmic bedding; ripple cross lamination | Thoroughly burrowed; thin to medium; wavy to nodular beds; bedding surfaces show diastems | Lamination may be minor; often massive beds; lenses of gradded sediment; lithoclastsand exotic blocks rhytmic beds | Slumps in soft sediments; foreset bedding; slope bioherms; exotic blocks | Massive organic structure or open framework with roofed cavities; Lamination contrary to gravity | Medium to large scale cross bedding; festooms common | Burrowing trace very prominent | Birdseye, stromatolites, mm lamination, gradded bedding, dolomite crusts on flats. Cross-bedded sand on channels | Anhydrite after gypsum; nodular, chickenwire, and blades; irregular lamination; carbonate caliche |
| **Terrigeneous clastics admixed or interbedded** | Quartz silt and shale; fine grain siltstone; cherty | Quartz silt, siltstone, and shale; well segregate beds | Some shales, silt, and fine grained siltstone | Some shales, silt, and fine grained siltstone | None | Only some quartz sand admixed | Clastics and carbonates in well segregated beds | Clastics and carbonates in well segregated beds | Windblow, land derived admixtures; clastics may be important units |
| **Biota** | Exclusively nektonic-pelagic fauna preserved in local abundance on bedding planes | Very diverse shelly fauna preserving both infauna and epifauna | Bioclastic detritus derived principally from upslope | Colonies of whole fossils organisms and bioclastic debris | Major frame building colonies with ramose forms in pockets; in situ communities dwelling in certain niches | Worn and abraided coquinas of forms living at or on slope; few indigeneous organisms | Open marine fauna lacking (e.g. echinoderms, cephalopods, brachiopods); mollusca, sponges, forams, algae abundant; patch reef present | Very limited fauna, mainly gastropods, algae, certain foraminifera (e.g. miliolids) and ostracods | Almost no indigeneous fauna, except for stromatolitic algae |

Figure 2.7. A schematic model of depositional facies across carbonate-shelf margins (modified after Wilson, 1975).

# CHAPTER III

# METHODOLOGY

The research aims mainly at examining the carbonate microfacies of the Dhruma Formation. There are essential criteria in microfacies that can be diagnosed in micro-scale. However, outcrop and sedimentological study are key to enhance the understanding of facies associations in this area. Complementary sample collection during fieldwork and sample analyses using a stereo microscope, and scanning electron microscopy (SEM) are the two primary methods that are relevant to examine carbonate microfacies (Flugel, 2010). The integration of these techniques is presented in a workflow in Figure 3.1.

## 3.1 Field Work

Field investigation began with a reconnaissance fieldwork to select suitable outcrops which represent the studied members. The outcrops selection was based on several factors, such as the accessibility to the location and the vertical-lateral continuity of each member in the study area. During fieldwork, detailed sedimentological description of each bed was performed and samples were collected from each representative bed to obtain high-resolution stratigraphic sequence. The samples were collected for every bed in the designated outcrops. For example, a bed of approximately 1 meters, the samples were taken from 3 distinctive parts of the bed (lower, middle and upper parts of the bed). The variation in sedimentary structures, grain size, color, and other key features were also photographically documented and described. Additionally, a detailed sedimentological

analysis is essential to recognize vertical and lateral variations in the studied area, and thus to construct the stratigraphic log of the measured sections.

The first outcrop (the Wadi outcrop section) attains a thickness of 33.56 meters in which over 50 samples had collected. The road-cut outcrop (Section 2) above the Wadi outcrop (Section 1), which likely represents the lower part of the D4 Unit, has a thickness of 7.43 meters and nearly 20 samples were collected. A 24.87-m thick outcrop (Section 3) located about 5 km from the first outcrop was also logged and sampled. A total of 41 samples were collected from this section.

## 3.2 Laboratory Work

Different techniques were employed to describe and understand the characteristic of the samples. A total of 110 carbonate samples from both localities were collected. All measurements have been prepared and measured in King Fahd University of Petroleum and Minerals.

All samples were slabbed, etched with 10% hydrochloric acid and described using an Olympus stereomicroscope model SZX7 (Figure 3.2a) at Center of Integrative Petroleum Research (CIPR) in King Fahd University of Petroleum and Minerals (KFUPM). This was used to identify the geological features such as grain types, sedimentary structure, and textures.

One-cubic centimeter chip of each of some selected samples was coated with a thin layer of gold to enhance conductivity and scanned using a JEOL 5900 LV-Oxford X-MaxN scanning electron microscope facility at the Research Institute of KFUPM to obtain their

micro-scale mineralogical composition, cement, micropore (less than 4 microns) and any inherent micro structures.

Small veneer trims of bulk samples and/ or trimmed plug ends were impregnated with blue epoxy and then polished for preparing the thin section. Half part of each thin section was stained with Alizarin Red-S to distinguish various minerals composition of the sample (stained calcite showed red to pink color while dolomite remains unstained, Dickson, 1965). The preparation and analysis of the thin sections were carried out at CIPR in thin section sample preparation laboratory. Visual estimation of the quantitative abundances of mineralogy, constituents, pore and cement types were performed using polarized Olympus microscope model BX51 with an attached Olympus DP71 camera to capture the photomicrographs of the samples (Figure 3.2b). A modified Dunham (1962) carbonate rocks classification scheme was used to define the microfacies. Pore types classification by Choquette and Pray (1970) has been used to describe the pore types under the thin sections. The detailed explanation about these two will be discussed further in the subsequent chapters.

Approximately 3 to 5 grams of powdered bulk samples were prepared and analyzed to obtain bulk mineralogical phases in each sample using a Rigaku Ultima IV X-Ray Diffractometer at Center of Engineering Research-KFUPM (Figure 3.2c). The diffractometer was operated at 2θ from 2° to 70° to determine the crystallinity of a compound. This analysis focused on identifying major carbonate minerals, such as calcite, aragonite, and dolomite. All peak positions were processed using the database in the Rigaku PDXL software to quantify the proportion of the minerals in each sample.

Porosity and permeability a part of routine core analysis, are essential measurements for understanding the reservoir quality of a sample. One-inch core plugs had been prepared for 60 samples at CIPR-RI, KFUPM. The criteria to select the samples were mainly based on two factors including rigidity of sample and sample size. Most core plugs were taken in the vertical direction, though few samples were plugged in both directions. The AP-608 Automated Permeameter-Porosimeter by Coretest Systems was operated at confining pressure using helium gas to test the samples (Figure 3.2d). After 10 to 20 minutes of measurement time, the AP-608 automatically generated both porosity and permeability values at 500psi confining pressure.

## 3.3 Microfacies Analysis

Microfacies analysis is based on detailed petrographic description of the samples under both hand specimens and thin-section. One of the quantitative methods which are widely used for accessing the microfacies is grain counting. To address the quantitative microfacies analysis, the visual estimation chart developed by Terry and Chilingar (1955) has been utilized to estimate the percentage of grains, matrix, cement, and visual pores in the samples. The naming scheme of each microfacies has been achieved by determining texture and adding the most abundant allochems as modifiers. Where present, sedimentary structures were added to significantly improve the value of naming of the microfacies. An accurate description and analysis of the microfacies through quantitative approach is necessary for developing its depositional environment.

The most widely used classification scheme for carbonate rocks is the Dunham classification (1962) that have been utilized herein to define carbonate rocks in both hand

specimen and thin section. The scheme was mainly based on the texture and supporting fabric which considers depositional energy (Dunham, 1962). The mud-supported facies or mudstone is defined as a facies which has abundant micrite (any allochems with a size between a range of >30 μm—2 mm). If mud concentration is more than 85% and less than 15% of large grains (>2 mm), can be referred to as wackestone. On the other hand, packstone is a grain-supported texture containing <15% mud (any particle with the size of 4—30 μm) and 10% of large grains (>2 mm) (Dunham, 1962). Another grain-supported facies known as grainstone is described as a facies with abundant grains and lack of micrite. In addition, if the original fabric cannot be determined and has been obliterated by replacement or recrystallization, then the termed of crystalline limestone or dolomitic limestone (predominantly of dolomite rhombs) will be applied. For further explanation of this classification, refer to Figure 3.3.

Furthermore, a classification by Choquette and Pray (1970) is used for describing the carbonate pore type. The classification is based on the pore space between or within grains, crystal and other physical structures of the rock (i.e., grain dissolution) as depicted in Figure 3.4. This classification has been useful for porosity evolution studies and to some extents, important for exploration (Lonoy, 2006). Generally, porosity of the carbonate rocks has been largely impacted by diagenetic processes (secondary porosity).

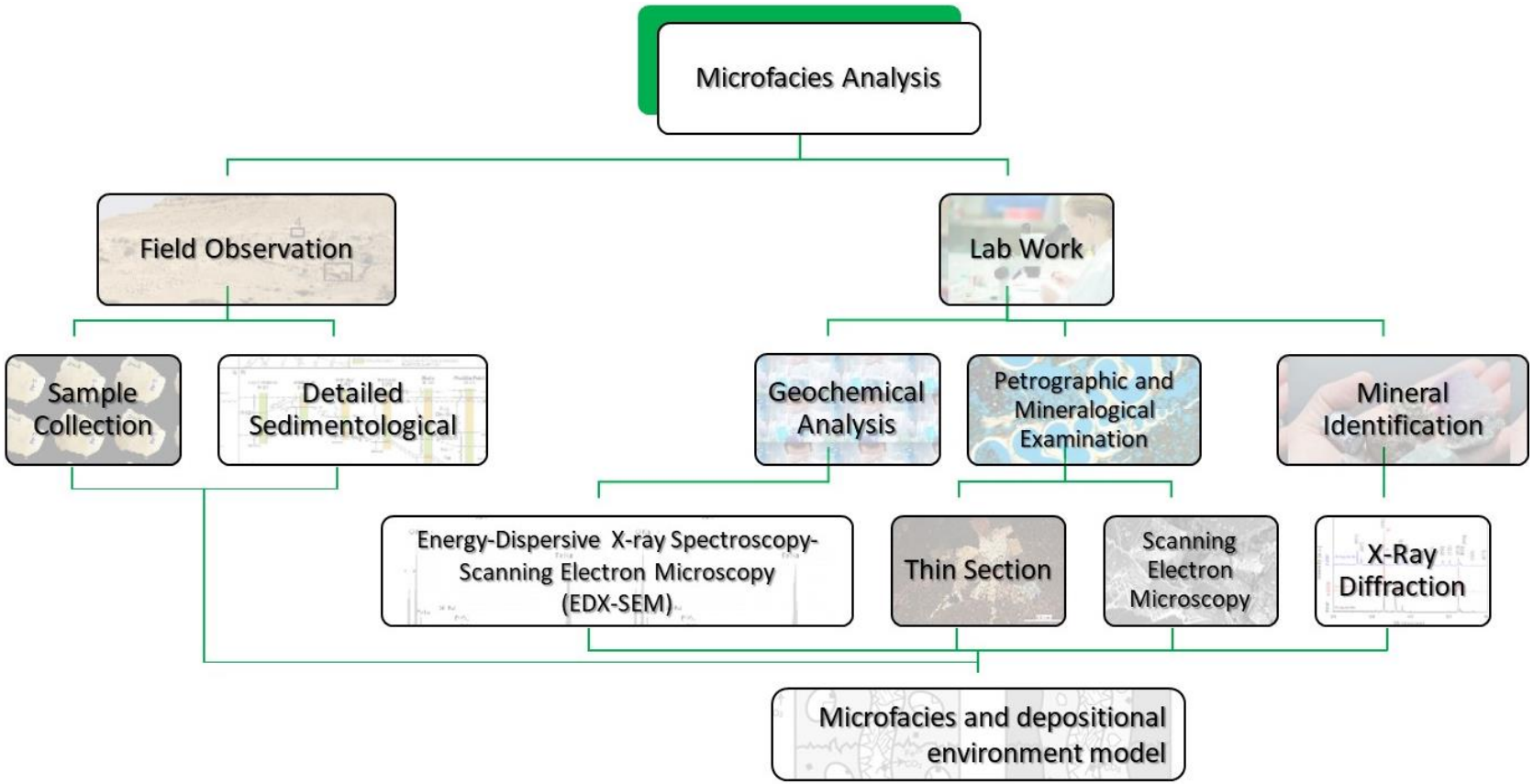


Figure 3.1. Schematic workflow of the study that is based on the integration of field observation and lab work to construct the depositional environmental model.

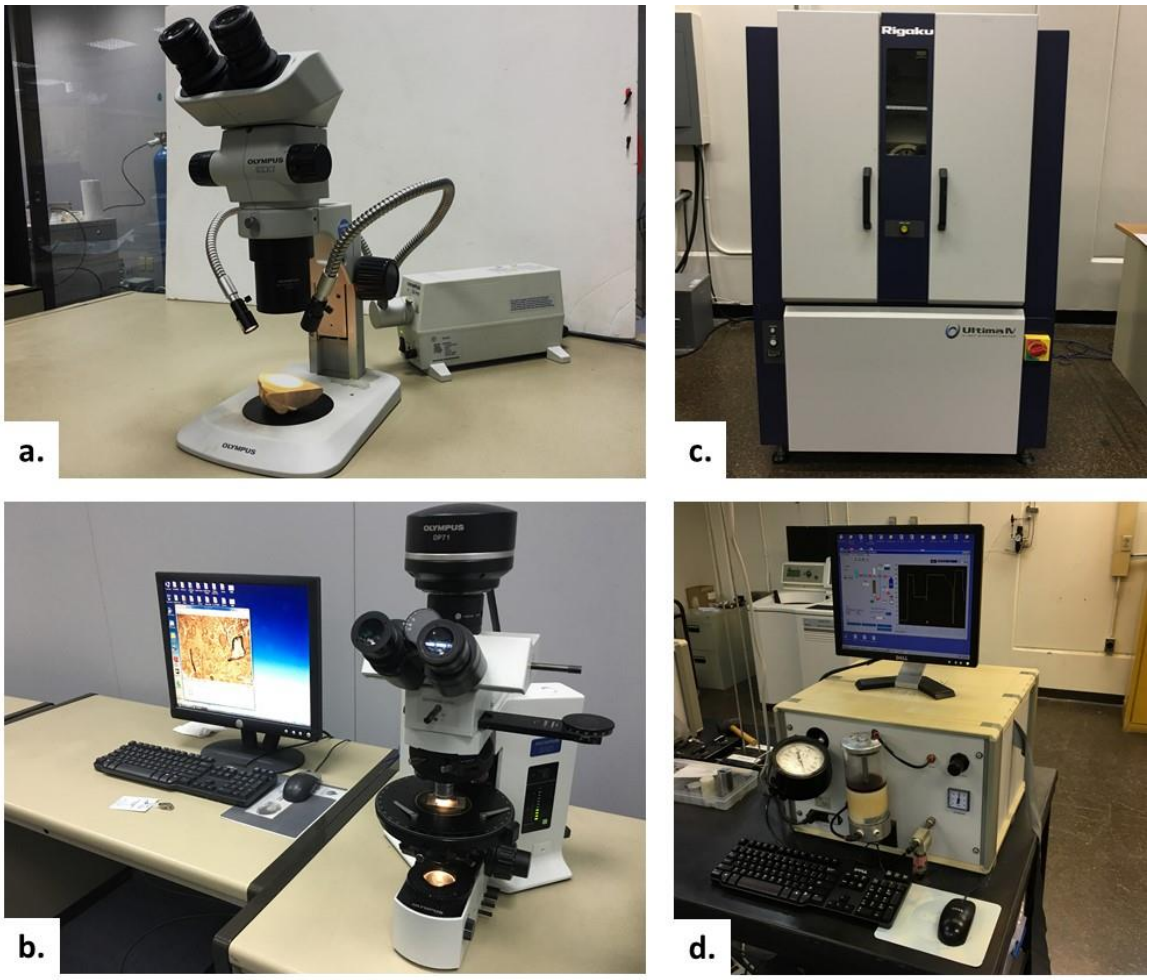


Figure 3.2. a & b. Stereo binocular (model : Olympus SZX7) and polarized (model : Olympus BX51) microscopes, c. X-Ray Diffractometer model Rigaku Ultima IV, d. Coretest System Automated Permeater-Porosimeter (APP) type AP-608.

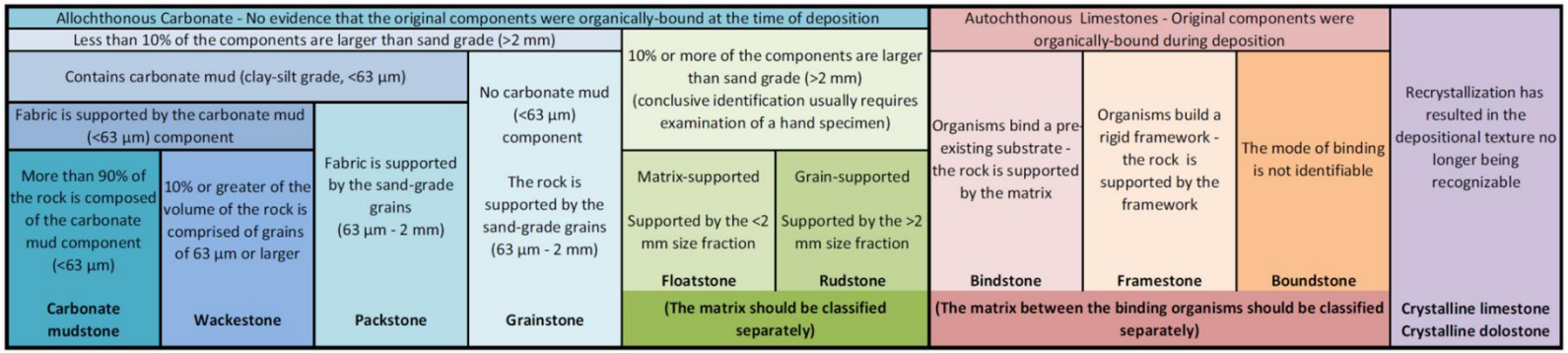


Figure 3.3. The modified Dunham classification by Embry and Klovan (1971)

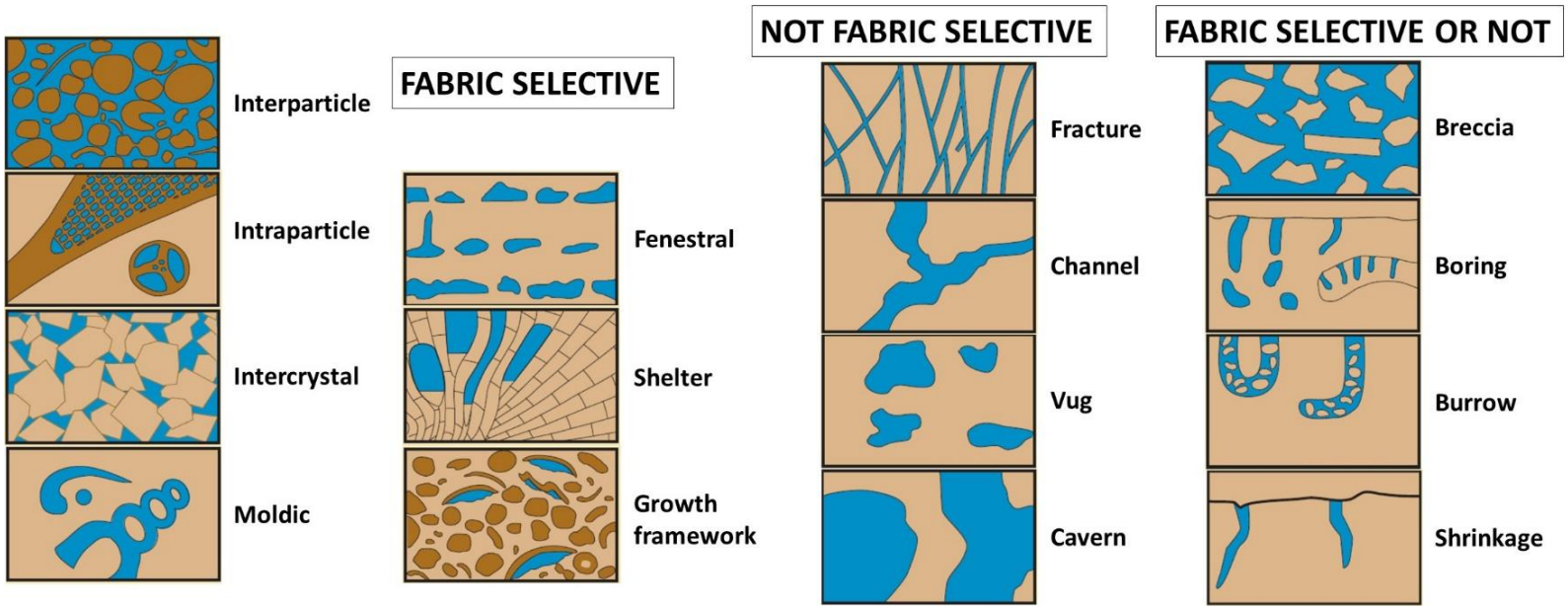


Figure 3.4. Porosity classification developed by Choquette and Pray (1970). For detail explanation about this classification, see text.

# CHAPTER IV

# RESULTS

The results including field description, petrographic analysis, and porosity-permeability measurements of Dhruma Formation investigated in the study area, are presented in three distinctive sub-chapters. In the field description sub-chapter explained any sedimentological feature captured during fieldwork. While petrographic analysis and porosity-permeability measurement were performed in the laboratory which covered the frequency analysis of microfacies data and revealed in which microfacies the porosity-permeability values are well-developed.

## 4.1 Field Description

The studied outcrops are positioned in Darma' Quadrangle, around 60 kilometers southwest of Riyadh city which is located between 24°00'—25°00' N, and 45°00'—46°30' E (Figure 1.3). The outcrops show good exposures of the D2 to D4 Units of the Dhruma in this study area.

The first section (Wadi section) represents the uppermost part of D2 Unit and lower to middle parts of Jufayr Member (D3 Unit). This section starts with a resistive, massive, indurated limestone bed of benthic foraminifera-rich facies which likely represents the uppermost D2 Unit, followed by a series of shallowing upward sequences, and capped by a thick accumulation of grainy facies represented by either peloidal or oolitic grainstones of the D3 Unit. The dominant the non-skeletal grains in the outcrop are peloids and ooids. Additionally, large skeletal fragments of mollusk (gastropods and bivalves) and

brachiopod are quite abundant. Numerous bioturbation in the forms and shapes of burrows are present from bottom to top of the section.

The roadcut outcrop (Section 2) which lies above section 1, which likely represents the lower part of the D4 Unit, commences with a massive, greyish yellow wackestone with few fragments of bivalves and local occurrences of stylolite. This is overlain by thickly interbedded skeletal rich-packstone and oolitic grainstone in the middle part and is capped by grain-dominated facies and thickly bedded packstone to grainstone facies at the top. Dolomitization occurs in basal part of the outcrop (Figure 4.1).

An outcrop section (Section 3) which represents the middle to upper parts of the D4 Unit, was measured along a cliff near a gas station in Hafirat Nisah district. This outcrop section is highly burrowed (Figure 4.2) and contains trace fossils identified as *Thalassinoides* (Figure 4.3). It is characterized by a series of interbedded grain-dominated facies (packstone to grainstone) and wackestone facies, overlain by a thickly interbedded mudstone to wackestone facies. The transition between these facies is marked by thin marl beds.

Complete stratigraphic sections of all the studied outcrops are presented in Figure 4.4, 4.5, 4.6, respectively. Figure 4.4 shows that the D3 Unit commenced with limestone which is rich in mollusk, bivalve fragments and abundant benthic foraminifera especially at the base of section 1. Figure 4.5 illustrates the bottommost of D4 Unit. Figure 4.6 is a stratigraphic column of top of D4 Unit.

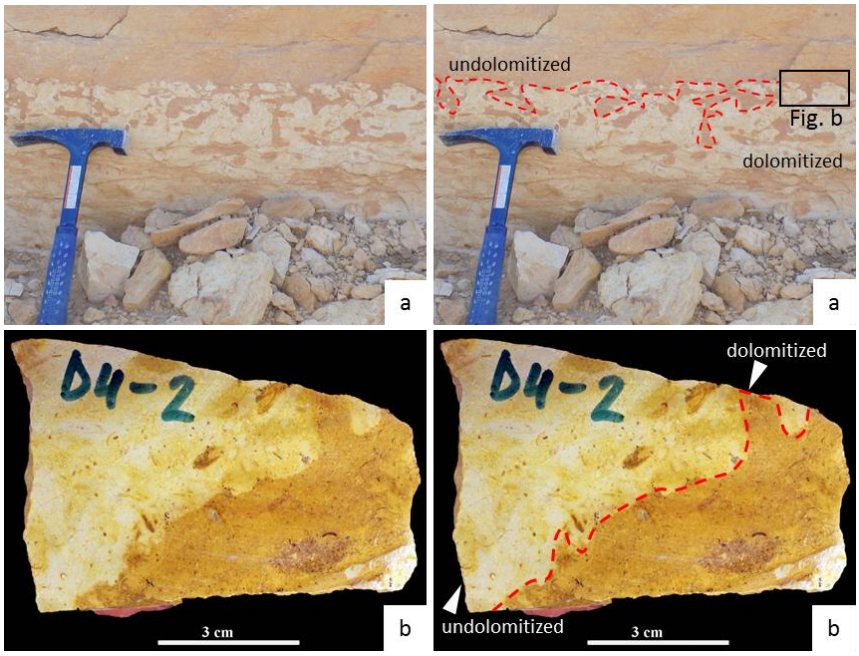


Figure 4.1. a. The boundary (red dash line) between undolomitized and dolomitized, b. hand specimen sample presenting burrow-mottled structure (red dash line).

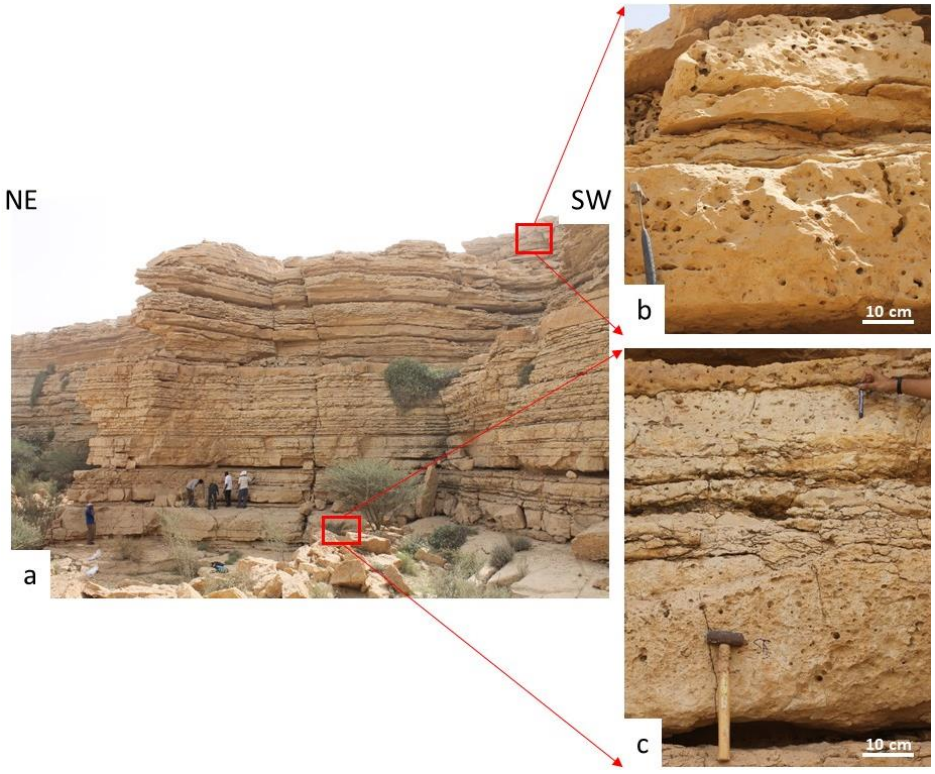


Figure 4.2. a. The D4 Unit showing burrows with the diameter of around 1 to 2 cm in average that has been significantly developed throughout the section especially in the topmost (b) and bottommost (c) of section 2.

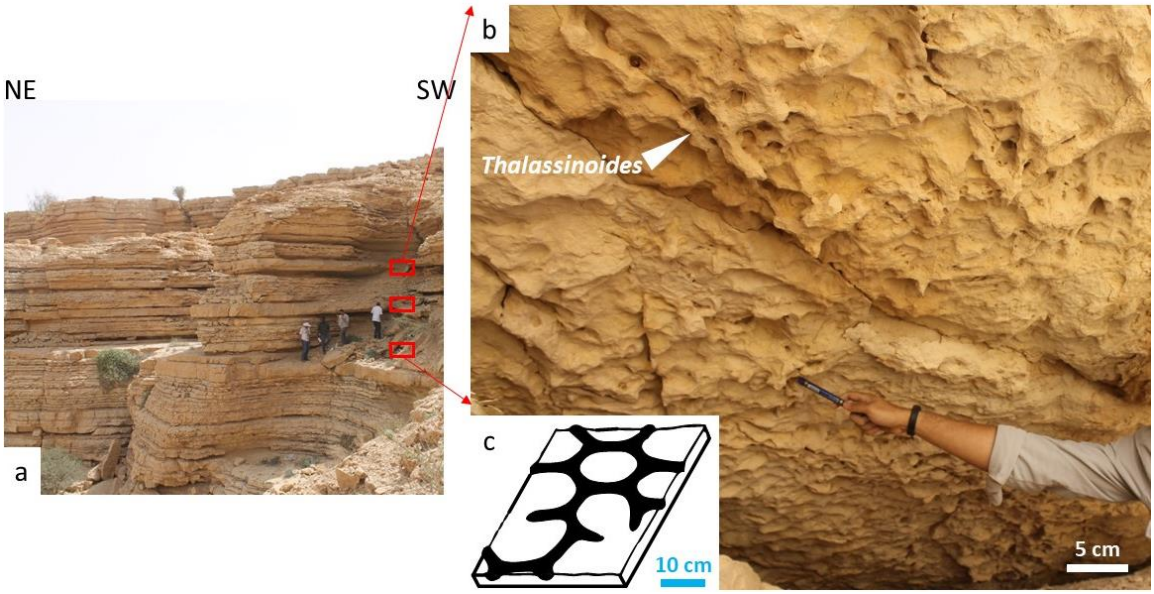


Figure 4.3. a. *Thalassinoides* trace fossils have been commonly found in the second section (red rectangles spot their location), b. Tunnel-shaped *Thalassinoides* exhibiting a diameter of around 2 to 3 centimeters, (c) A cartoon showing the shape of Jurassic *Thalassinoides* (modified after Seilacher, 2007).

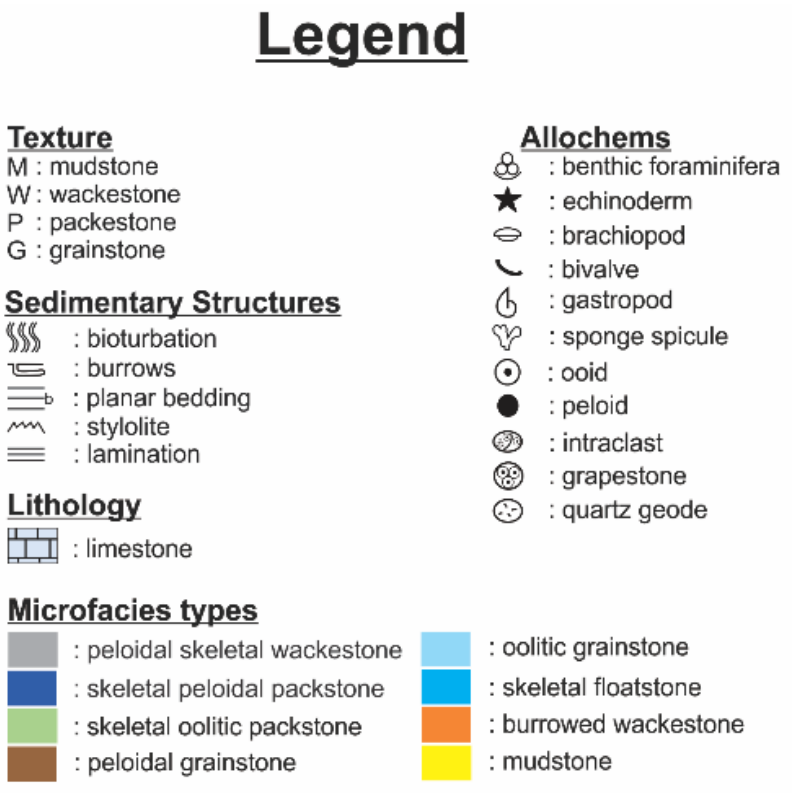


Nomenclature for all symbols and microfacies types used in the study area

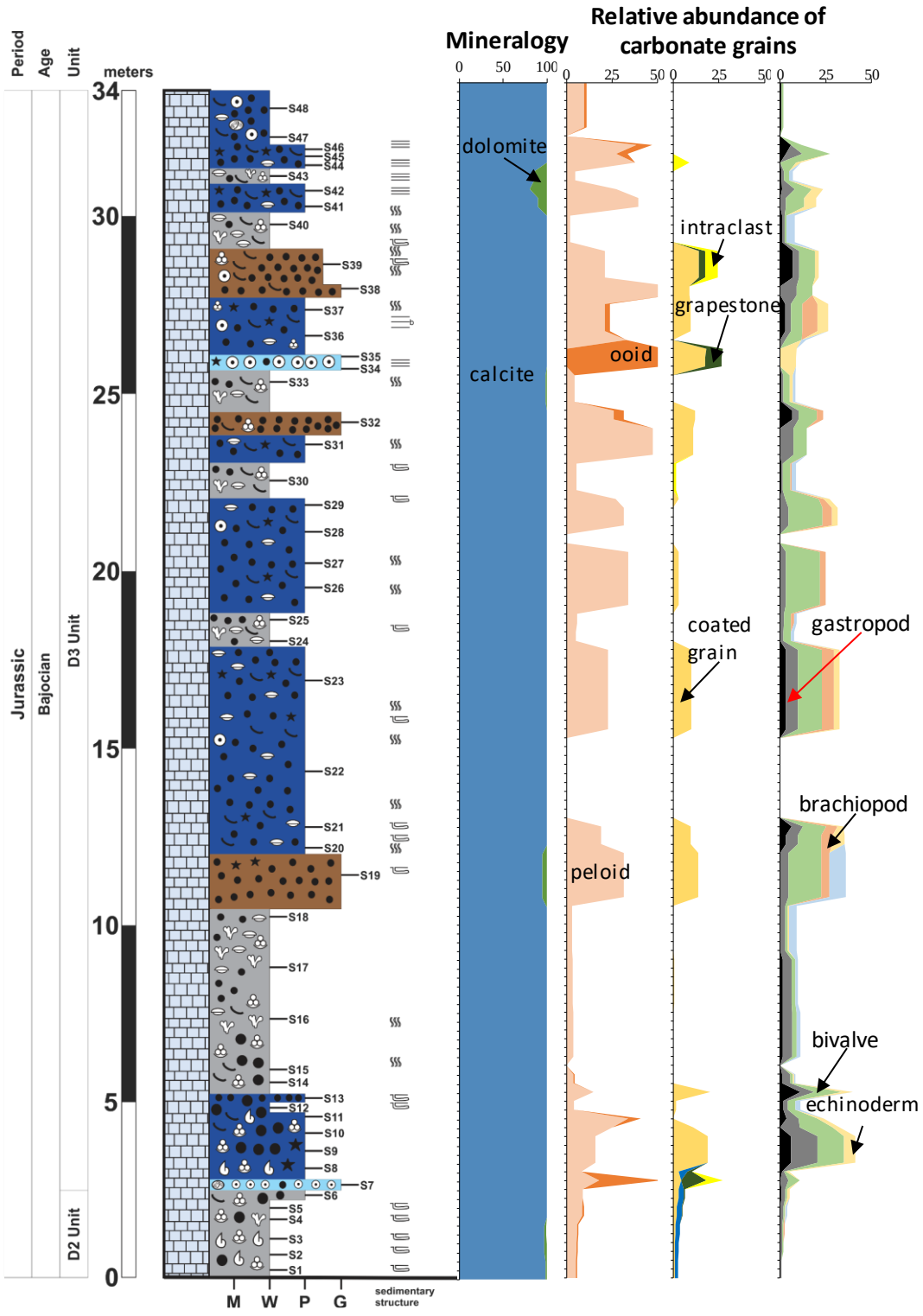


Figure 4.4. Stratigraphic column of section 1 which represents D3 Unit. For the explanation of the symbols, see page 40.

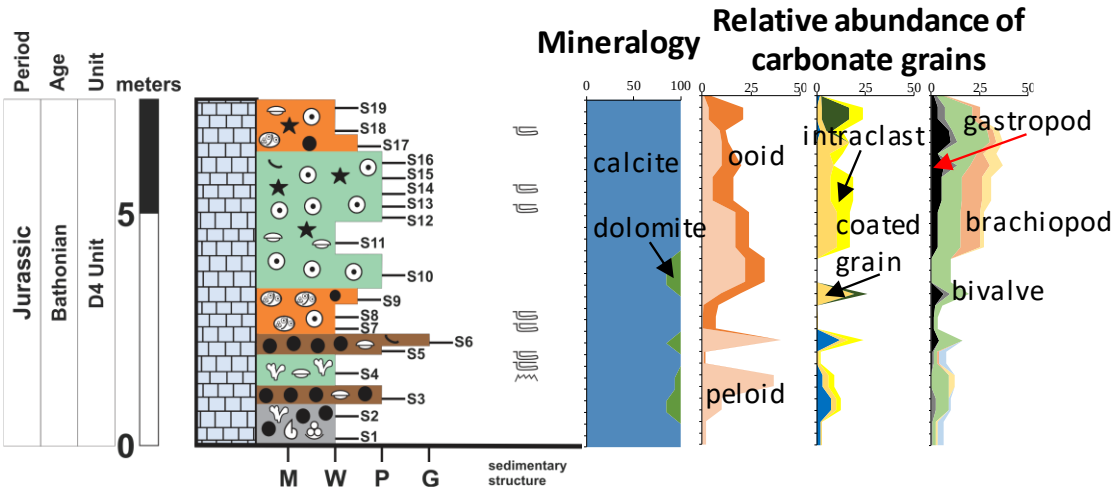


Figure 4.5. Stratigraphic column of section 2 which represents lowermost D4 Unit. For the explanation of the symbols, see page 40.

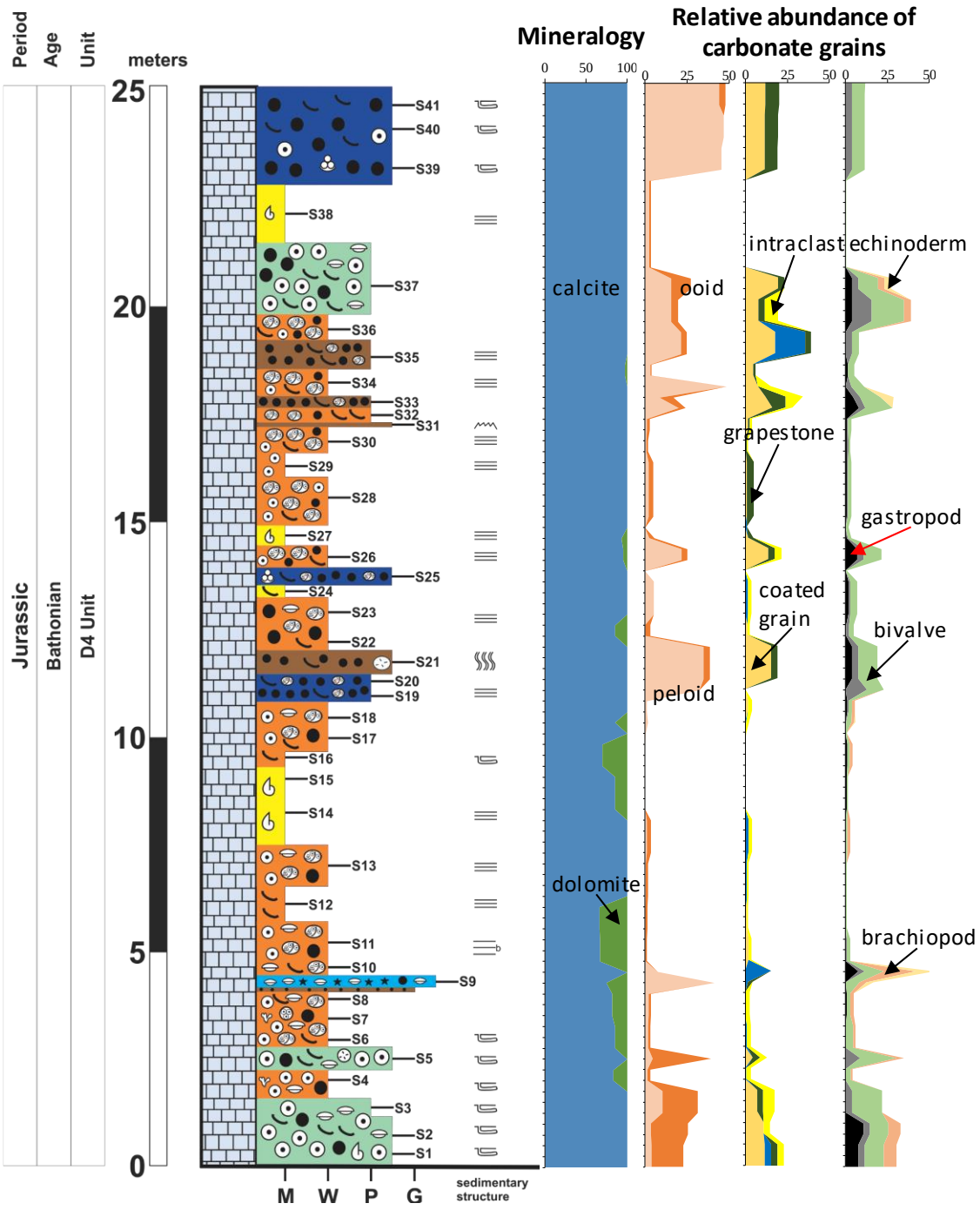


Figure 4.6. Stratigraphic column of section 3 which represents upper part of D4 Unit. For the explanation of the symbols, see page 40.

## 4.2 Quantitative Microfacies Analysis

Each microfacies have been described and interpreted according to the data collected from field and petrographic examinations. Summaries of the characteristics of all the microfacies are presented in Tables 1 and 2. The percentages of all microfacies are depicted in Figure 4.7. The identified microfacies and their association are listed below and described in the subsections that follow:

1. MF 1: Peloidal Skeletal Wackestone
2. MF 2: Skeletal Peloidal Packstone
3. MF 3: Skeletal Oolitic Packstone
4. MF 4: Peloidal Grainstone
5. MF 5: Oolitic Grainstone
6. MF 6: Skeletal Floatstone
7. MF 7: Burrowed Wackestone
8. MF 8: Mudstone

Table 1. Summary of the quantification of interpreted microfacies along with their reservoir potential presented as an average value. These results are based on petrographic analysis, XRD, and porosity-permeability measurements

| Microfacies | Total samples | Abundance (%) | Composition (%) | | | Porosity (%) | Permeability (mD) |
|---|---|---|---|---|---|---|---|
| | | | Calcite | Dolomite | Anhydrite | | |
| **MF 1: Peloidal Skeletal Wackestone** | 20 | 19 | 92.75 | 2.20 | - | 4.83 | 0.0382 |
| **MF 2: Skeletal Peloidal Packstone** | 23 | 26 | 98.75 | 1.25 | - | 6.60 | 0.0271 |
| **MF 3: Skeletal Oolitic Packstone** | 13 | 12 | 97.46 | 2.31 | 0.23 | 12.26 | 0.0330 |
| **MF 4: Peloidal Grainstone** | 12 | 11 | 95.75 | 4.25 | - | 10.23 | 0.1428 |
| **MF 5: Oolitic Grainstone** | 3 | 2.8 | 100 | - | - | - | - |
| **MF 6: Skeletal Floatstone** | 1 | 1 | 98 | - | - | - | - |
| **MF 7: Burrowed Wackestone** | 25 | 23 | 93.44 | 6.48 | - | 11.0 | 0.3593 |
| **MF 8: Mudstone** | 23 | 26 | 98.75 | 1.25 | - | 6.69 | 0.0005 |
| | **104** | **100** | **96.14** | **3.19** | **0.03** | **6.48** | **0.0748** |

Table 2. Summary of the identified microfacies types in the study area

| Microfacies Association | Microfacies | Major and minor grain types | Sedimentary structure | Pore types | Depositional environment |
|---|---|---|---|---|---|
| Lagoon | MF 1: Peloidal Skeletal Wackestone | Large diversity of skeletal grains such as echinoderms, bivalves, brachiopods, gastropods, relatively abundant benthic foraminifera of *Pfenderina* sp., *Nautiloculina* sp. and *Redmondoides* sp., *Globivalvulina* sp.. Monoxon and triaxon spicules are common. Dasyclad green algae fragments are found locally. The non-skeletal grains are dominated by peloids, ooids, and few intraclasts. | lamination | moldic, interparticle, intraparticle | relatively low energy, open lagoon |
| | MF 2: Skeletal Peloidal Packstone | Abundant peloids, followed by coated grain, grapestone and intraclasts. The skeletals are largely dominated by mollusks, brachiopods, and few *Nautiloculina* sp. | lamination | interparticle, moldic, intraparticle | low energy, restricted lagoon |
| Shoal complex | MF 3: Skeletal Oolitic Packstone | Abundant concentric ooids, common coated grain, grapestones and intraclasts. Allochems are largely dominated by mollusks, brachiopod, and benthic foraminifera of *Nautiloculina* sp. Lime mud are also presented as matrix. | lamination | interparticle, moldic | moderate to high energy, back- or foreshoal. |
| | MF 4: Peloidal Grainstone | Abundant peloids, common skeletal grains including brachiopod, echinoderm, bivalve fragments and benthic *foraminifera of Trocholina* spp. Other non-skeletal grains which are mostly dominated by coated grains of skeletal fragments are minor. | - | leached dolomite rhombs, intercrystalline, intraparticle | moderate to high energy, back- or foreshoal |
| | MF 5: Oolitic Grainstone | Abundant well-sorted, radial-fabric ooids as the major non-skeletal grain, then followed by concentric-radial ooids, and intraclasts. Minor skeletals including bivalve, foraminifera, gastropod | - | moldic, intraparticle, interparticle | moderately high energy, shoal crest |
| Open Marine | MF 6: Skeletal Floatstone | Abundant fragment of skeletals (i.e., echinoid, bivalve, and brachiopod). | scour surface | intraparticle | high energy, between FWWB and SWB |
| | MF 7: Burrowed Wackestone | Allochthonous ooids filling burrow, moderate skeletal fragments in the form of bivalve, brachiopod, and foraminifera. Monoxon spicule are found locally in several beds. Highly dolomitized. | burrowing | leached dolomite, moldic | moderate energy, below SWB |
| | MF 8: Mudstone | Absence of grains, abundant micrite mud, few mollusks fragments. | lamination | no visible porosity, probably micropores | low energy, proximal outer ramp |

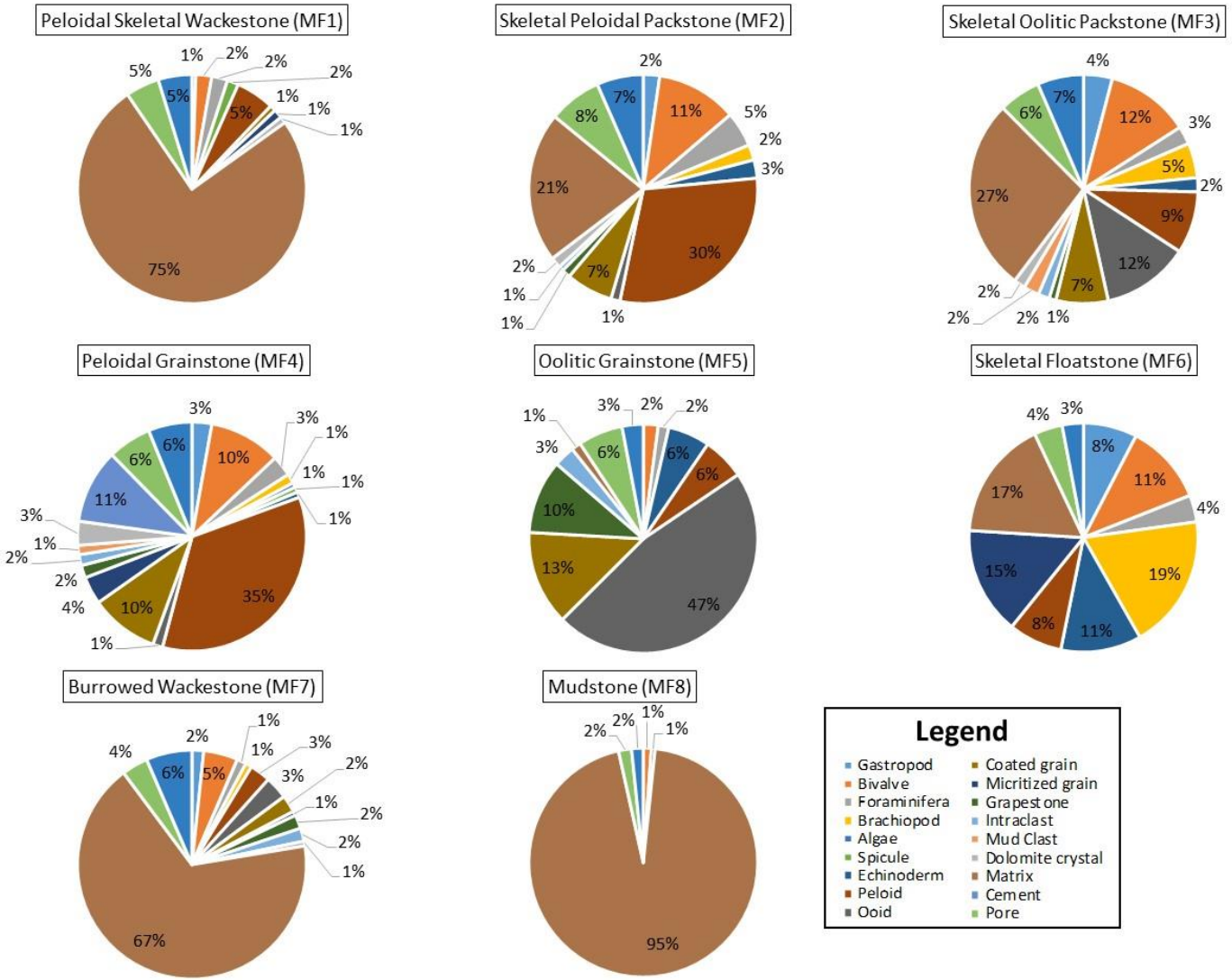


Figure 4.7. Microfacies types and relative amount of point-count group.

### 4.2.1 MF 1: Peloidal Skeletal Wackestone

This beige to dark brown colored peloidal skeletal wackestone has an average thickness of 1 meter in appearance (Figure 4.8a). In the field, this microfacies occurred mostly in Section 1, few meters in Section 3, and mostly associated with skeletal peloid packstone. The rock fabric is wackestone with the concentration of calcite lime mud around 75% on the average. It is characterized by a high diversity of skeletal grains such as echinoderms and gastropods (av. 5%; Figure 4.7), bivalves (av. 2%), brachiopods (av. 1%), relative abundance of benthic foraminifera (av. 3%) species *Pfenderina* sp. commonly associated with *Nautiloculina* sp. *Redmondoides* sp., and *Globivalvulina* sp. (Figure 4.8c and d). Monoxon and triaxon spicules are common in thin section (less than 5%). Dasyclad green algae fragments are found locally (Figure 4.8b). The non-skeletal grains are dominated by peloids (over 4%), followed by ooids (av. 2%) which are commonly observed as a single cortical ooid or as the part of intraclasts. No porosity has been observed under microscope.

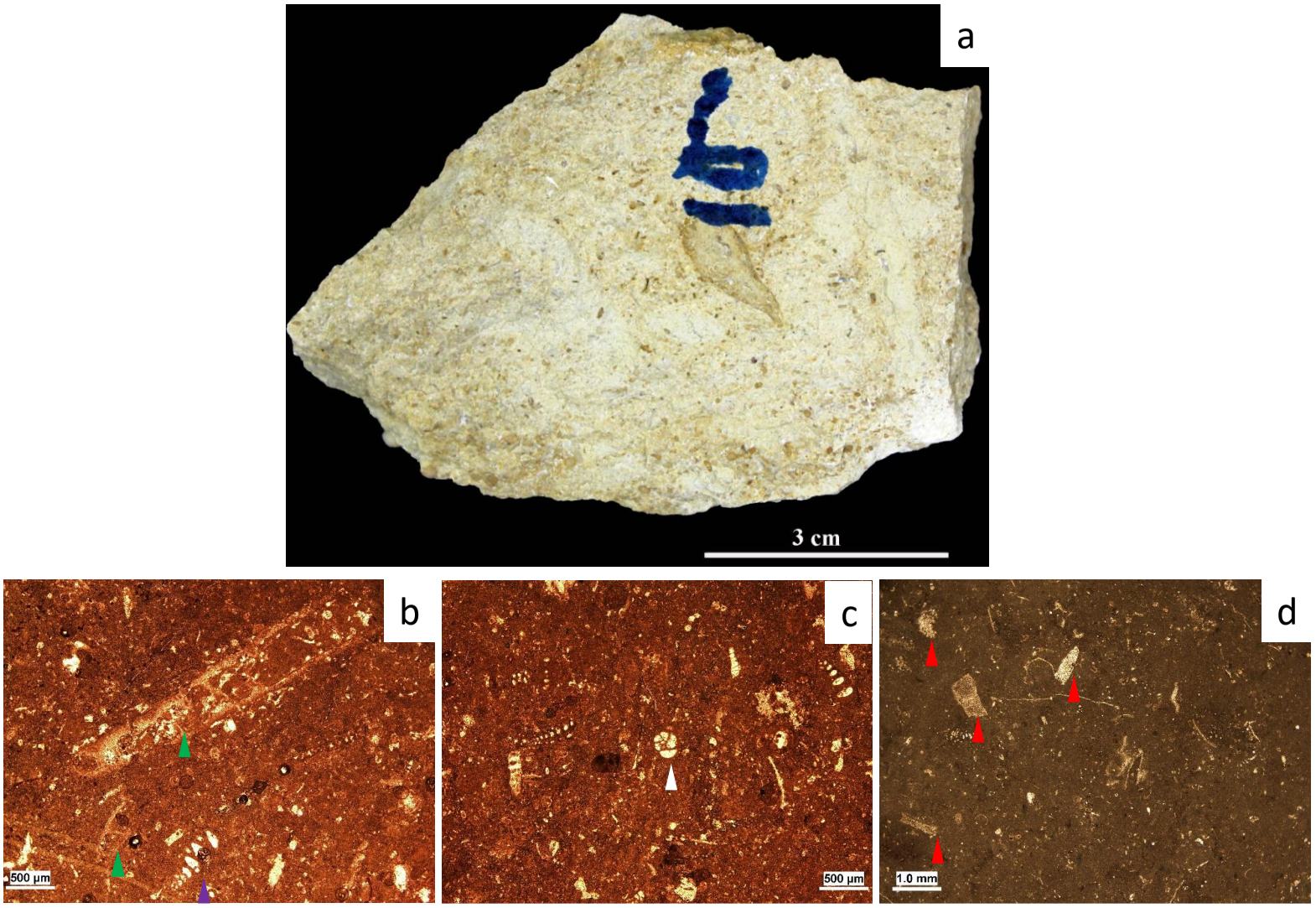


Figure 4.8. a. Polished surface of this microfacies contains of abundant skeletal, b. Dasyclad green algae fragments (green arrow) and (purple arrow) are found rare to common, c and d. Globivalvulina sp. (white arrow) along with other assemblages of benthic foraminifera, and echinoderm plates (red arrow) are embedded in carbonate mud.

### 4.2.2 MF 2: Skeletal Peloidal Packstone

This microfacies is yellowish to brownish in color (Figure 4.9a) and has an average thickness of 1 meter. Peloid is the most dominant grain type in the facies (av. 30%; Figure 4.7). It is also noticeable that the facies, is commonly interbedded with peloidal skeletal wackestone and often capped by peloidal or oolitic grainstone, especially in the middle to upper parts of section 1. This microfacies occurred mostly in Section 1 (48%; Figure 4.18) and only within a few meters in Section 3. The matrix is predominantly of carbonate mud (micrite) (av. 21%; Figure 4.9b). Skeletal grains including bivalves (av. 5%; Figure 4.7), brachiopods, gastropods, and echinoderms (av. 2%) benthic foraminifera of *Trocholina* spp. (av. 1%; Figure 4.9c and d) account for 25—30% of the total grain components in the facies. Other non-skeletal grains which are mostly dominated by coated grains and micritized grain of the skeletal fragment are minor. The visual porosity is estimated to be less than 7%. The porosity types are mainly intraparticle, moldic and intergranular. Calcite is the dominant mineral with the percentage up to 98%.

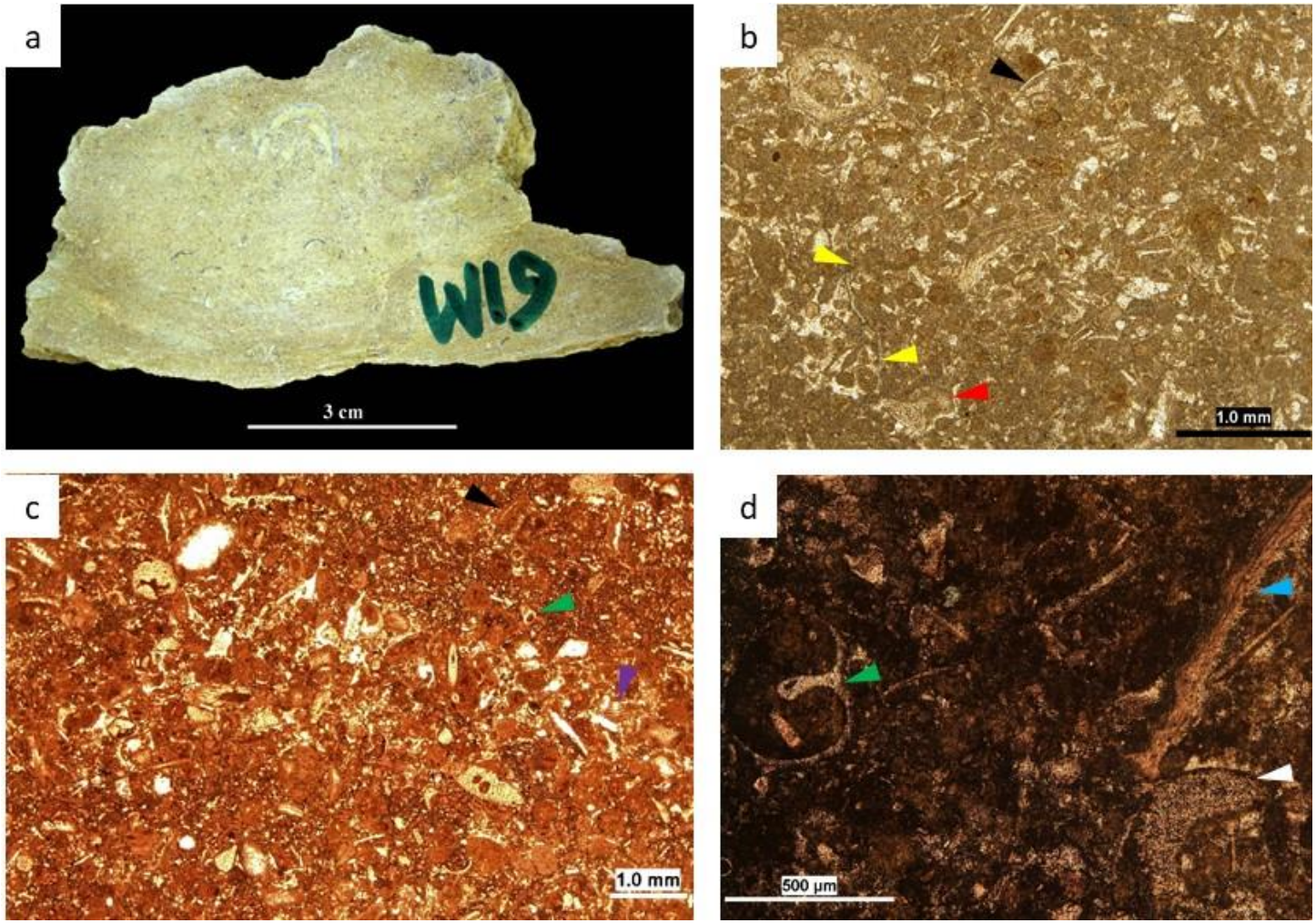


Figure 4.9. a. Slabbed sample of this microfacies is comprised mainly of gastropod and echinoid fragments and rare benthic foraminifera. b. PPL photomicrograph of brachiopod (red arrow) and bivalve (black arrow) fragments coated by thin micritic envelope along with fracture pore (yellow arrow), c. Trocholina spp. (purple arrow), gastropod (green arrow), coated grain of bivalve fragment (black arrow) appear in the thin section d. Cross-polarized photomicrograph showing gastropod cemented by thin isopachous calcite (green arrow), honeycomb-like structure of echinoid with micrite coating (white arrow), and brachiopod (blue arrow) fragments.

### 4.2.3 MF 3: Skeletal Oolitic Packstone

Skeletal oolitic packstone is characteristically grain-rich and pale yellowish orange to grayish orange in appearance (Figure 4.10a). The facies with thickness ranging from 1 to 1.75 meters, is relatively thick. The microfacies appeared mostly in Section 3 and is often associated with the burrowed wackestone facies. The most abundant constituents are non-skeletal grains represented largely by concentric ooids (av. 25%; Figure 4.7), followed by coated grain (av. 10—15%), grapestones (av. 6%) and intraclasts (av. 5%) (Figure 4.10b). Concentric-fabric ooids mostly exhibit a size range of 600-700 microns (Figure 4.10c). The skeletal grains are largely dominated by mollusks (av. 20—25%), brachiopod (av. 10%), and benthic foraminifera of *Nautiloculina* sp. (av. 1%) (Figure 4.10d). Lime mud is also presented as matrix (av. 30%; Figure 4.7). The facies is comprised of nearly 5% of calcite cement and around 4% interparticle porosity on the average. Diagenetic features recorded in this facies are authigenic anhydrite and ferroan calcite cements, partial dissolution of ooids lamellae which led to moldic porosity (Figure 4.10b).

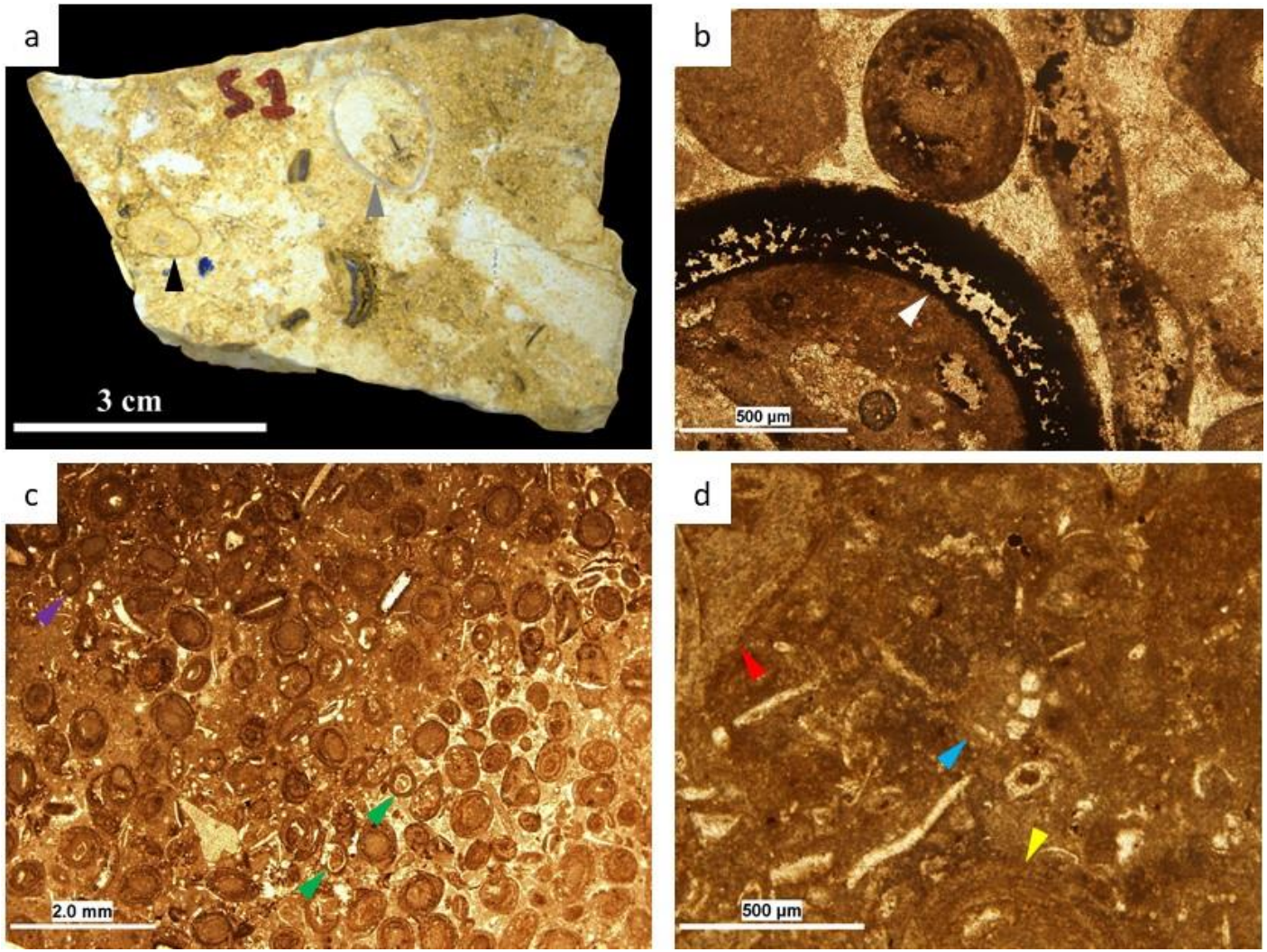


Figure 4.10. a. Polished sample showing an ooid-formed intraclast coated by thin micritic envelope (black arrow) and bivalve (grey arrow) b. Microboring in a bivalve fragment, c. Grapestone (purple arrow) and ooids with concentric lamellae (green arrow), d. Thin micritic envelope on brachiopod fragment, Nautiloculina sp.? (blue arrow), concentric fabric of ooid (yellow arrow) are characterizing this microfacies.

### 4.2.4 MF 4: Peloidal Grainstone

Peloidal grainstone is a yellowish to brownish, 50—75 cm thick interval (Figure 4.11a). It commonly occurs in the three investigated sections and acts as a cap of shallowing upward sequence. The facies which is generally associated with skeletal peloidal packstone, is characterized by the abundance of peloids with an average of 35% (Figure 4.7) as the major non-skeletal grains. Peloids are fine grained, moderately to well sorted with an average size of 70—100 microns (Figure 4.11b-d). Other non-skeletal grains are partially micritized concentric ooids (over 5%), micritized grain of mollusk fragments (more than 2%), and intraclasts (around 2%). Gastropod and brachiopod fragments (av. 3%; Figure 4.7) found scattered in the thin sections, constitute more than 15% of the total grains. Visual porosity is low (av. 5%; Figure 4.7). The porosity types mainly occur as moldic (around 70% of the visual porosity), followed by intragranular by an average of 20%, and fracture by an average of 10%. Equant calcite cement (av. 3%) commonly occludes pores in the microfacies. Micritization and hematite cement are observed under plain light microscopy. Besides, dolomitization and later calcitization are considered as other diagenetic features which may be affecting porosity.

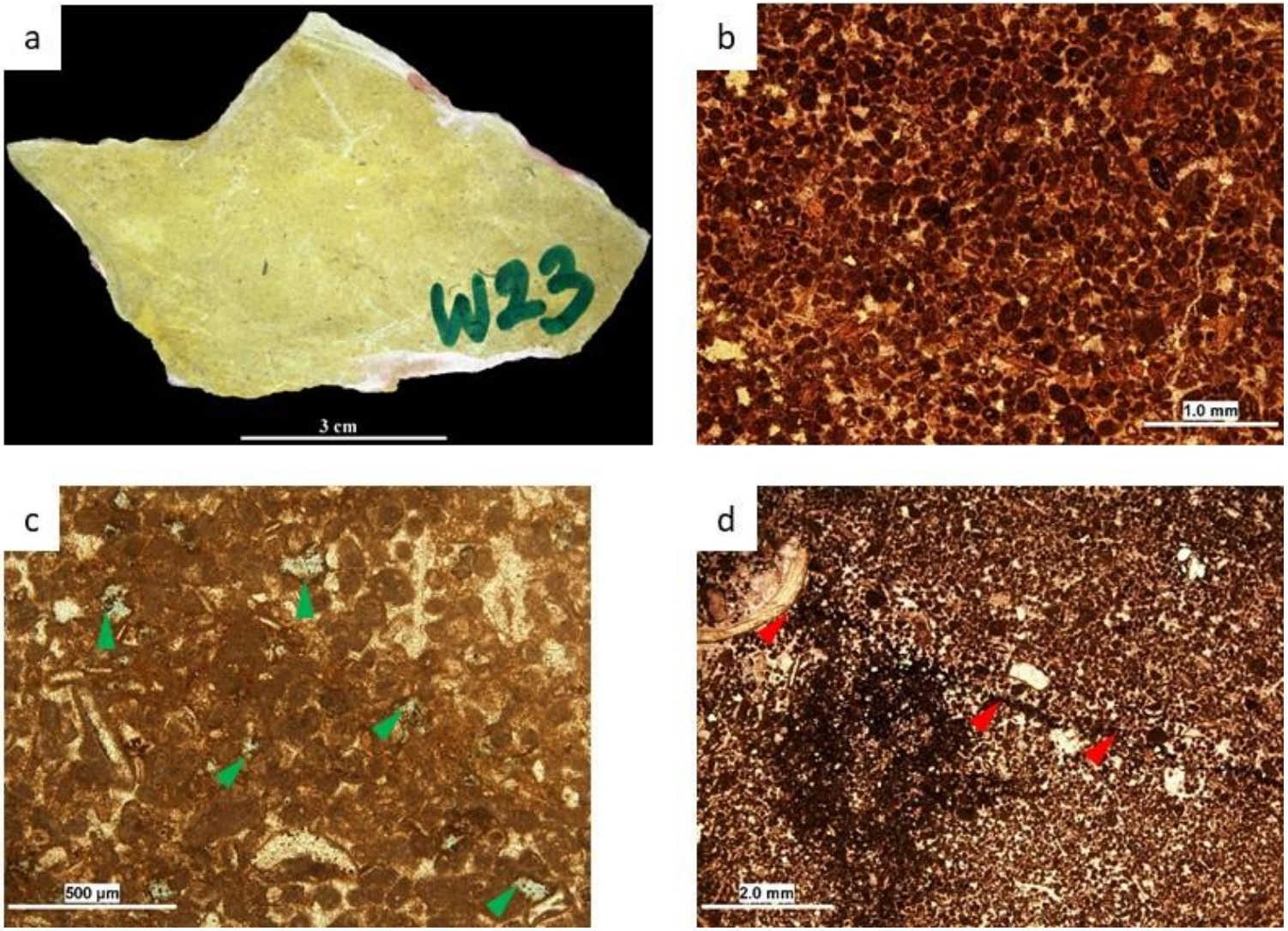


Figure 4.11. Peloidal grainstone is characterized by abundant peloids as showing in the hand specimen (a) and thin section (b). PPL photomicrograph showing secondary porosity in this facies, c. Dolomite dissolution (green arrow) d. Low-amplitude microstylolites (red arrow) overlapped brachiopod fragment.

### 4.2.5 MF 5: Oolitic Grainstone

This microfacies is characterized by yellowish to brownish in color, with about 35-centimeter thick bed (Figure 4.12a). In the field, this microfacies occurred only in Section 1 and was interchangeable with peloidal grainstone as a cap of shallowing upward sequence. The major allochems which accounts for 35 to 40% of total constituents is well-sorted ovoid-shaped ooids with mostly radial fabric structures. It ranges from 300─500 μm in size with an average of 400 μm (Figure 4.12b and c). Peloids (av. 6%; Figure 4.7), grapestones (av. 5%) and intraclasts (av. 3%) are commonly present within this microfacies. Benthic foraminifera (i.e., *Nautiloculina* sp., and *Trocholina* spp.) are commonly observed in the nuclei of ooids and intraclasts. Minor quantity of lime mud matrix is up to 3%. Equally-spaced ooids are cemented by equant calcite cement (av. 3%). In addition to that, fracture-filled calcite is also observed under light microscope (Figure 4.12d). Dissolution of radial fabric commonly occurs as pore (secondary porosity).

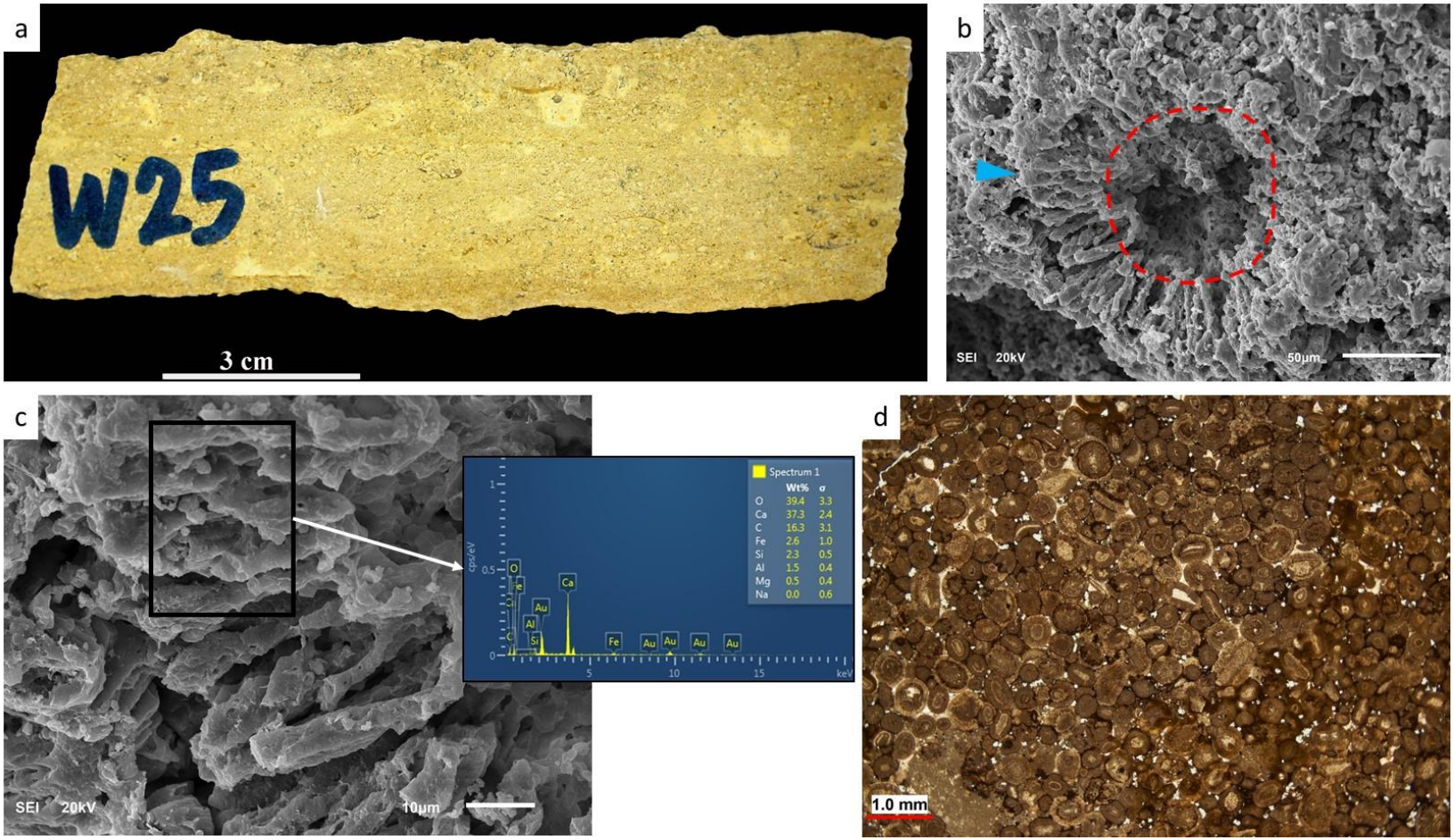


Figure 4.12. a. Slabbed rock of well-sorted ooids grainstone, b. SEM photomicrograph of radial-fabric ooid (blue arrow) showing nucleus has been leached thus may boost its porosity as intraparticle pore (red dash rectangle), c. Radial crystal length varies between 40-45 µm and commonly defines the thickness of lamellae. This crystal may originally low-Mg calcite supported by relatively high concentration of Ca (37.3 %) and low Mg concentration (0.5 %) as observed by EDX-SEM analysis (spectrum 1), d. Abundant single-laminae ooids.

### 4.2.6 MF 6: Skeletal Floatstone

This microfacies is yellowish to brownish and has a thickness of 2—3 centimeters (Figure 4.13a). The microfacies is occurred only in Section 3 and is typified by poorly-sorted grains and scour base. Abundant echinoderms (av. 15%; Figure 4.7), followed by brachiopods (av. 15%), and bivalves (av. 10%) fragments are the characteristics of this microfacies. These skeletal grains made up to 90% of the total grains in the microfacies. Non-skeletal grains dominated by peloids (less than 15% of the total grains). The matrix is made up of carbonate mud (micrite) (Figure 4.13b—d). The visual porosity (less than 3%) difficult to identify under plain light microscope. However, intraparticle and moldic pores have been found either in a partially or completely dissolved grains. Calcite is the dominant mineral with the percentage of 100% as examined under plain light microscope.

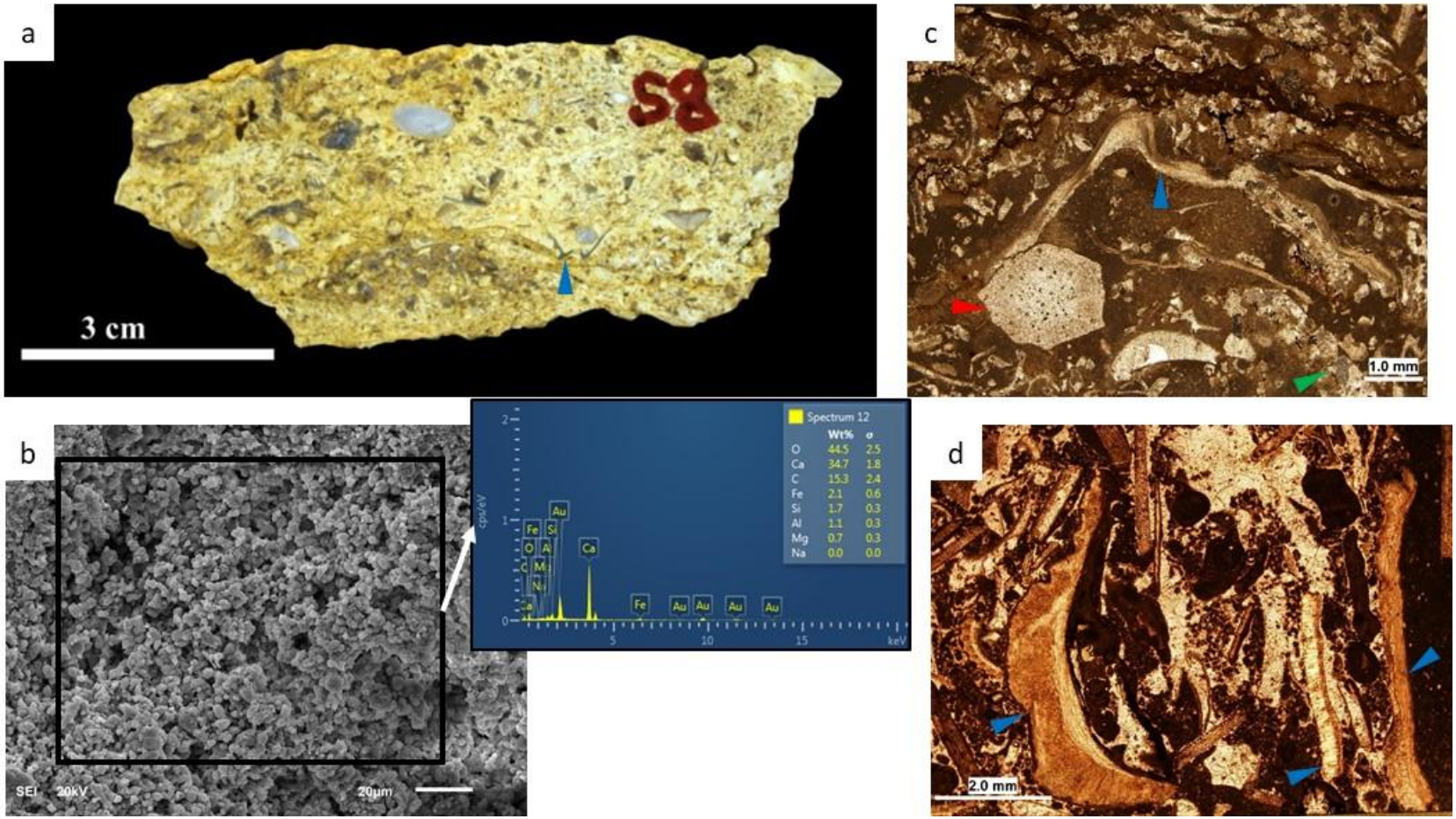


Figure 4.13. a. Slabbed rock of skeletal floatstone microfacies is composed of irregular shape of skeletal which are mainly dominated by echinoderm and brachiopod (blue arrow) fragments. b. SEM photomicrograph of micrite is predominantly of calcite with abundant micropores, c. Cross-polarized photomicrograph showing that fragments of echinoderm (red arrow), brachiopod (blue arrow), and neomorphosed mollusk (green arrow) embedded in lime mud, d. Brachiopod fragments (blue arrow) and fine-grained, moderately sorted peloids are cemented by blocky calcite.

### 4.2.7 MF 7: Burrowed Wackestone

This microfacies forms typically thin massive beds that are generally 50—60 centimeters in thickness (Figure 4.14a). The texture varies from wackestone to mudstone. The distinct feature in this microfacies is the presence of burrows filled by ooids (Figure 4.14b). In the outcrop, this microfacies is found mostly in Section 3 and is often associated with peloidal grainstone and mudstone. Ooids fabric is generally cortical and often micritized (Figure 4.13c). Tangential lamellae of ooids occur and can be observed under the microscope. *Cladocoropsis* fragments are present in a few samples (Figure 4.14d). Skeletal fragments are also present in the form of bivalves, brachiopods, and foraminifera. Monaxon spicules are observed in several beds (Figure 4.14d). The porosity encountered in thin section is rather low, around 4—8%. Leached-dolomite through calcitization is also present. Stratigraphically, this facies is commonly associated with skeletal oolitic packstone and peloidal grainstone.

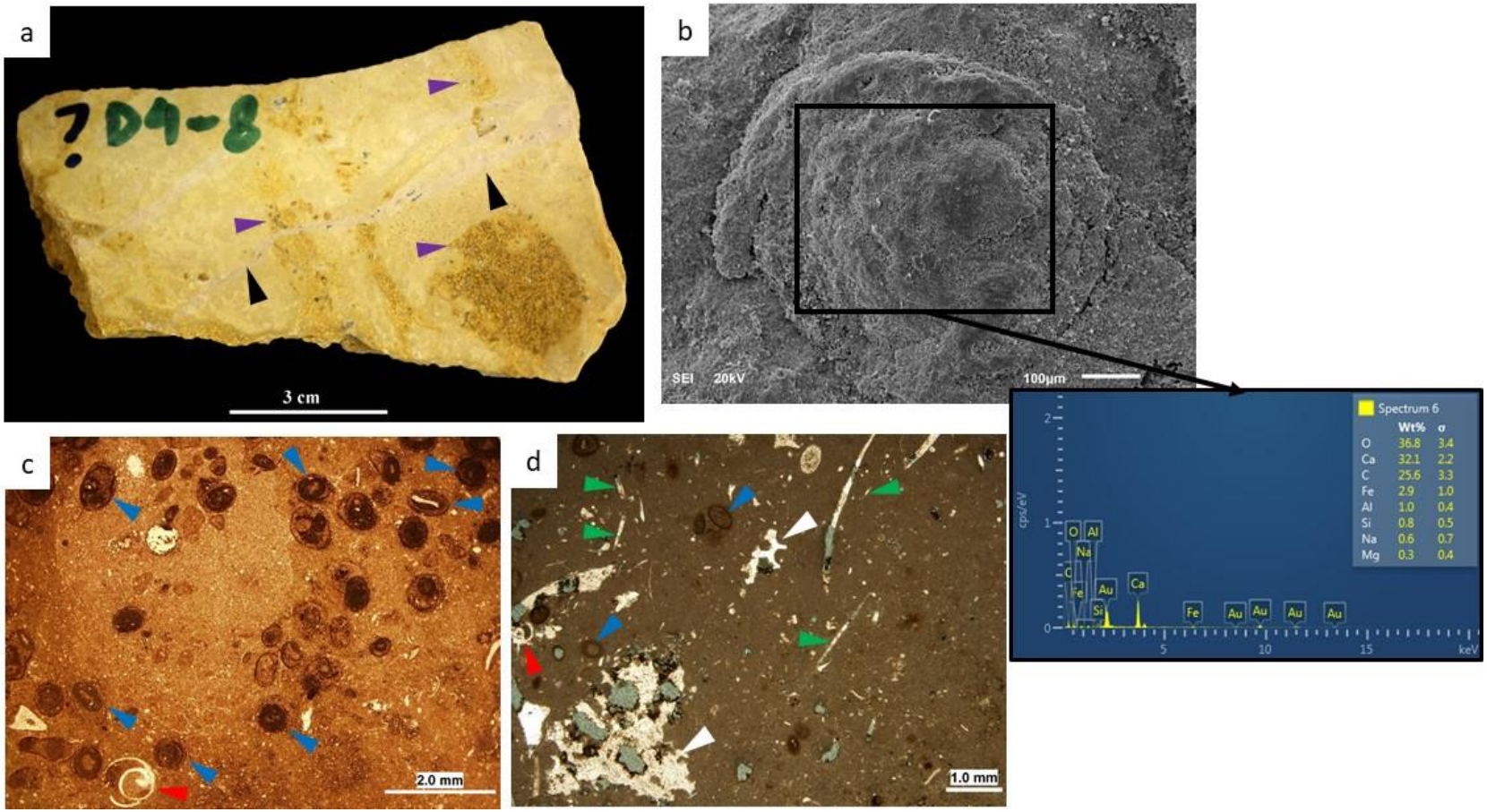


Figure 4.14. a. Hand-specimen sample of this microfacies showing burrows filled by ooid (purple arrow) cut by fracture (black arrow), b. SEM photomicrograph of micritic ooid resulting in calcite origin with Ca content of about 32%, c. Sparse micritic ooids (blue arrow) and gastropod mold (red), d. Monoxon spicules (green), micritic ooids (blue arrow), gastropod (red arrow), and presumably Cladocoropsis fragment (white arrow).

### 4.2.8 MF 8: Mudstone

The mudstone is characterized by homogeneous, a pale to greyish yellow color sediments (Figure 4.15a). The thickness of this microfacies varies from 40 centimeters to 2 meters, and it occurred only in Section 3. Micrite matrix dominates this microfacies (mud-supported, > 95% matrix; Figure 4.7). Allochems are rarely present, however, a minor quantity of gastropod and bivalve fragments with a percentage of less than 3% are found embedded in the matrix (lime mud) (Figure 4.15b-d). Fractures filled by calcite are also presented in both hand-specimen and thin sections. Thin sections frequently show low porosity (< 3%). Moldic pore may be locally present, and micropore of less than 10 microns observed in the SEM. Calcite is the dominant mineral (mean: 92%), followed by dolomite (av. 7%; Figure 4.7). Diagenetic features including dolomitization exist especially in association with burrowed wackestone.

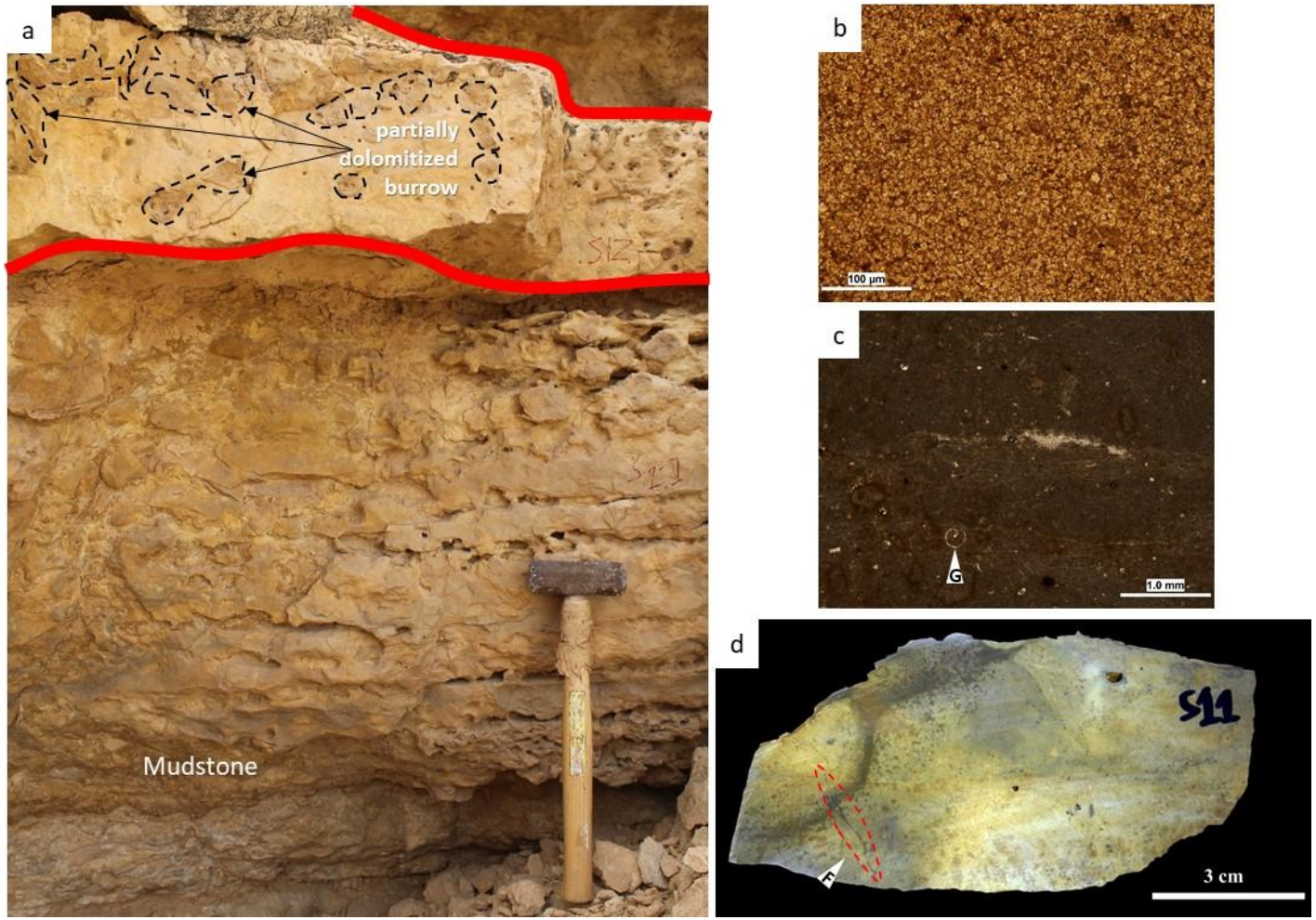


Figure 4.15. a. This microfacies is commonly associated with partially-dolomitized burrow facies (note that mottled appearance where burrows are located, b. PPL photomicrograph of complete dolomitization of micrite resulting fine subhedral to anhedral rhombs of fine dolomite c. Gastropod fragment (G) embedded in lime mud, d. Slabbed rock sample of bioclastic mudstone showing fracture (F) filled by calcite.

## 4.3 Mineralogical Composition

A quantitative method of microfacies yielded a visual estimate of mineralogical composition through petrographic analysis, then compare its results with XRD analysis for validation. The representative of over 80 samples from both sections have been analyzed using XRD which was mainly used to compare and identify the carbonate minerals such as calcite, aragonite, dolomite and minor quantities of clastic mineral (i.e., quartz and kaolinite). As a result, the first section which represents the D2 and D3 Units of the Dhruma shows dominantly calcite (91—97% average), dolomite (> 5%) and minor amount of clay minerals (< 2%). Silica content which are represented by quartz and kaolinite in the D2—D3 Units is rather low (< 2%). Another section which represents the D4 Unit indicates increasing dolomite content in the upper part (~8% average) with a slight decline of calcite (90% average). Dolomitization in the D4 Unit is mostly represented by non-fabric preserved dolomite as partially dolomitized micrite matrix and complete dolomitization in burrows which are generally concentrated in the lower part of section 2 and section 3. A comparison between petrographic and XRD analyses shows consistency as depicted in Figure 4.16. Figure 4.17 shows the percentages of the average mineralogical composition for each microfacies. Calcite is the dominant mineral, then dolomite which is characteristically absent or less than 2% in some microfacies including oolitic grainstone, skeletal floatstone, and skeletal peloidal packstone.

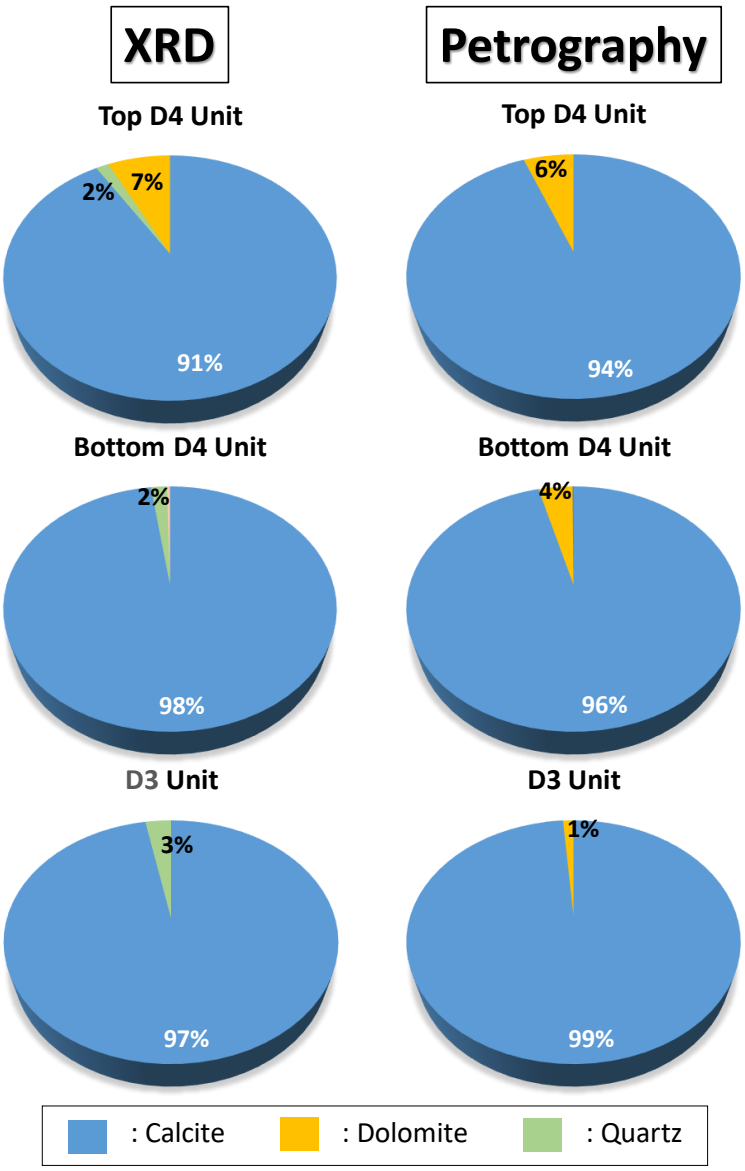


Figure 4.16. Comparison between XRD (left) and petrography (right) result. Calcite is the dominant mineral (over 90%), followed by dolomite (less than 10%) and silica minerals (i.e., quartz and kaolinite)

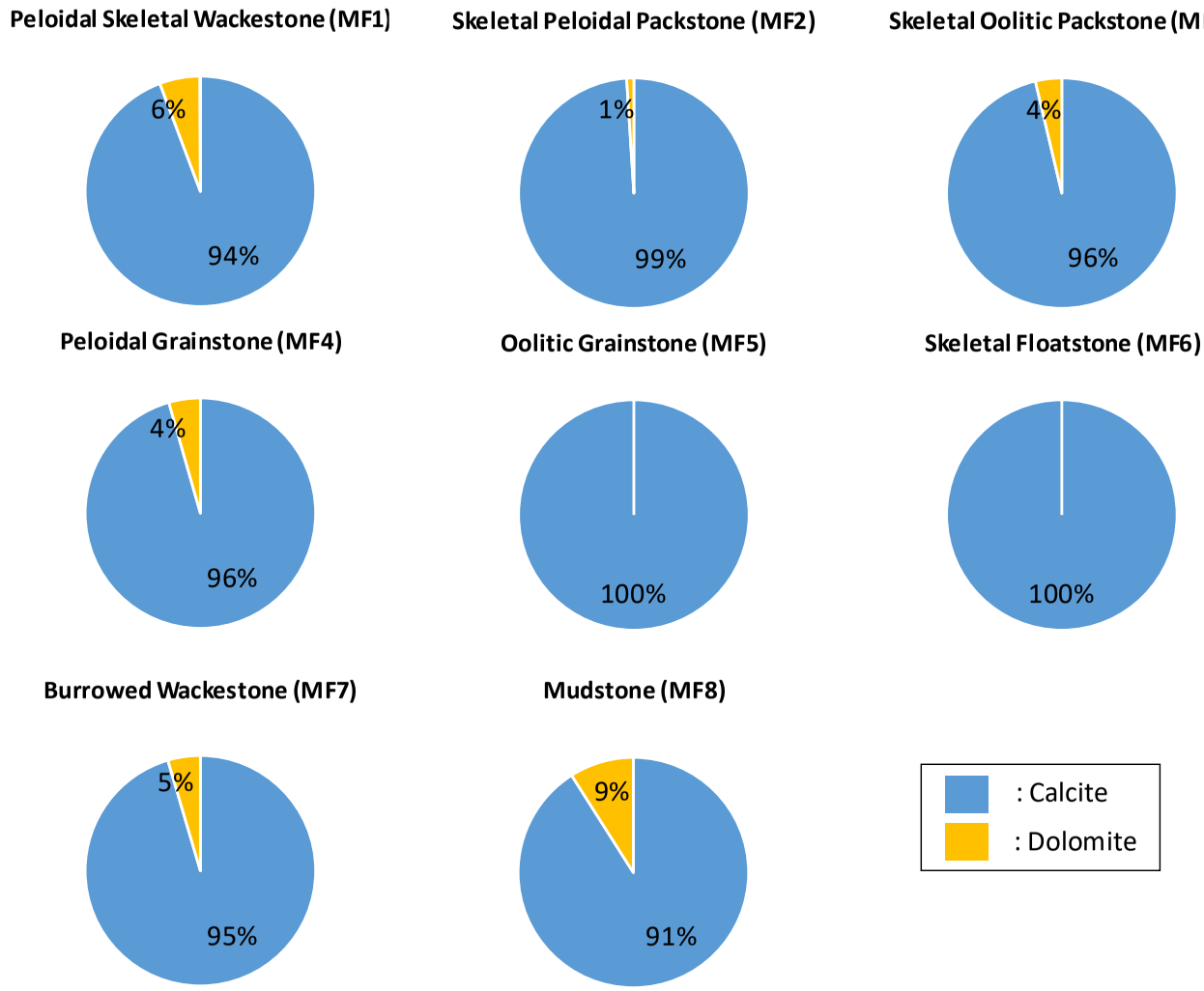


Figure 4.17. Mineralogical composition of each microfacies is presented above. Calcite is the most abundant mineral, then followed by dolomite.

## 4.4 Microfacies Distribution

Among the eight microfacies, skeletal peloidal packstone and burrowed wackestone occur as the most abundant microfacies in the study area (Figure 4.18). Skeletal peloidal packstone is mostly found in the D3 Unit of section 1, whereas burrowed wackestone is commonly found in the D4 Unit of section 2. The D3 Unit is generally characterized by thickly-bedded skeletal peloidal packstone and peloidal skeletal wackestone. In contrast, the D4 Unit is characterized by thickly-interbedded peloidal and oolitic grainstone-mudstone.

Peloid is the major non-skeletal grain throughout all the sections. These are commonly formed by micritization on ooids or skeletal grains. Another major grain is ooid which generally formed either concentric, radial and mixed concentric-radial fabric. Tangential ooids characterize burrowed wackestone and skeletal oolitic packstone, while radially-arranged crystals of ooids are common to abundant in oolitic grainstone. Additionally, some microfacies including oolitic grainstone, skeletal oolitic packstone contain grapestones and intraclasts made up from ooids and bivalve shells.

Mollusk fragments including gastropods and bivalves are moderately abundant throughout both sections. Benthic foraminifera reach great diversity in the lower part of section 1 and display lower diversity up-dip towards the D4 Unit. Echinoderms and brachiopods are rarely found in the lower part of section 1, while sponge spicules of monoxon and triaxon are common.

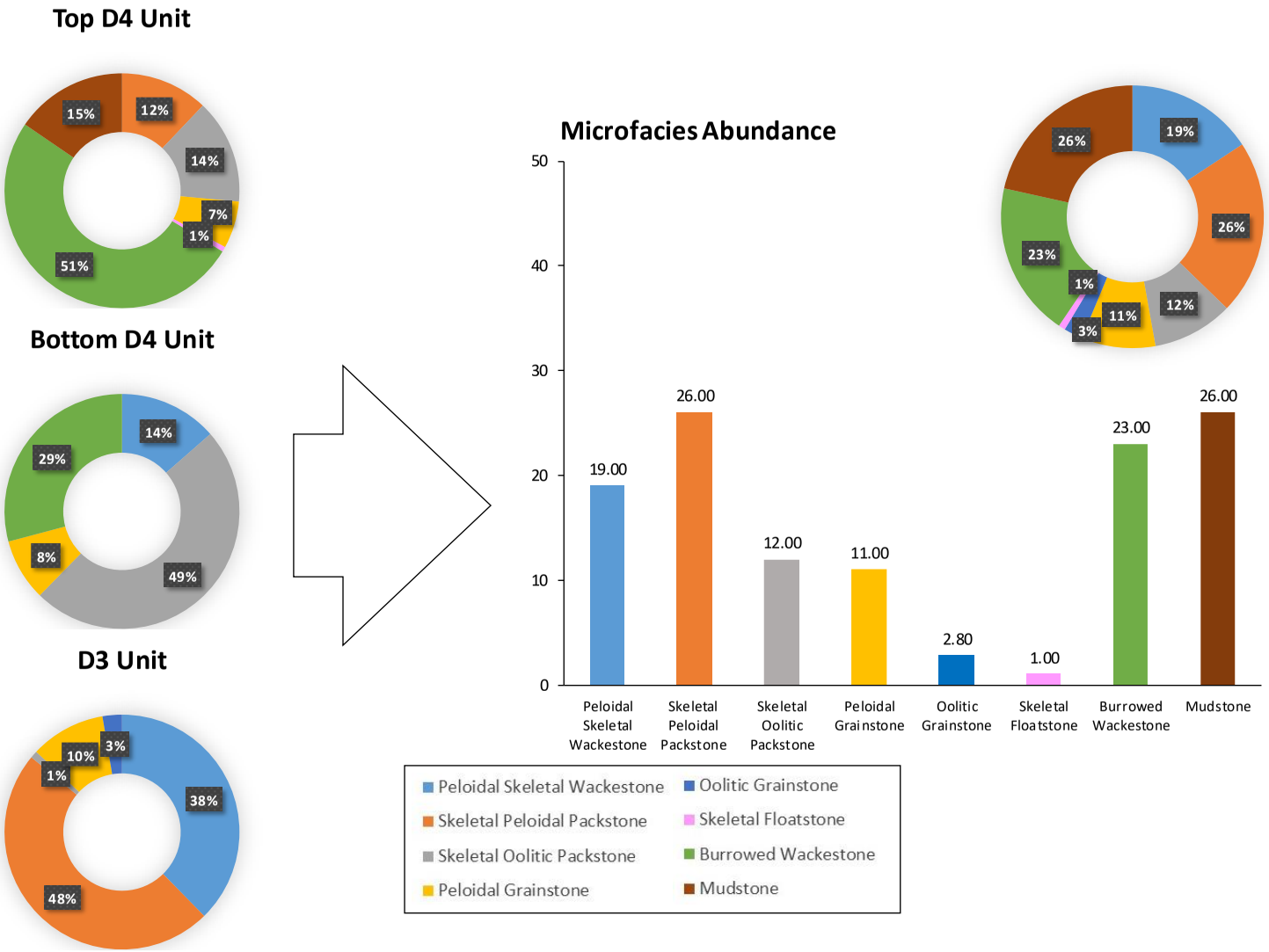


Figure 4.18. Microfacies abundance in the study area.

## 4.5 Biofacies Analysis

The biofacies analysis of fossils in the study area is based on a semi-quantitative analysis of hundreds of thin sections. The interpretation is generally representative due to a consistency with the interpreted depositional environments inferred from microfacies analysis. Biofacies zones in the study area are classified as 3 distinctive biofacies zones including biofacies A, biofacies B, and biofacies C. These groups based on the presence of a within these biofacies in association with the which later can provide evidence for accessing paleoenvironments.

Biofacies A contains generally abundant benthic foraminifera including *Globivalvulina* sp., *Pfenderina* sp., *Redmondoides* sp., and *Nautiloculina* sp. (Figure 4.19). These benthic foraminifera are commonly associated with gastropod, echinoderm, bivalve, and brachiopod fragments. The abundant foraminifera assemblage in low-energy environment corresponds to limited non-skeletal grains (i.e., ooids, intraclasts, and grapestones).

Biofacies B is characterized by the benthic foraminifera *Trocholina* spp. which is often associated with gastropod fragments. This biofacies is commonly encountered in the oolitic grainstone facies as whole grain that may be coated by a thin micritic envelope.

Biofacies C constitutes fragments of *Cladocoropsis*, monoxon and triaxon sponge spicules. These fossils are found in association with gastropod fragments. Sponge spicules of monoxon and triaxon are frequently found along with foraminiferal assemblages of *Pfenderina* sp., *Nautiloculina* sp., *Redmondoides* sp., *Globivalvulina* sp. especially in the peloidal skeletal wackestone microfacies. Figure 4. displays the relative

abundant fossils in the study area which showed low and high diversity of each faunas as indicated by two different lines.

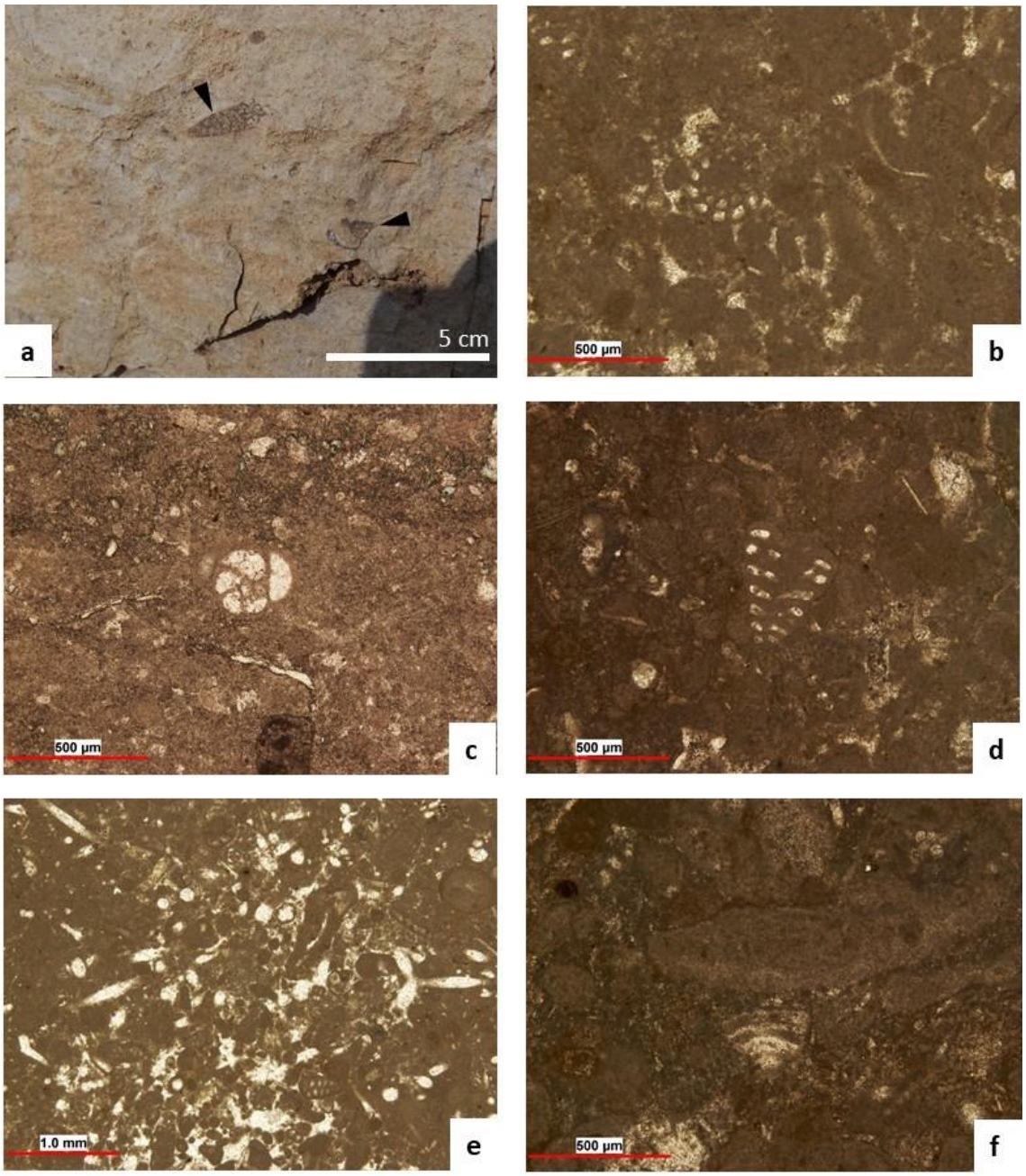


Figure 4.19. Representative fossils of a. Large gastropods, b. *Nautiloculina* sp. c. *Globivalvulina* sp., d. *Redmondoides* sp., e. Monoxon and triaxon sponge spicules, f. *Trocholina* spp.

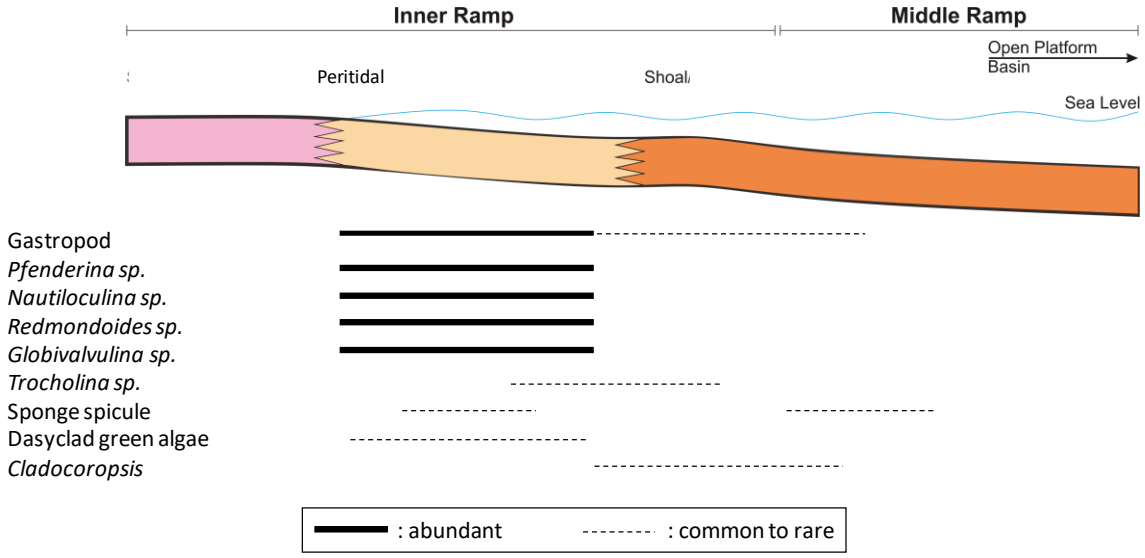


Figure 4.20. Paleoenvironment indicator and its relationship with fossil assemblages in the study area extracted from this study

## 4.6 Porosity and Permeability Distribution

A total of 69 core plugs from the studied sections have porosity values ranging from 1% to 30.2% with an average of 12.5%. Permeability ranges from 0 to 8 mD with an average of 0.22 mD. Porosity-permeability plots of all the microfacies are illustrated in Figure 4.21. There is no trend in the plot and this might have been due to diagenetic processes which might have either destroyed or enhanced porosity. All porosity types in the study area are presented in Figure 4.22. The low porosity-permeability values correspond to mud-supported facies (Figure 4.22a) and the highest porosities are associated with skeletal oolitic packstone. Higher porosity is attributed to moldic porosity produced by leached ooid grains (Figure 4.22b) and interparticle (Figure 4.22c), while lower porosity is caused by abundant lime mud and highly cemented microfacies (Figure 4.22d). Another secondary porosity which may improve the porosity is due to leaching of dolomite rhombs caused by calcitization which mainly occurs in the D4 Unit (Figure

4.22e). Additionally, some microfacies have developed fracture pore that can also enhance porosity (Figure 4.22f).

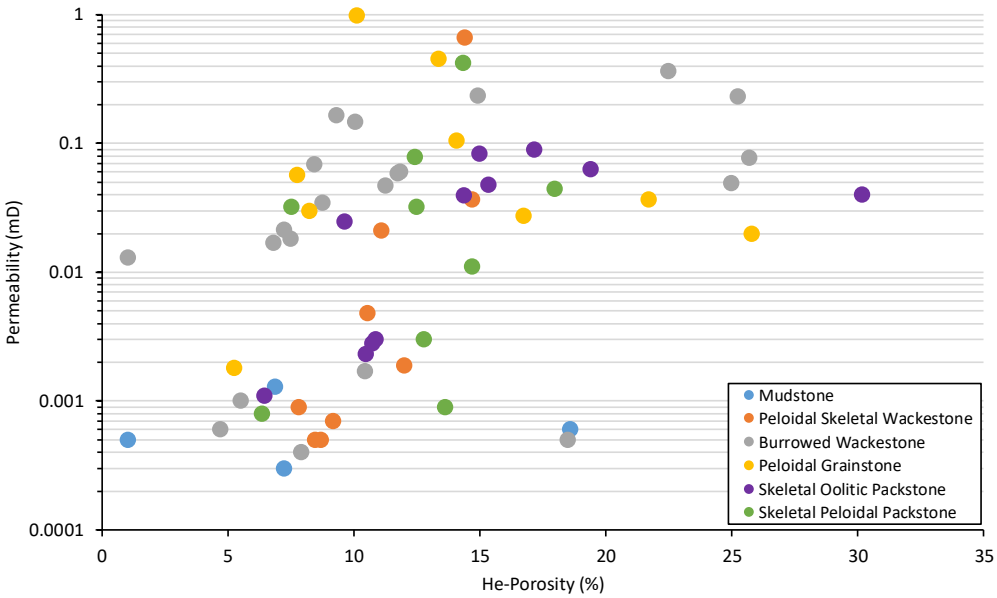


Figure 4.21. Porosity-permeability cross plot of all the microfacies

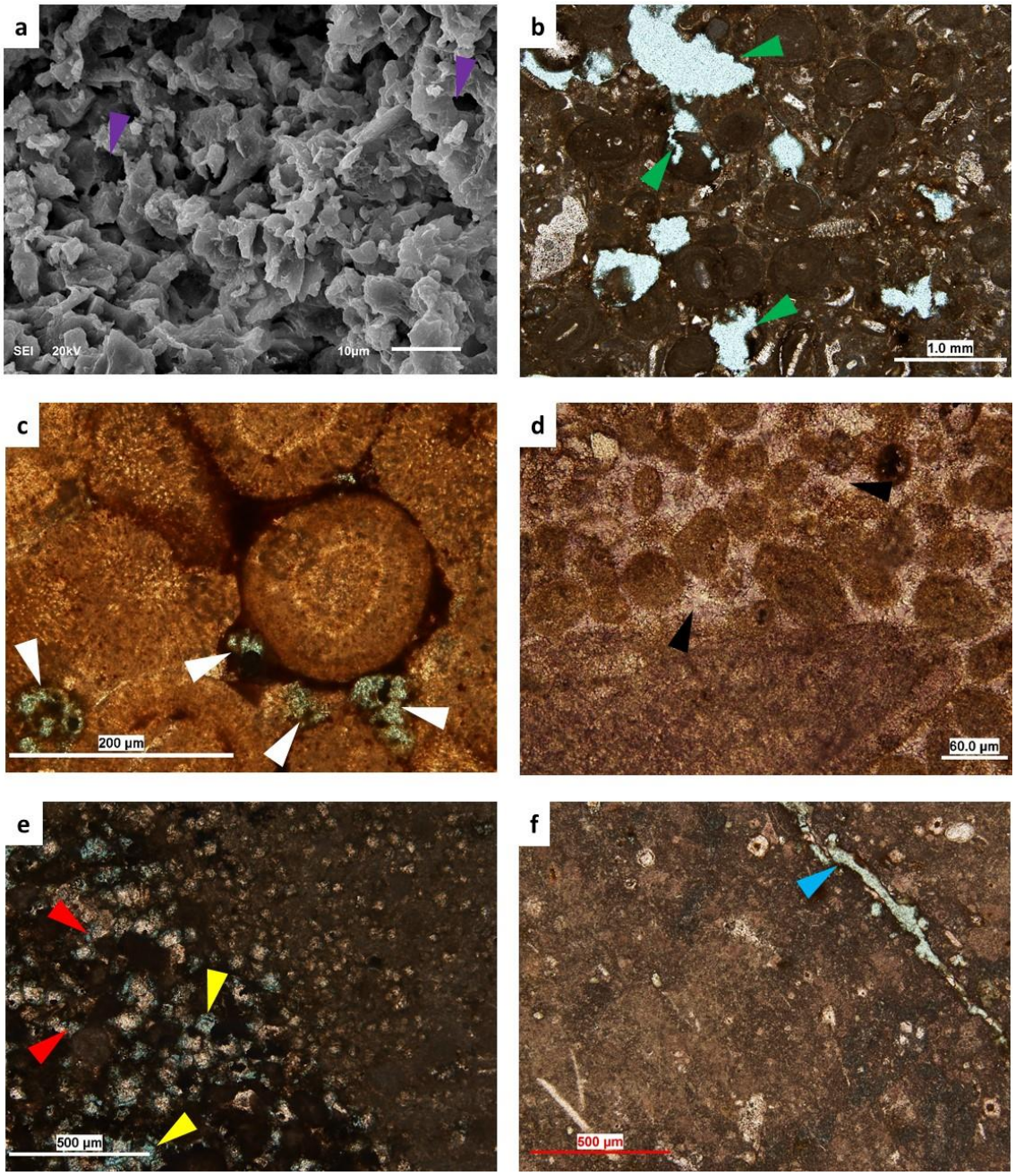


Figure 4.22. a. Micropores (purple arrow) is commonly found in micrite mud, b. Secondary porosity point in green arrow (probably moldic pores of ooids) generally found in skeletal ooids packstone, c. Intergranular porosity (white arrow) between radial-fabric ooids, d. Destruction of porosity by extensive calcite cementation in peloidal grainstone, e. Partial dissolution of fabric-destructive dolomite concentrated only particularly in burrow (?). Note the location of intercrystalline (red arrow) and leached dolomite (yellow arrow) pores, f. Fracture (blue arrow) developed in a mud-supported facies.

# CHAPTER V

# DISCUSSIONS

## 5.1 Depositional Environment

Interpreting the depositional environment of the studied sections involves the integration of all related information from macro- (i.e., sedimentary structure and hand-specimen samples) to micro-scale (i.e., grain and fossil components). Few information on sedimentary structures including burrows and lamination has been recorded from the field work. The information derived from XRD and petrographic analyses showed that minor quantities of silica (i.e., quartz and kaolinite) are locally concentrated in section 1 which represent the mud-supported facies of the D3 Unit. This indicates a low influx of detrital sediments during the depositional time of the investigated sequence.

According to Manivit (1985), the Middle Dhruma Formation in the study area was deposited in a subtidal environment. The D3 Unit in the study area starts with a thin bed of oolitic limestone. This is consistent with the findings of Manivit (1985) who stated that the D3 Unit commenced with limestone rich in ooids at Khashm adh Dhibi. Likewise, the D4 Unit in the study area is consistent as defined by Manivit (1985). It is composed mainly of abundant non-skeletal grains (i.e., peloids, ooids, grapestones, and intraclasts) and less commonly skeletal grains (i.e., mollusks, brachiopod, foraminifera, algae).

Evidence from sedimentary structure and associated grains in all the microfacies suggests deposition within inner to outer ramp as shown below in Figure 5.1 as a 3D model and Figure 5.2 as a 2D transect along an inner to outer ramp.

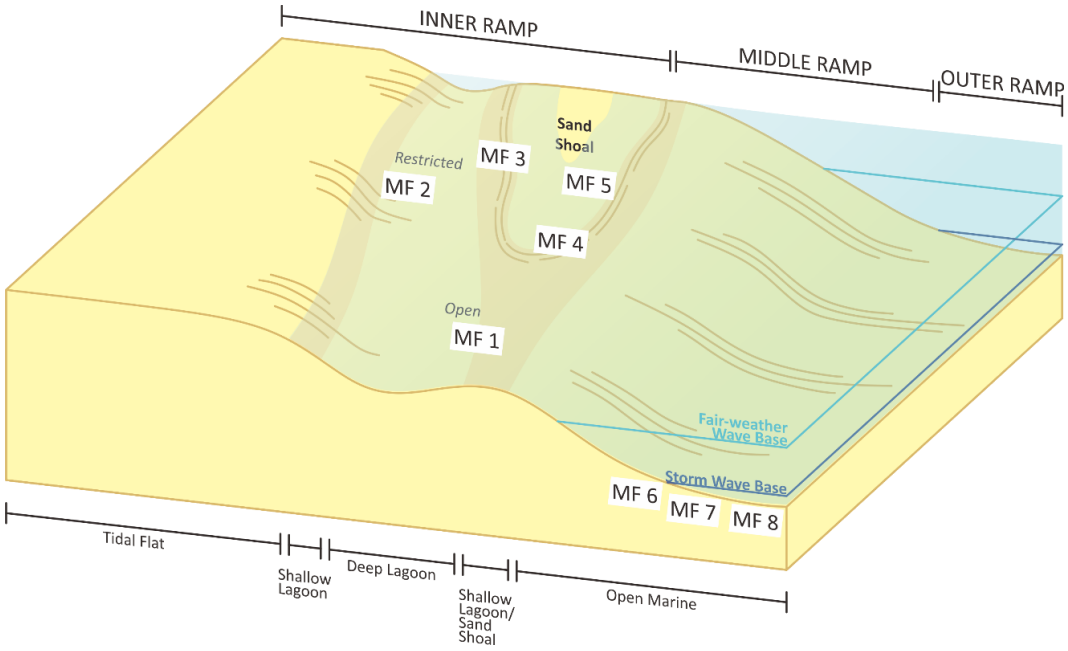


Figure 5.1. Depositional environment of the studied member spanning from lagoon to open marine setting (from distal inner ramp to proximal outer ramp). Note that scale is vertically and laterally exaggerated.

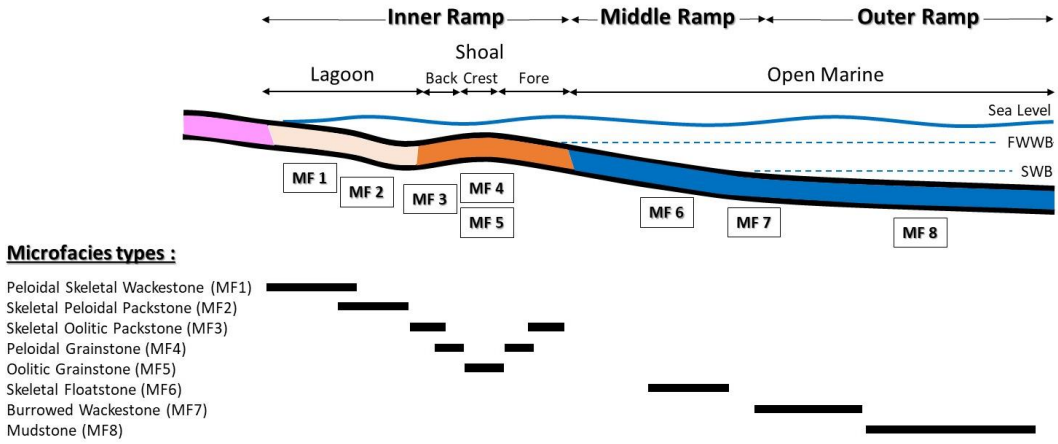


Figure 5.2. Schematic 2D depositional environment model.

The lagoonal setting comprises microfacies 1 and 2 as shown in the figure above. Peloidal skeletal wackestone and skeletal peloidal packstone contain abundant to common foraminifera assemblages. This environment corresponds to biofacies A, which is mainly found in restricted to open lagoon environment.

Peloidal skeletal wackestone was deposited in a moderate energy because of these factors including relatively diverse grain associations (i.e., peloids, mollusk and brachiopod fragments) and abundance of lime-mud. Besides, relative abundance of benthic foraminiferal species (i.e., *Pfenderina* sp., *Nautiloculina* sp. *Redmondoides* sp., and *Globivalvulina* sp.) and spicule of monoxon and tetraxon types which generally found in open marine setting are evidence of open marine environment (Hughes, 2004; Al-Dhubaib, 2010). Less occurrences of ooids with concentric-fabric which were likely transported from high-energy shoal are an indicative of open setting, lagoon environment (Strasser, 1986). Another line of evidence is provided by the presence of *Thalassinoides* that mostly occurs in the transition zone between continental and shallow marine (Seilacher, 2007). Addditionally, similar case was observed in the Jurassic carbonate of Arab Formation in Saudi Arabia that such burrow could be formed in inner to outer ramp with the maximum vertical penetration depth from a few tenths of meter to 2.4 m (8 ft) (Lindsay et al., 2006).

Skeletal peloidal packstone composes of abundant equal-sized, fine-peloids and moderate faunal diversity suggesting a normal salinity, low to moderate water circulation, restricted lagoon setting. This is supported by the idea of the occurrence of *Trocholina* spp. which was commonly found in shallow to deep lagoon environment (Hughes, 2004). In addition, the presence of green algae in this microfacies is an indicative of a lagoonal environment (Hughes, 2004).

The shoal complex is dominated by moderate-energy microfacies of peloidal grainstone, oolitic grainstone, and skeletal oolitic packstone, and corresponds to biofacies B. Peloidal

grainstone and oolitic grainstone are located slightly up-dip than skeletal oolitic packstone which may be deposited in back- or fore shoal environment (Figure 5.2).

Skeletal oolitic packstone composes of abundant concentric-radial ooids and common skeletal grains of gastropod and mollusk. This microfacies is interpreted to be deposited in a relatively calm, protected shallow marine environment. A line of evidence is supported by common cortical-fabric ooids which could be formed in a high-energy wave agitation and may suggest shoal complex (Strasser, 1986). Additionally, the presence of lagoonal foraminifera belonging to *Nautiloculina* sp. and gastropods acted as ooid nucleus have transported from their origin (shallow to deep lagoon) to this environment (Hughes, 2004).

Peloidal grainstone has a characteristic of abundant well-sorted peloids. This may suggest a shallow and moderately agitated environment. The lack of benthic foraminifera is another line of evidence to support the prevalence of moderate to high-energy waves at the time the facies was deposited. Based on these factors, this microfacies was likely deposited in a shoal complex and has close relationship with oolitic grainstone, which is also deposited in a similar environmental setting.

Oolitic grainstone is interpreted to be deposited in a high-energy, wave-agitated shoal complex (Tucker and Wright, 1990), up-dip position compared with skeletal oolitic packstone and peloidal grainstone. These lines of evidence are supported by the occurrence of mixed forms of ooids with relatively abundant radial fabric over other types of fabric and the presence of micritized ooids in which large variability of wave-agitation is suggested to facilitated the formation of ooids (Flugel, 2010). Similarly,

radial fabric ooids from Arab Formation of Saudi Arabia were interpreted to have been deposited on a high energy grain shoal in platform interior (Cantrell, 2006). Additional evidence is provided by the presence of benthic foraminifera namely *Nautiloculina* sp., and *Trocholina* spp. which were frequently found in a relatively calm, shallow marine environment and adjacent to shoal complex (Hughes, 2004). Some of which act as the nucleus of ooids, and their tests are heavily micritized and dumped along with other grains. Those foraminifera may probably be allochthonous fossils from a neighboring environment (i.e., lagoon) that have been swept by water agitation to be deposited in this environment.

Additionally, mixed form of ooids with relatively abundant radial-fabric ooids over concentric-, concentric-radial fabric and highly preserved lamellae may imply that either they were originally stable or were stabilized over time through diagenesis (Strasser, 1986; Cantrell, 2006). Ancient radial ooids during the Jurassic were originally of calcite mineralogy with radially oriented crystal (Cantrell, 2006) and tended to be formed in a relatively calm to moderate-energy environment with a different level of salinity (Strasser, 1986) compared with modern ooids in the Arabian Gulf that are primarily aragonite and form in a high-energy, wave- or tide-dominated environment (Amao and Al-Ramadan, 2017). These phenomena are because the period of the Calcite Sea during the Jurassic as stated by Sandberg (1983) favored ooids precipitation as calcite, rather than as aragonite.

The open marine setting is mostly dominated by mud-supported facies of burrowed wackestone, mudstone, and relates to biofacies C. Another microfacies in the open

marine setting is the skeletal floatstone and interpreted as a derived-skeletal bank deposit. This microfacies is interpreted to be a product of storm deposit as evidenced by the occurrences of the following features: 1. moderate to poor sorting, disorganized grains of echinoid, brachiopod, and bivalve fragments, 2. relatively high mud concentration (over 30%) may indicate further basinward, 3. a sharp contact (erosional base) with the underlying beds (Carozzi, 1988 p. 61; Flugel, 2010).

Burrowed wackestone is composed of allochthonous ooids with concentric fabric and the occurrence of *Cladocoropsis* fragments that is commonly deposited in a lagoonal environment (Hughes, 2004). This microfacies is suggested to be deposited in a proximal middle ramp because of storm/ wave agitation. In addition, sparse sponge spicules of monoxon which are commonly associated with *Cladocoropsis* fragments can easily be transported by storms and redeposited in the proximal middle ramp (Lindsay et al., 2006). Abundant micritic matrix suggests that this facies might have been deposited in a moderate to low energy environment (Tucker and Wright, 1990). Based on these factors, the interpreted depositional environment is suggested to have been in the basinward part of the shoal complex and below the fair-weather wave base (FWWB), above the storm-wave base (SWB).

Mudstone is interpreted to be deposited on a middle ramp below the SWB and represented the deepest part of the section in the study area. Evidence to support the interpretation, are provided by the absence of grains and is often associated with a highly burrowed microfacies (burrowed wackestone) (Flugel, 2010). Abundant microcrystalline carbonate mud is also another indication of a restricted, low-energy setting (Tucker and

Wright, 1990). An occasional occurrence of brachiopod and mollusk fragments that commonly accumulated in a shallower setting is an indicative of allochthonous origin. Although this type of microfacies can be deposited in shallower marine settings (i.e., open lagoon), the absence of calcareous algae is another line of evidence which may suggest low-energy environments below wave base, middle to outer ramp (Flugel, 2010)

## 5.2 Comparison to Other Ancient Carbonate Ramp Settings

The Dhruma Formation in the study area resembles other carbonate ramp settings, for example in Oman. Schlaich and Aigner (2017) reported that the Dhruma Formation in Oman was deposited on an epeiric carbonate ramp. The authors subdivided the Dhruma paleoenvironmental setting into 3 distinctive zones including low-, medium-, and high-energy zones. Their analysis of the sediments that were deposited in a low to high-energy zone, correlates to the lagoon to shoal cycles in the present study (Figure 5.3a). Moreover, shallowing upward cycle of open marine to shoal in this study corresponds to the low- to high-energy zone of the Dhruma Formation in Oman (Figure 5.3b).

The lagoonal setting in the study area is represented by a coarsening upward sequence with a thickness of 3 meters. This cycle commences with peloidal skeletal wackestone and is eventually capped by oolitic grainstone. Comparing these findings with the study of Schlaich and Aigner (2017) their interpreted cycle starts with thick massive mudstone with common skeletal grains and peloids, then followed by another low-energy lithofacies of wacke-packstone with common gastropods, bivalves, brachiopods fragments, and non skeletal grains including peloids and ooids, and is finally capped by

oolitic grainstone. The present study and the study of Schlaich and Aigner reveal abundant bioturbation, especially in the low-energy setting.

A shallowing upward sequence from open marine to shoal in the present study is indicated by mudstone, overlain by burrowed wackestone, and finally overlain by peloidal grainstone. Likewise, interbedded wackestone and massive pack- to grainstone are indicative of low-energy basinward, then this lithology gradually changes to peloidal grainstone which represents the high energy zone. The low-energy zone of massive pack- to grainstone contains bivalves, brachiopods, gastropods, echinoderms, peloids, and ooids. This lithology is comparable to burrowed wackestone which is composed of common skeletal grains of bivalves, ooids and peloids and rare gastropods.

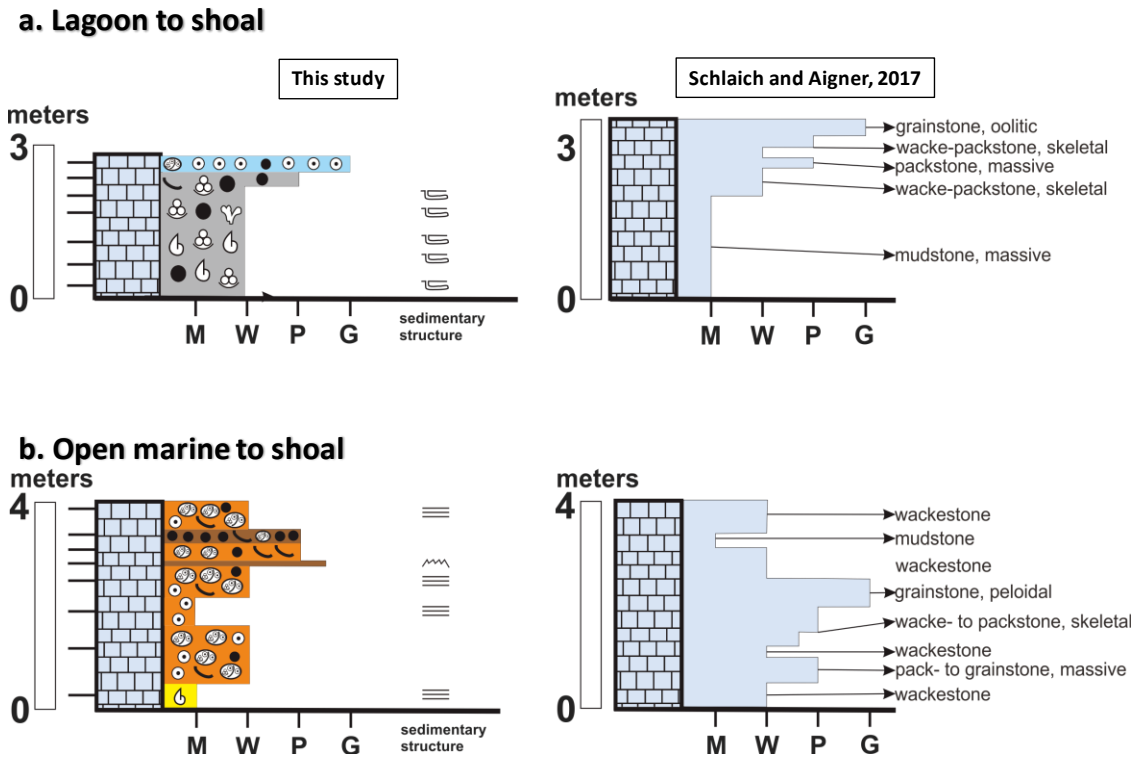


Figure 5.3. Comparison of ancient carbonate ramp along the western margin of Paleo-Tethys Sea in (a) lagoon to shoal and (b) open marine to shoal setting.

## 5.3 Petrophysical Properties of the Middle Dhruma

Over 50 % of the world's hydrocarbon reservoirs are found in carbonate rocks (Warren, 2000; Ehrenberg and Nadeau, 2005). Apart from primary porosity (i.e., intra- and interparticle, etc.) which is commonly developed during depositional time, most of carbonate porosity are developed after deposition (secondary porosity). The studied members show how dolomite rhombs can increase porosity when calcitization (dedolomitization) process takes place especially in the D4 Unit. Porosity in the mud-supported microfacies in D3 Unit is moderate to low (less than 15% average) as compared to D4 Unit. Therefore, discussion on the petrophysical properties are concentrated exclusively on the D4 Unit.

Figure 5.4, 5.5, and 5.6 show porosity-permeability values of 3 distinctive microfacies association including lagoon, shoal complex, and open marine. Lagoonal environment shows slightly less porosity-permeability values ranging from 5 to 17 % porosity with permeability values of less than 1 mD (Figure 5.4). Other environments such as the shoal complex and open marine, on the contrary, are characterized by a wide range of porosity-permeability values (por: 2-30%) which may suggest high and low reservoir potentialities at the same time. Low porosity values in lagoon environment are expected due to abundant lime mud. While high porosity values in shoal and open marine environments could be attributed to dissolution of ooid (moldic pores) and dolomite rhombs in burrows (intra-, intercrystalline pores), respectively.

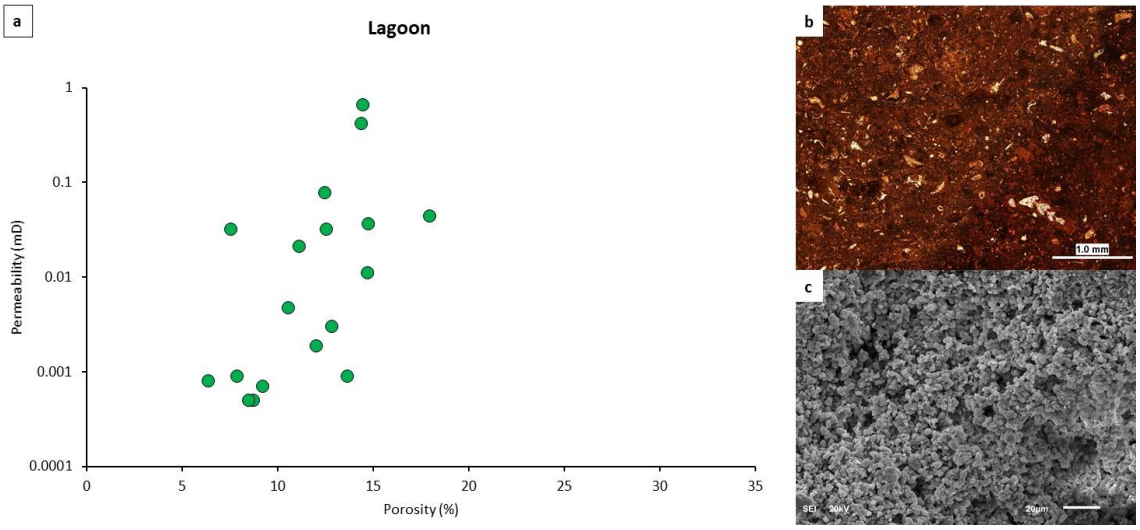


Figure 5.4. Helium porosity-permeability plot of microfacies association of lagoon environment (a). Although visual porosity can be seen under thin section (b), porosity enhancement by micropores (c).

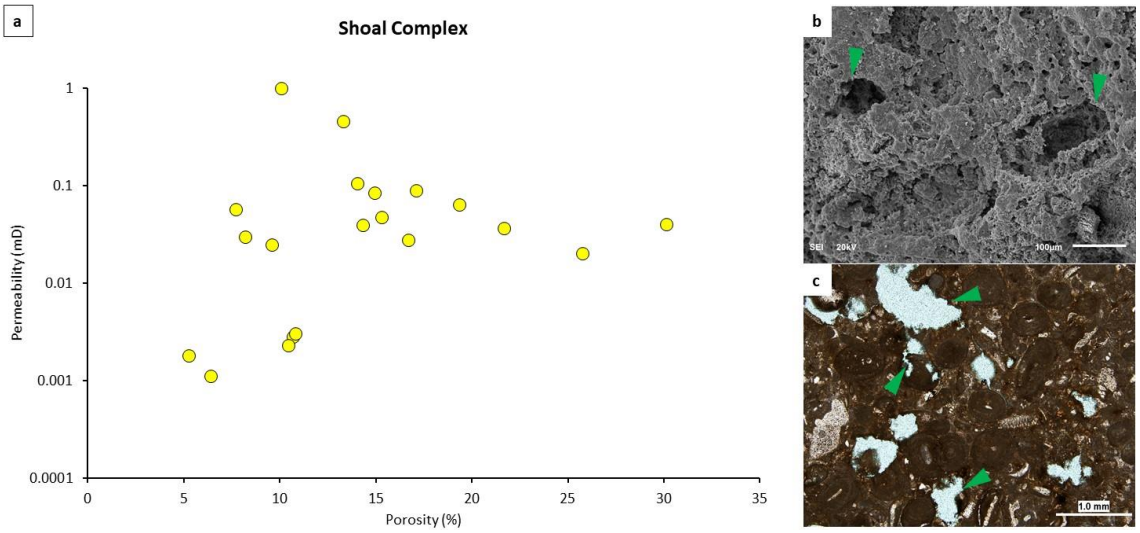


Figure 5.5. Helium porosity-permeability plot of microfacies association of shoal complex environment (a). SEM (b) and thin section (c) photomicrographs provided evidence of the dissolution of ooid grains.

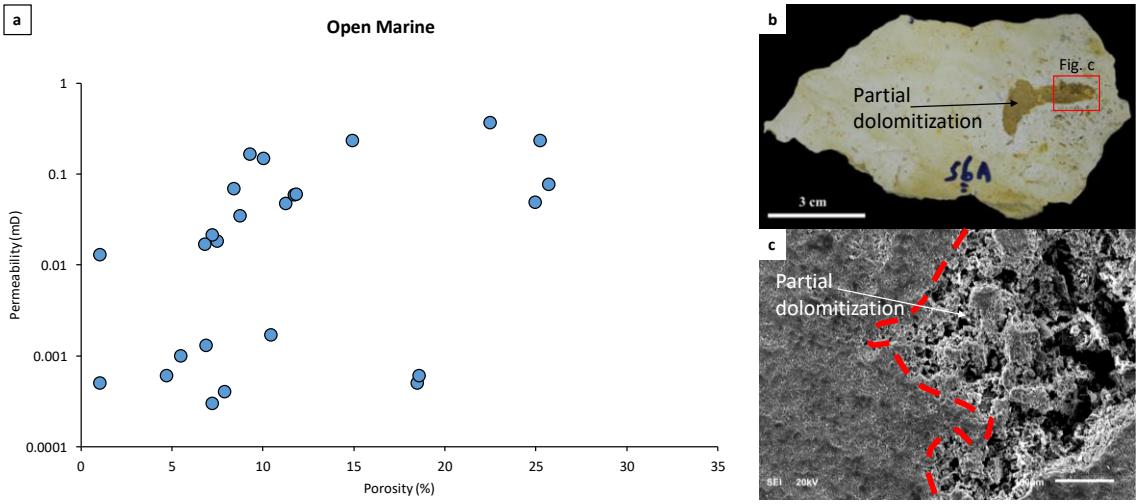


Figure 5.6. Helium porosity-permeability plot of microfacies association of open marine environment (a). High porosity values (> 17 %) can be attributed to partial dolomitization in burrows as shown in slabbed rock (b) and SEM (c).

The lower D4 Unit as seen in Figure 5.7, is slightly dolomitized in the lower part and shows a slight increase in porosity and permeability compared to surrounding beds. Likewise, the upper D4 Unit generally contains relatively high porosity and permeability values in the lower part as depicted in Figure 5.8. Relatively high porosity (up to 27 %) relates to calcitization or dedolomitization process in burrowed wackestone.

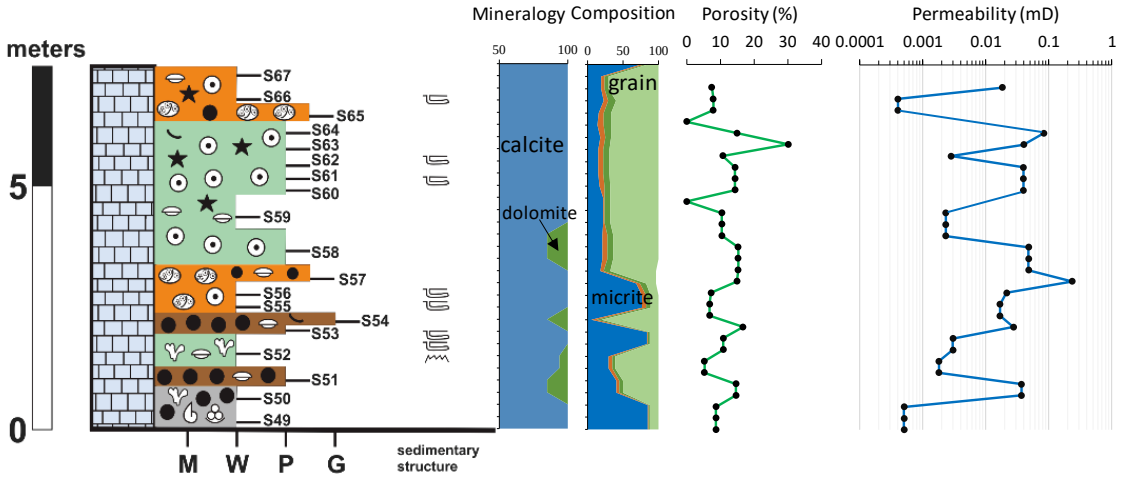


Figure 5.7. Vertical variations in the petrophysical characteristics of Lower D4 Unit. See page 41 for the explanation of color code.

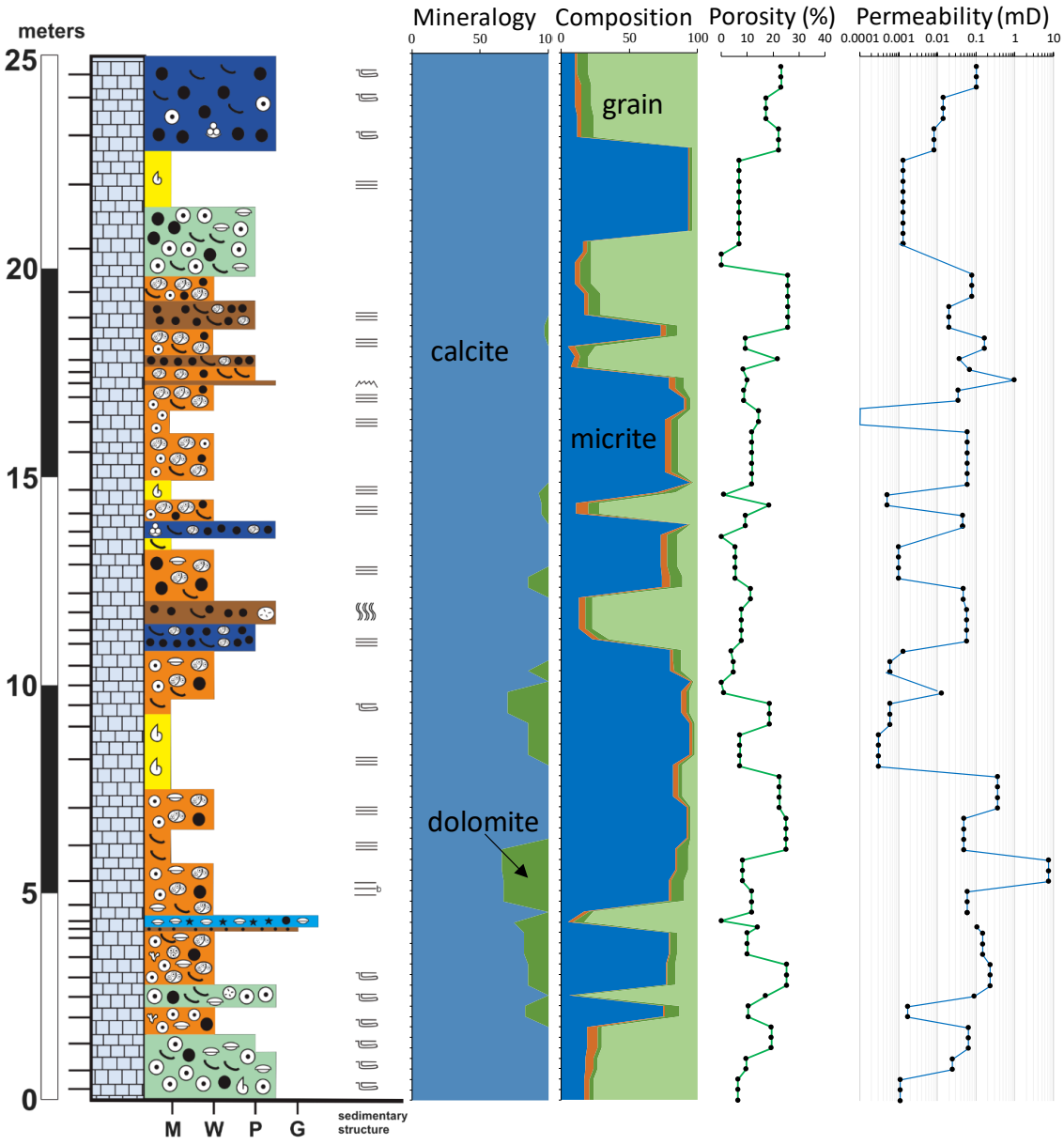


Figure 5.8. Vertical variations in the petrophysical characteristics of Upper D4 Unit. See page 41 for the explanation of color code.

Partial dolomitization typically occurs in the D4 Unit especially in burrows (Figure 5.6b and c) and be a factor to vertical and lateral heterogeneity in terms of mineral, texture and pore-type (Lindsay et al., 2006). One dolomite phase, called non-fabric preserved dolomite, exists in the studied units. Non-fabric preserved (NFP) dolomite selectively

filled burrows in burrowed wackestone and some are found scattered in the lime mud. Such dolomite has lost the original limestone fabric and have been completely obliterated. Dolomite in the study area has crystal sizes ranging from 50 to 120 microns (fine-size crystals) and crystal shapes of euhedral to subhedral. This dolomite type occurrs in the basal to middle parts of D4 Unit and is commonly associated with skeletal oolitic packstone in which the presence of anhydrate as a cement is found. The presence of evaporite relics provide the source of Ca-rich solution and can suggest the timing for calcification reaction (Warren, 2000). In comparison, NFP dolomite in subsurface well of Arab Formation is considered as to be of poor reservoir quality with a porosity of over 10 % and permeability value of less than 1 mD (Lindsay et al., 2006). The reason is that there is no dolomite dissolution, instead, dolomite has filled the pores by dolomitization process at the nucleation site.

# CHAPTER VI

# CONCLUSIONS AND RECOMMENDATIONS

## 6.1 Conclusions

The Dhruma Formation in the study area presents an important role in investigating ancient carbonate ramp in a passive margin. This study investigates vertical stacking patterns in the D2, D3 and D4 Units using sedimentological and petrography studies in Hafirat Nisah area.

Sedimentological and petrographic descriptions revealed 8 different microfacies types including Peloidal Skeletal Wackestone, Skeletal Oolitic Packstone, Skeletal Peloidal Packstone, Peloidal Grainstone, Oolitic Grainstone, Skeletal Floatstone, Burrowed Wackestone and Mudstone. These facies were deposited in a shallow marine (peritidal to open marine) without pronounced abrupt clastic influx and relatively calm, warm water environment. These microfacies were further classified into 3 major setting including lagoon (i.e., Skeletal Peloidal Packstone, Peloidal Skeletal Wackestone), shoal complex (i.e., Skeletal Oolitic Packstone, Peloidal Grainstone, Oolitic Grainstone), and open marine (i.e., Mudstone, Skeletal Floatstone, Burrowed Wackestone).

Biofacies analysis supports the interpretation of the depositional environments by providing fossils and non-skeletal grains relationship. The biofacies in the outcrop sections is categorized as 3 major depositional settings, biofacies A correspond to lagoon environment, biofacies B characterized the transition zone between lagoon-shoal-open marine, biofacies C is predominantly of open marine/ outer ramp setting.

Reservoir quality in the studied outcrops can be attributed to limestone with a significant dissolved dolomite rhomb in burrowed wackestone and peloidal grainstone microfacies, moldic pores of skeletal oolitic packstone microfacies, interparticle and moldic pores of oolitic grainstone microfacies. High amount of cementation and the abundance of lime mud are considered the reducing factors of the reservoir quality in the identified microfacies.

## 6.2 Recommendations

Based on this study, rock physics and property modeling approaches using micro-Computed Tomography Scan and mercury injection capillary pressure (MICP) can lead to a better understanding of vertical and lateral continuity of burrows with respect to porosity and permeability. Additionally, diagenetic study is crucial and will be needed to better understand the post-depositional control on reservoir quality of the D3 and D4 Units.

# REFERENCES


Ahr, W. M., 1967, The Carbonate Ramp : An Alternative to the Shelf Model: Gulf Coast Association of Geological Societies Transactions, v. 23, p. 221–225.

Al-Dhubaib, A. J., 2010, Taxonomy and Palaeoenvironments of Middle and Late Jurassic Foraminifera and its associations of Saudi Arabia: University College London, 401 p.

Al-Husseini, M. I., 1997, Jurassic Sequence Stratigraphy of the Western and Southern Arabian Gulf: GeoArabia, v. 2, no. 4, p. 361–382.

Al Ibrahim, M. A., J. F. Sarg, N. Hurley, D. L. Cantrell, and J. D. Humphrey, 2017, Depositional environments and sequence stratigraphy of carbonate mudrocks using conventional geologic observations, multiscale electrofacies visualization, and geochemical analysis: The case of the Tuwaiq Mountain and Hanifa Formations in a basinal settin: AAPG Bulletin, v. 101, no. 5, p. 683–714, doi:10.1306/08051615221.



Al Ibrahim, M. A., J. F. Sarg, N. Hurley, D. L. Cantrell, and J. D. Humphrey, 2017, Depositional environments and sequence stratigraphy of carbonate mudrocks using conventional geologic observations, multiscale electrofacies visualization, and geochemical analysis: The case of the Tuwaiq Mountain and Hanifa Formations in a basinal settin: AAPG Bulletin, v. 101, no. 5, p. 683–714, doi:10.1306/08051615221.



Al-Mojel, A. S. I., 2010, High-Resolution Sequence Stratigraphy of the Middle Jurassic Lower Fadhili Reservoir in Khurais Complex, Central Saudi Arabia: King Fahd University of Petroleum and Minerals, 117 p.

Alsharhan, A. S., and C. G. Kendall, 1986, Precambrian to Jurassic Rocks of Arabian Gulf and Adjacent Areas: Their Facies, Depositional Setting, and Hydrocarbon Habitat: AAPG Bulletin, v. 70, no. August, p. 977–1002.

Alsharhan, A. S., and K. Magara, 1994, The Jurassic of the Arabian Gulf basin: Facies, depositional setting, and hydrocarbon habitat: Canadian Society of Petrolem Geologist Memoir, v. 17, p. 397–412.

Alsharhan, A. S., and A. E. M. Nairn, 1997, Sedimentary Basins and Petroleum Geology of the Middle East: 934 p.

Amao, A. O., and K. Al-Ramadan, 2017, Discussions on Arabian Gulf ooids: Carbonates and Evaporites, doi:10.1007/s13146-017-0396-8.

Arkell, W. J., B. Y. R. A. Bramkamp, and M. Steineke, 1952, Jurassic ammonites from Jebel Tuwaiq, Central Arabia: 241-309 p.

Beydoun, Z. R., 1986, The petroleum resources of the Middle East: A review: Journal of Petroleum Geology, p. 5–28.

Burchette, T. P., and V. P. Wright, 1992, Carbonate ramp depositional systems: Sedimentary Geology, v. 79, p. 3–57.

Cantrell, D. L., 2006, Cortical fabrics of Upper Jurassic ooids , Arab Formation , Saudi Arabia : Implications for original carbonate mineralogy: Sedimentary Geology, v. 186, p. 157–170, doi:10.1016/j.sedgeo.2005.11.015.

Cantrell, D. L., P. G. Nicholson, G. W. Hughes, M. A. Miller, A. G. Buhllar, S. T. Abdelbagi, and A. K. Norton, 2014, Tethyan Petroleum Systems of Saudi Arabia, *in* AAPG Memoir: p. 613–639, doi:10.1036/13431867M1063615.

Carozzi, A. V., 1988, Carbonate rock depositional models: A microfacies approach: New Jersey, Prentice Hall, 604 p.

Choquette, P., and L. Pray, 1970, Geologic Nomenclature and Classification of Porosity in Sedimentary Carbonates: AAPG Bulletin, v. 54, no. 2, p. 207–250, doi:10.1306/5D25C98B-16C1-11D7-8645000102C1865D.

Cuvillier, J. E. A. N., 1952, La notion de" microfaciès" et ses applications., *in* VII Convegno Nationale del Metano et del Petrolio: p. 3–7.

Dunham, R. J., 1962, Classification of Carbonate Rocks According to Depositional Textures, *in* AAPG Memoir: p. 108–121.

Edgell, S., 1992, Basement tectonics of Saudi Arabia as related to oil field structures, *in* Basement Tectonics: p. 169–193, doi:10.1007/978-94-011-2654-0_10.

Ehrenberg, S. N., and P. H. Nadeau, 2005, Sandstone vs. carbonate petroleum reservoirs: A global perspective on porosity-depth and porosity-permeability relationships: AAPG Bulletin, v. 89, no. 4, p. 435–445, doi:10.1306/11230404071.

El-Sorogy, A. S., M. A. Galmed, K. Al-Kahtany, and A. Al-Zahrani, 2017, Microfacies and diagenesis of the Middle Jurassic Dhruma carbonates, southwest Riyadh, Saudi Arabia: Journal of African Earth Sciences, v. 130, p. 125–133, doi:10.1016/j.jafrearsci.2017.03.019.

Embry, A. F., and J. E. Klovan, 1971, A Late Devonian reef tract on northeastern Banks Island, NWT: Bulletin of Canadian Petroleum Geology, v. 19, no. 4, p. 730–781.

Enay, R., C. Mangold, Y. Almeras, and G. W. Hughes, 2009, The Wadi Ad-Dawasir “delta”, central Saudi Arabia : A relative sea-level fall of Early Bathonian age: GeoArabia, v. 14, no. 1, p. 17–52.

Fischer, J. C., Y.-M. Le Nindre, J. Manivit, and D. Vaslet, 2001, Jurassic gastropod faunas of central Saudi Arabia: GeoArabia, v. 6, no. 1, p. 63–100.

Flugel, E., 2010, Microfacies of Carbonate Rock: Analysis, Interpretation and Application: Berlin, Springer-Verlag, 984 p., doi:10.1007/10.1007/978-3-642-03796-2.

Hubbard, R. J., 1988, Age and significance of sequence boundaries on Jurassic and Early Cretaceous rifted continental margins: AAPG Bulletin, v. 72, no. 1, p. 49–72.

Hughes, G. W., 2004, Middle to Upper Jurassic Saudi Arabian carbonate petroleum reservoirs: biostratigraphy, micropalaeontology and paleoenvironments: GeoArabia,

v. 9, no. 3, p. 79–114, doi:10.1007/3-540-45482-9_10.

Hughes, G. W., M. Al-Khalid, and O. Varol, 2009, Oxfordian biofacies and palaeoenvironments of Saudi Arabia: Volumina Jurassica, v. VI, p. 47–60.

J.S. Brown, 1943, Suggested use of the word microfacies: Economic Geology, v. 4, p. 325.

James, N. P., and B. Jones, 2015, Origin of Carbonate Rocks: Chicago, John Wiley & Sons, 320 p.

Kaminski, M. A., S. Chan, R. Bale, H. M. Gull, A. O. Amao, and L. O. Babalola, 2018, Middle Jurassic planktonic foraminifera in Saudi Arabia - A new biostratigraphical marker for the J30 maximum flooding surface in the Middle East: Stratigraphy, v. 15, no. 1, p. 37–46, doi:10.29041/strat15.1.37-46.

Konert, G., A. M. Afifi, S. A. Al-Hajri, and H. J. Droste, 2001, Paleozoic stratigraphy and hydrocarbon habitat of the Arabian Plate: GeoArabia, v. 6, no. 3, p. 407–442, doi:TBA.

Lindsay, R. F., D. L. Cantrell, G. W. Hughes, T. H. Keith, H. W. Mueller III, and S. D. Russell, 2006, Giant Hydrocarbon Reservoirs of the World: From Rocks to Reservoir Characterization and Modeling, *in* E. A. Mancini, ed., Giant Hydrocarbon Reservoirs of the World: From Rocks to Reservoir Characterization and Modeling: Tulsa, Geological Society Publishing House, p. 97–138.

Lonoy, A., 2006, Making sense of carbonate pore systems: AAPG Bulletin, v. 90, no. 9, p. 1381–1405, doi:10.1306/03130605104.

Malik, M. H., 2016, Micropalaeontology and sequence stratigraphy of Middle Jurassic D4-D5 Members of Dhruma Formation, Central Saudi Arabia: King Fahd University of Petroleum and Minerals, 156 p.

Manivit, J., C. Pellaton, D. Vaslet, Y.-M. Le Nindre, J.-M. Brosse, J.-P. Breton, and J. Fourniguet, 1985, Explanatory notes to the geologic map of the Darma Quadrangle, Sheet 24 H, Kingdom of Saudi Arabia: Ministry of Petroleum and Mineral Resources of Saudi Arabia, 33 p.

Murris, R. J., 1980, Middle East: Stratigraphic Evolution and Oil Habitat: AAPG Bulletin, v. 64, no. 5, p. 597–618.

Okla, S. M., 1987, Algal microfacies in Upper Tuwaiq Mountain Limestone (Upper Jurassic) near Riyadh, Saudi Arabia: Palaeogeography, Palaeoclimatology, Palaeoecology, v. 58, p. 55–61.

Okla, S. M., 1986, Litho- and Microfacies of Upper Jurassic Carbonate Rocks Outcropping in Central Saudi Arabia: Journal of Petroleum Geology, v. 9, no. 2, p. 195–206, doi:10.1111/j.1747-5457.1986.tb00381.x.

Powers, R. W., L. F. Ramirez, C. D. Redmond, and E. L. Elberg, 1966, Geology of the Arabian Peninsula: Sedimentary Geology of Saudi Arabia: Washington, USG Survey Professional Paper, 154 p.

Read, J. F., 1982, Carbonate platforms of passive (extensional) continental margins: Types, characteristics and evolution: Tectonophysics, v. 81, no. 3–4, p. 195–212, doi:10.1016/0040-1951(82)90129-9.

Sandberg, P. A., 1983, An oscillating trend in Phanerozoic non-skeletal carbonate mineralogy: Nature, v. 305, no. 5929, p. 19–22, doi:10.1038/305019a0.

Schlaich, M., and T. Aigner, 2017, Facies and integrated sequence stratigraphy of an Epeiric Carbonate Ramp Succession: Dhruma Formation, Sultanate of Oman: The Depositional Record, v. 3, no. 1, p. 92–132, doi:10.1002/dep2.28.

Schlumberger, 2007, Carbonate Reservoirs : Meeting unique challenges to maximize recovery: 8 p.

Schlumberger, 2009, Schlumberger Annual Report: 102 p.

Seilacher, A., 2007, Trace fossils analysis: 1-226 p., doi:10.1007/978-3-540-47226-1.

Sharland, P. R., D. M. Archer, R. B. Casey, S. H. Davies, A. P. Hall, A. D. Heward, A. D. Horbury, and M. D. Simmons, 2001, Arabian Plate Sequence Stratigraphy: Manama, Bahrain, Gulf Petrolink, 371 p.

Steineke, M., 1939, Arabian Geology and Topography: AAPG Bulletin, v. 12, no. 23, p. 1877–1878.

Steineke, M., B. Y. R. A. Bramkamp, and N. J. Sander, 1958, Stratigraphic Relations of Arabian Jurassic Oil: 1294-1329 p.

Stewart, S. A., 2017, Hormuz salt distribution and influence on structural style in NE Saudi Arabia: Petroleum Geoscience, v. 23, no. 3.

Strasser, A., 1986, Ooids in Purbeck limestones (lowermost Cretaceous) of the Swiss and French Jura: Sedimentology, v. 33, no. 5, p. 711–727, doi:10.1111/j.1365-3091.1986.tb01971.x.

Terry, R. D., and G. V. Chilingar, 1955, Summary of “Concerning some additional aids in studying sedimentary formations” by M.S. Shvetsov: Journal of Sedimentary Research, v. 25, no. 3, p. 229–234, doi:10.1306/74D70466-2B21-11D7-8648000102C1865D.

Tucker, M., and V. P. Wright, 1990, Carbonate Sedimentology: Blackwell Sciences Ltd., 482 p.

Vaslet, D., J. Delfour, J. Manivit, Y.-M. Le Nindre, J.-M. Brosse, and J. Fourniguet, 1983, Explanatory notes to the Geologic Map of the Wadi Ar Rayn quadrangle, Sheet 23 H, Kingdom of Saudi Arabia: Ministry of Petroleum and Mineral Resources of Saudi Arabia, 46 p.

Warren, J., 2000, Dolomite: occurrence, evolution and economically important associations: Earth-Science Reviews, v. 52, no. 1–3, p. 1–81, doi:10.1016/S0012-8252(00)00022-2.

Wilson, J. L., 1975, Carbonate Facies in Geologic History: 472 p., doi:10.1007/978-1-

4612-6383-8.

Wilson, J. L., 1974, Characteristics of Carbonate-Platform Margins: AAPG Bulletin, v. 58, p. 810–824.

Ziegler, M. A., 2001, Late Permian to Holocene Paleofacies Evolution of the Arabian Plate and its Hydrocarbon Occurrences: GeoArabia, v. 6, no. 3, p. 445–504.

# VITAE


Name : Aviandy Widya Ismanto

Nationality : Indonesian

Date of Birth : 18/03/1991

Email : aviandy18@gmail.com

Address : 14th Jambangan, Surabaya 60232, East Java, Indonesia

Academic Background : BSc. Geophysics, University of Gadjah Mada, Indonesia


Prior to joining CPG-KFUPM, he joined a private consultant in Yogyakarta as a junior geophysicist for about 2 years where he developed various experiences in some carbonate reservoirs in Indonesia with respect to seismic analysis and interpretation. His main interests are sedimentology, geostatistical reservoir modeling, seismic analysis and interpretation.

**Published article:**

- **Aviandy W. Ismanto,** Septriandi A. Chan, Khalid A. Al-Ramadan, Michael A. Kaminski, Lamidi O. Babalola. 2018. Micro- and foraminiferal biofacies analyses of Middle Dhruma Carbonates of Saudi Arabia (in preparation).